UiT The Arctic University of Norway

Faculty of Science and Technology
Department of Physics and Technology

Assessment of the Remaining Carbon Budget: Incorporation of Nonlinear Feedbacks in a Simple Response Model

Endre Falck Mentzoni

EOM-3901 Master's Thesis in Energy, Climate and Environment

June 2020

Abstract

Anthropogenic emission of greenhouse gases is causing an unbalance in the Earth's climate system, leading to global climate change. The implications of these changes are dramatic, with a need for a global-scale assessment. The remaining carbon budget (RCB) is a measure of the amount of greenhouse gasses (GHGs) that can be emitted if we are to reach a specific temperature target. Traditionally, carbon budgets are assessed from experiments in Earth System Models (ESMs) or less complicated reduced complexity models, such as the Model of the Assessment of Greenhouse Gas Induced Climate Change (MAGICC). The large spread between ESMs implies that one would need to study an ensemble of models. An alternative approach, which so far has remained unexplored is to use simple response models to assess RCBs and to build in a non-linear effect framework explicitly.

The construction of a simple response model (SRM) and estimated likelihood plots for the RCB show that the SRM estimates are consistent with MAGICC. A non-linear forcing effect framework enables the implementation and study of non-linear Earth system feedbacks. The estimates use a combination of emulators of 14 ESMs from the Coupled Model Intercomparison Project 5 (CMIP5) ensemble, to even out the climate sensitivity of each model.

Acknowledgements

First and foremost, I would like to thank my supervisor, Professor Martin Rypdal, for all the guidance, ideas and feedback through each stage of the process of my thesis.

I also want to give a special thanks to my dear friends and research partners Andreas Johansen and Andreas Rostrup Martinsen. It definitely would not have been as pleasant without both of you.

Finally, I would like to thank my friends and family, my father Kjell Olav for proofreading the thesis, my classmates and «Barista Boyz», who has made the last five years at university a memorable time.

Table of Contents

List of Tables

List of Figures

Acronyms

AR5	Assessment Report 5
BAU	Business-as-usual
CCS	Carbon capture and storage
CI	Confidence interval
CMIP5	Coupled Model Intercomparison Project 5
EMIC	Earth system Model with Intermediate Complexity
ESM	Earth system model
GDP	Gross domestic product
GHG	Greenhouse gas
GIS	Greenland ice sheet
GMST	Global mean surface temperature
IAM	Integrated Assessment Model
IPCC	Intergovernmental Panel on Climate Change
MAGICC	Model of the Assessment of Greenhouse Gas Induced Climate Change
MISI	Marine ice sheet instability
NASA	National Aeronautics and Space Administration
NOAA	National Oceanic and Atmospheric Administration
PPB	Particles per billion
PPM	Particles per million
RCB	Remaining carbon budget
RCP	Representative Concentration Pathways
SR15	Special Report on Global Warming of 1.5°C
SRM	Simple response model
SROCC	Special Report on the Ocean and Cryosphere in a Changing Climate
SSP	Shared Socioeconomic Pathways
SST	Sea surface temperature
TCRE	Transient Climate Response to cumulative Emissions of CO_2
WAIS	West-Antarctic ice sheet

1 Introduction

Global climate change is one of the defining issues of our time. In 2019 the global mean surface temperature (GMST) has increased by 1.1±0.1°C relative to the industrial revolution, with a baseline period between 1850-1900 (World Meteorological Organization, 2020). The main factor for this warming is rising greenhouse gas (GHG) concentrations from emissions associated with consumption and production of fossil fuels driven by a dramatic increase in the use of global resources (Allen et al., 2018; J. Rogelj et al., 2018).

Through the Paris Agreement and its signatories, most of the global community aims to hold global average temperature well below 2°C and at the same time aspiring to constrain the warming below 1.5°C above a pre-industrial revolution average. According to results of the latest Special Report on Global Warming of 1.5°C (SR15) by the Intergovernmental Panel on Climate Change (IPCC), there is at least 66% probability that the 1.5°C-target will already fail between 2030 and 2052 (J. Rogelj et al., 2018). With a specified temperature target, it is possible to estimate an approximate remaining carbon budget (RCB) through a simple physical relation known as the transient climate response to cumulative emissions of CO_2 (TCRE) (see Section 2.4). Often, RCBs are estimated using complex Earth System Models (ESMs), with substantial variation between models. An alternative approach is to use reduced complexity models such as Model of the Assessment of Greenhouse Gas Induced Climate Change (MAGICC). However, since there are few such models, there is a risk to underestimate the model uncertainty.

As a part of the fifth and last year of my integrated bachelor and master's degree, I am participating in a research project with fellow students Andreas Johansen and Andreas Rostrup Martinsen, and our supervisor Martin Rypdal. The research project focuses on the construction of a simple response model (SRM) for estimates of the RCB. We verify our model results through Martinsen (2020) comparison with MAGICC6, demonstrate the estimate of the RCB with linked likelihoods for a given mitigation target, and analyse the impact on the RCBs when including the Arctic amplification factor.

This study also reviews the concept of RCBs and how they are generally estimated, with the impact and challenges that arise from including or excluding different forcing factors, and feedback-mechanisms.

The SRM is a pure-play on the scenario-based approach. As of now, it consists of four forcing factors, with emissions from carbon dioxide and methane, emissions from anthropogenic aerosols, and an implemented non-linear forcing framework dependent on the GMST. In this study, we implement an example of non-linear forcing through the GHG release from the warming of wetlands and abrupt permafrost thaw, due to the interest in the Arctic amplification factor (Johansen, 2020).

We can, with little effort, implement other forcing factors or feedback mechanisms in the flexible SRM framework. For a given emission scenario of CO_2 (typically given as $GtCO_2$ per year), the model estimates a concentration through our simple carbon response model. Due to the nature of the different forcing factors, the relationship between concentrations and forcing is described separately for each forcing agent using standard relations of atmospheric physics. From the forcing estimates, we estimate the global temperature response using linear box-type climate models with parameters fitted to the different models in the Coupled Model Intercomparison Project 5 (CMIP5) ensemble.

Even though climate change is a global challenge, the impacts are felt locally (Allen et al., 2018). Modelling and observations show that there is an Arctic amplification factor for global warming. The temperature increase in the Arctic succeeds the GMST. For instance, GISTEMP model shows mean surface temperature north of 64°N in 2019 of 2.71°C (Dai, Luo, Song, & Liu, 2019; Lenssen et al., 2019; Team, 2020). As a part of our project, we have estimated and implemented the Arctic amplification factor to obtain RCBs for temperature targets for the Arctic (Section 3.7 and (Johansen, 2020)).

Rather than studying scenarios that exceed the more optimistic temperature targets like 1.5°C or 2.0°C from the Paris Agreement, we focus on avoidance- and overshoot-scenarios (see Section 2.4.4). Findings in SR15 underline that in order to limit global warming to more ambitious mitigation targets such as 1.5°C there has to be an almost pivotal shift in the global society, with the decoupling of GHG emissions from economic growth (Allen et al., 2018). If we continue in a business-as-usual (BAU) scenario for too long, the number of policy options diminishes quickly, leading to considerable challenges and a higher risk of failure for both the mitigation and adaptation efforts, likely leading to amassing total costs (Hurlbert et al., 2019).

Another uncertain factor is the impact of human mitigation and adaptation choices, underlining the need for an RCB estimate framework with a capability to run a high number of scenarios with several model combinations. This is where the SRM shows its forte, because of its simplicity, low runtime, flexible framework and the included likelihood estimates.

2 Theory and background

2.1 Climate change

Observations from the National Aeronautics and Space Administration (NASA) and National Oceanic and Atmospheric Administration (NOAA) show that 2019 was the second warmest year on record since 1880, as illustrated in Figure 2.1 (NASA Earth Observatory, 2020). The estimated GMST in 2019 was 1.1±0.1°C above pre-industrial levels, i.e., a baseline period of 1850-1900. Four of the past five years were the warmest since modern instrumental temperature recording started in 1880, and it is quite clear that the long-term trend of global warming seems to be continuing (NASA Earth Observatory, 2020; World Meteorological Organization, 2020).

There is a broad consensus among climate scientists that rising concentration of GHGs in the atmosphere from anthropogenic emissions is the key factor in climate change and rising global temperatures. The most important greenhouse gases are carbon dioxide (CO_2), methane (CH_4) and nitrous oxide (N_2O). In 2019 the average atmospheric concentration of CO_2 was around 411 particles per million (ppm), which, compared to pre-industrial levels, increased 47% from around 280 ppm (National Research Council, 2020; J. Rogelj et al., 2018). This rise in global CO_2 concentration reflects how the unbalance between the sources and sinks has changed due to an increasing ratio of anthropogenic emissions when comparing it to the carbon uptake by the ocean and biosphere (World Meteorological Organization, 2020).

Both rising temperatures and the increasing unbalance in the changing climate system can lead to severe environmental effects and socio-economic impacts. The Special Report on the Ocean and Cryosphere in a Changing Climate (SROCC) concluded with 80% probability that climate change in the ocean and the cryosphere is leading to an increase in both single extreme weather events and extreme weather patterns, on a global scale (Collins et al., 2019).

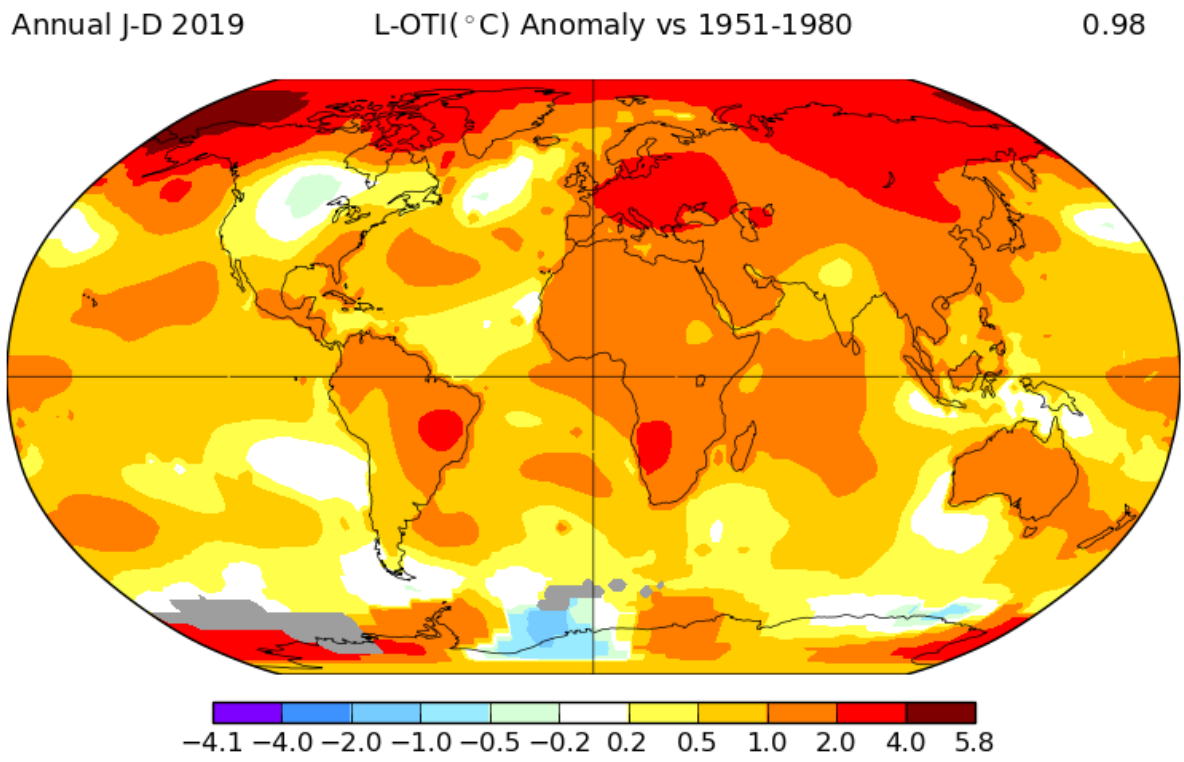

Figure 2.1: Global annual surface temperature anomalies (°C) in 2019 relative to a baseline period from 1951 to 1980, using a 1200 km smoothing radius. The estimates of the global average temperature anomaly led to 0.98°C. Reproduced from (Lenssen et al., 2019; Team, 2020).

Warming of the mean sea surface temperatures (SST) of 0.11°C per decade since the 1970s, has been leading to a warming of the ocean's upper layer (depths of 0-700m). These changes leads to an increasing stratification of the upper ocean, thus lowering the carbon uptake (Hoegh-Guldberg et al., 2018). In addition to a lower carbon uptake, it leads to an increased probability of marine heatwaves. The IPCC defines a marine heatwave as a short-term extreme warming event where the daily SST lies above the 99% confidence interval (CI) for a given local area for the period between 1982-2016 (Collins et al., 2019).

Model results from ESMs indicate that with at least 90% probability, 84-90% of all the marine heatwaves on a global scale between 2006-2015 is attributable to the increase in GMST compared to an 1850-1900 baseline. Frölicher, Fischer, and Gruber (2018) states that if the temperature exceeds 2°C, almost 100% can be attributed to global warming. The marine heatwaves will become increasingly frequent, with an estimated factor increase of 16-24 under a Representative Concentration Pathway (RCP) scenario, RCP2.6, in 2081-2100 relative to 1850-1900. These changes can push the marine ecosystems to the brink of their systems elasticity, thus maybe leading to irreversible changes (Collins et al., 2019; Frölicher et al., 2018).

Negative impacts on ecosystems often accompany climatic- and extreme weather events. In the case of marine ecosystems, there are impacts on fisheries and the globally and locally dependent economies (Collins et al., 2019). An example is the detrimental hurricane season in 2017 along the coastlines of the southern United States and the Caribbean, with hurricane Harvey being one of the most costly, causing estimated damage of USD$ 125 billion, compared to USD$ 265 billion for the 2017 hurricane season in total (Blake & Zelinsky, 2018; Collins et al., 2019). In comparison, the Norwegian gross domestic product (GDP) for 2018 was USD$ 434 billion (The World Bank, 2020).

2.2 The economics of climate-change mitigation

The SR15 discovers through analysis of Integrated Assessment Models (IAMs), that for scenarios with temperature targets between 1.5°C and 2.0°C there is an increase in GDP of 240% and an increase in energy consumption of 20% and 50%, respectively by the year 2050 (J. Rogelj et al., 2018). An analysis of 31 developing countries, shows evidence of significant causality between CO_2 emissions, energy consumption and economic growth (Aye & Edoja, 2017). The world population is estimated to increase to between 8.5-10 billion people by 2050, and since population, in general, is a significant factor in economic growth, the need for climate action is urgent (KC & Lutz, 2017; Peterson, 2017).

All of the stated factors above, underline the need for the transition to low-, zero-, and negative carbon technologies like e.g. renewable energies and carbon capture and storage (CCS) (Aye & Edoja, 2017). To be able to meet a 1.5°C temperature target outlined in the Paris accord, drastic and immediate changes to the global society is required, with the combination of climate mitigation and adaptation. It requires a shift away from the causality between economic growth, the emissions of greenhouse gases, and the consumption of fossil fuels (Allen et al., 2018; Newman, 2017).

In 2015, the global fossil fuel subsidies accounts for around 6.3% of the global GDP at around USD$4.7 trillion, where the coal and petroleum industries are responsible for about 85% of the total subsidies (Coady, Parry, Le, & Shang, 2019). These numbers includes both the direct price subsidies and indirect costs through both lost environmental and economic benefits. Through

the phase-out of fossil fuel subsidies, the global carbon emissions can decrease by 28% and raising the global GDP with almost 4% when comparing to 2015 numbers (Coady et al., 2019).

However unlikely an abrupt stop in the fossil fuel subsidies is, it will be a drastic mitigation effort towards a 1.5-2°C temperature target. It will also come with many benefits for the global society in the form of, e.g. a reduction in aerosol emissions, leading to improvements in public health (further discussed in Section 2.4.2) (Allen et al., 2018).

Even though mitigation action is the most critical factor for reaching the Paris accord temperature target of 2°C, climate adaptation is needed. Examples of adaptive measures is the transition to green infrastructure and strengthening its resilience, increasing sustainability in water management, ecosystem restoration and improving the public health system. The abovementioned measures are feasible and cost-effective (de Coninck et al., 2018), but, in general, adaptive measures will likely be very costly with considerable uncertainties in the effectiveness, with estimates for yearly costs in 2030 in the range of USD$ 140-300 billion (UNEP, 2018). Findings in AR5 also indicate that there might exist a considerable gap between the actual need for global adaptation efforts and the available funding (IPCC, 2014). It is also found to in general be notably more cost-effective to focus on mitigation efforts, thus reducing greenhouse gas emissions instead of covering the damage costs induced by climate change (Sánchez et al., 2016).

Understanding where these limits lie is thus an area of research that needs focus. Findings in Assessment Report 5 (AR5) underline that present knowledge of adaptation limits is insufficient, with a lacking understanding of how the warming climate can impact the as of now characterised limits. These problems in combination with a lack of or inadequate planning may lead to maladaptation, possibly increasing the vulnerability of certain areas or people (IPCC, 2014; Klein et al., 2014). This knowledge gap underlines the need for adaptation frameworks that are flexible to changes in scientific knowledge, leading to varying risks of success for the adaptation efforts and their results both in an economic and climatic manner (UNEP, 2018).

As briefly discussed in Section 3.7, global climate change will lead to uneven regional impacts and thus varying needs for adaptive measures and thus potentially higher adaptation costs. Findings in the Adaptation Gap Report 2018 showed that for a 1.5°C mitigation target, ecosystem services and biodiversity would likely be the most vulnerable areas. These sectors were also

among the sectors with considerable lack of funding for adaptive measures and with a knowledge gap that likely leads to an increase in the adaptation costs, often located in many of the world's poorest regions (UNEP, 2018).

2.3 Radiative forcing and feedbacks

To be able to analyse and quantify the impact natural and anthropogenic emissions of greenhouse gases, aerosols, and other forcing factors have on the Earth's climate system, one can use different metrics. The one most commonly practised is radiative forcing. Forcing is generally defined through the net change in the energy balance of the Earth's climate system caused by a small change in the system (see Section 2.7.1 for further explanation). The standard unit is W/m^2 and will vary with time and space (Myhre et al., 2013).

In 2017, the observed total radiative anthropogenic forcing when not including aerosols, with respect to the pre-industrial levels in 1750 was 3.1 W/m^2, an increase of 0.3 W/m^2 compared to 2011 levels. The main factors are carbon dioxide, methane and nitrous oxide, contributing about 2.0 W/m^2, 0.5 W/m^2 and 0.2 W/m^2, respectively (Bruhwiler et al., 2018). Other forcing factors, such as aerosols is more complicated with effects on both the radiation and interactions with clouds which in turn can lead to other feedback effects. In general, there is a consensus that aerosols produce a negative global mean radiative forcing of -0.35 W/m^2 with an uncertainty range of -0.85 W/m^2 to 0.15 W/m^2, thus likely causing a cooling effect (Myhre et al., 2013).

Some factors of the greenhouse effect are not forcing factors, but instead, feedback agents. Water vapour is an example, playing a principal role in the climate system as the main greenhouse gas in the atmosphere. Changes in atmospheric concentrations of water vapour come from increasing air temperature rather than directly from emissions of greenhouse gases (Myhre et al., 2013). This is an example of what is known as positive feedback. A general definition of a positive feedback mechanism can be a reaction to the climate system that increases initial warming. In contrast, negative feedback leads to a cooling effect.

Feedbacks can also lead to increasing or decreasing carbon fluxes to the atmosphere as a result of the warming temperatures and are then usually called carbon cycle-climate feedbacks

(Bruhwiler et al., 2018). An example can be increasing frequencies of forest fires through, e.g. warming and thus drying of soils, leading to linked emissions in the form of, e.g. burned biome or permafrost thaw, leading to non-linear forcing effects (discussed in Section 2.5.1) (Gibson et al., 2018). In an isolated manner, forest fires can also lead to negative feedbacks through a higher albedo due to, e.g. less forest cover, leading to a higher surface reflectivity, even if the net feedback might be positive.

2.4 The remaining carbon budget

Since the release of AR5 in 2013, the use of climate budgets has become the principal tool to guide climate policies around the world (Messner, Schellnhuber, Rahmstorf, & Klingenfeld, 2010). A standard definition of an RCB is the finite and total amount of CO_2 that can be emitted into the atmosphere by human activities while still holding the warming of global temperature to a given temperature limit (Rogelj, Forster, Kriegler, Smith, & Seferian, 2019).

The concept behind the RCB builds on the anthropogenic influence on the global climate-carbon cycle system. Its main component is the TCRE, and the approximately linear relationship between cumulative anthropogenic CO_2 emissions since the industrial revolution and its effect on the global temperature. Through this relationship, one can calculate a specific carbon budget for an assigned mitigation target, as illustrated in Figure 2.2.

RCBs can be estimated using observational data or through simulations by using, e.g. ESMs, which includes a dynamic representation of the global carbon cycle, or from the observational record. The models are of varying complexity, where some of them only include CO_2 forcing while others use multi-gas simulations (J. Rogelj et al., 2018).

The IPCC estimates that 77% of the anthropogenic forcing is a result of CO_2 emissions while the remainder comes from non-CO_2 sources, including both greenhouse gases and aerosols. Since the TCRE's include different forcing factors, their respective carbon budgets also differ. Carbon budgets that only use CO_2 emissions as forcing are known as CO_2-only carbon budgets, while the ones that include other greenhouse gases and forcing factors are called effective carbon budgets (Myhre et al., 2013).

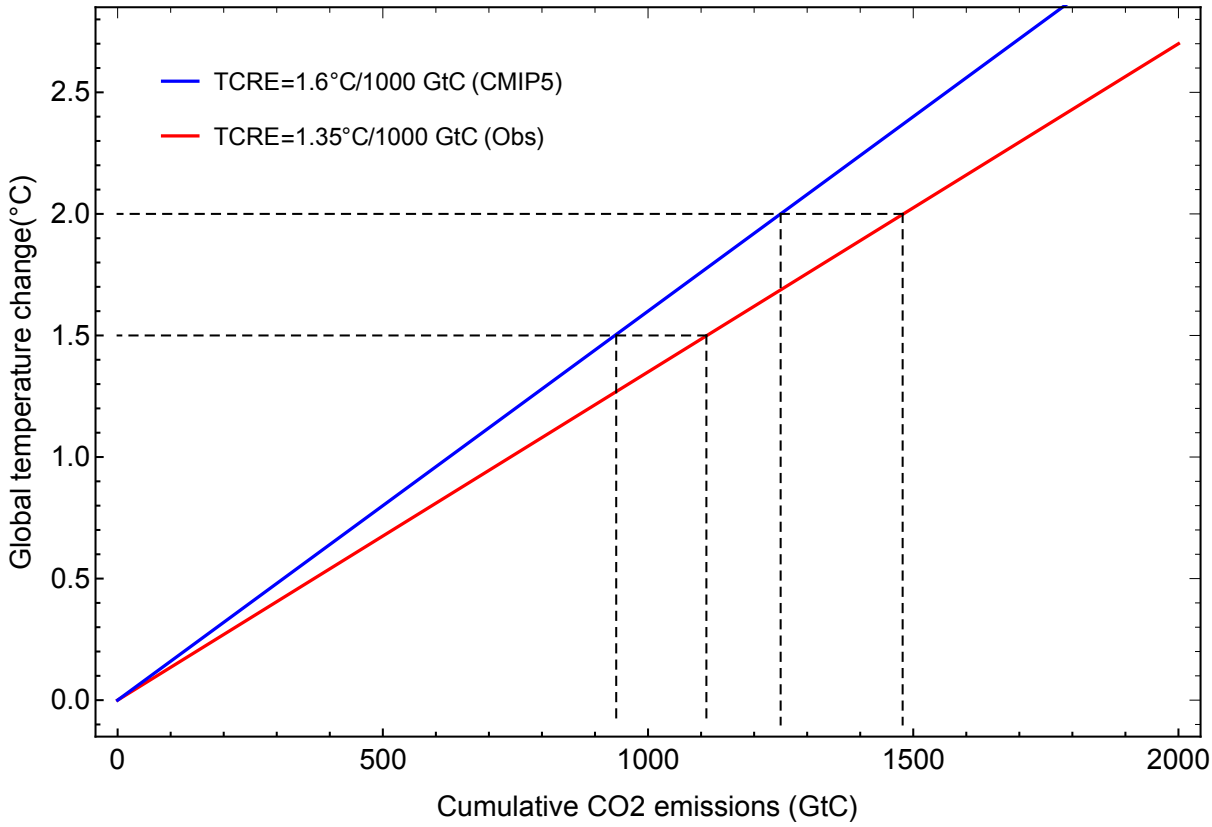

Figure 2.2: Estimates of two TCREs in a CO_2-only carbon budget. The red line illustrates the estimate using observed temperature data, with a median value of 1.35°C/1000 GtC. The blue line represents an estimate using the CMIP5 model ensemble with a best estimate of 1.6°C/1000 GtC. The dashed lines show how TCREs affect the associated carbon budgets. The TCRE estimates were found in (Matthews et al., 2017).

2.4.1 CO_2-only carbon budgets

Carbon budgets that only include CO_2 as a forcing factor will never be accurate estimates. However, they can form a sort of upper limit for emissions.

When using observational records to estimate a CO_2-only TCRE, one needs to identify the amount of observed warming that is attributable to CO_2 alone from fossil fuels and land-use change. Gillett, Arora, Matthews, and Allen (2013) estimates a TCRE with a 90% CI (5-95) of 0.7-2.0°C/1000 GtC with a median of 1.35°C/1000 GtC. When using the CMIP5 model ensemble, Matthews et al. (2017) estimates an interval of 0.8-2.4°C/1000 GtC, with a best estimate of 1.6°C/1000 GtC (5-95% range).

Figure 2.2 illustrates the resulting carbon budgets for these estimates. For the model-based TCRE, the 1.5°C and 2°C targets have resulting carbon budgets of 940 GtC and 1250 GtC,

respectively, while the observation-based TCRE (with its lower slope) suggests larger carbon budgets of 1110 GtC and 1480 GtC for the 1.5°C and 2°C targets. Thus about 18% larger carbon budgets for the observationally-based TCRE from Gillett et al. (2013) than for the model-based TCRE.

The difference between model-based estimates and estimates from observational data underlines the considerable uncertainty the temperature response to CO_2 emissions. Also, there are other factors like non-CO_2 greenhouse gases and aerosol emissions. We should note, however, that the model estimates have wider CIs than the estimates from observations (0.8-2.4 vs 0.7-2.0), which means that the models are more uncertain than what we can infer from the observed data. We also note that the carbon budget becomes practically path-independent when only using CO_2 forcing as a geophysical factor.

2.4.2 Effective carbon budgets

The carbon-climate cycle depends on forcing factors like non-CO_2 greenhouse gases, aerosol emissions and effects like changes in the surface albedo due to land-use. The IPCC forcing estimate of non-CO_2 emissions is about 23% of total anthropogenic forcing, and this implies that disregarding other forcing factors will give an inaccurate assessment of the climate system (Myhre et al., 2013). Due to a large number of forcing factors, with their varying lifetimes, there is no simple way of linearising it into a scaling factor to account for all the non-CO_2 emissions in the TCRE.

There are several ways of simplifying this problem. One way is to adopt the IPCC estimates that 77% of the observed warming is attributable to CO_2 emissions and thus define an "effective TCRE" which is adjusted to include the effect of non-CO_2 forcing. Matthews et al. (2017) define the "effective TCRE" as the change in global mean temperature in relation to an 1861-1880 average (0.99°C according to numbers from the Global Warming Index (Haustein et al., 2017)) and total historical CO_2 emissions between 1870-2015 (555 GtC according to (Le Quéré et al., 2015)). This translates from 0.99°C/555 GtC to 1.78°C/1000 GtC. It only uses CO_2 emissions but is scaled by the observed global mean temperature change from all emissions from 1870 until 2015, which then should account for a temperature change from all forcing factors. The effective TCRE to the CO_2-only TCRE should give a factor around 0.77 according to the IPCC forcing estimates. As it turns out, the factors for 2015 estimates indicates that this method might work as a simplification (1.35/1.78=0.76).

There are, however, problems with this approach. By assuming a constant factor one neglects the fact that mitigation efforts in different scenarios will affect the forcing ratios. Matthews et al. (2017) argue that the ratio can stay relatively constant for the next decade or two due to mitigation efforts linked to aerosol emissions which can keep the ratio nearly constant. Countries like China and India have seen an expansive industrial growth over the last few decades, fuelled by fossil fuels like coal, which leads to a strong increase in aerosol emissions in contrast to the global trend that is decreasing (Figure 2.3).

With an increase in air pollution, China experienced harmful public health effects and resulting deaths. In 2013 they launched a clean-air policy to reduce the air pollution through lowering aerosol emissions by improving industrial emission standards, removing outdated industry and promoting cleaner fuels (Zhang et al., 2019). From 2013 to 2017, the policy resulted in a national decrease in yearly emissions of sulphur dioxide (SO_2) and particle matters with a diameter smaller than 2.5 micrometres ($PM_{2.5}$) of 59% and 33%, respectively. The reduction gave a decrease in yearly deaths due to $PM_{2.5}$ by 0.41 million persons (95% CI: 0.38-0.43 million). Compared to the estimated global deaths in 2015 due to aerosols of 8.9 million (95% CI: 7.5-10.3 million) it was a decrease of around 5% (Burnett et al., 2018).

The motivation in China was to improve their public health mainly, and not necessarily to mitigate climate change through the promotion of, e.g. greener energies, even though they did so as an indirect effect when solving air pollution problems.

Even more recently, government confinement policies due to the COVID-19 pandemic leads to drastic changes in the global energy demand. Estimates from Le Quéré et al. (2020) show a decrease in daily global CO_2 emissions by -17% ($\pm 1\sigma$ CI (-11%,-25%)) in early April in relation to mean 2019 levels, corresponding to emission concentrations in 2006. The temporary emission reductions depend on the level and duration of the confinement globally. A return to pre-COVID-19 conditions between June 2020 and 2022 will result in an estimate of annual emission decrease between -4.2% and -7.5%, which would need to continue for several decades to meet a 1.5°C mitigation target (IPCC, 2018; Le Quéré et al., 2020).

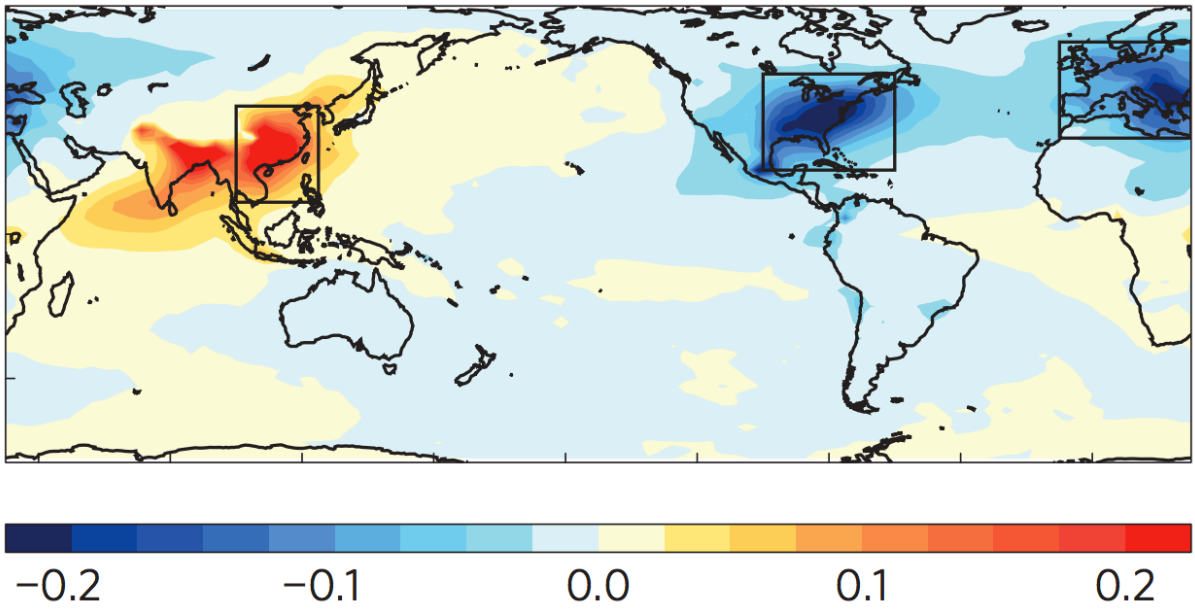

Figure 2.3: Global aerosol concentration trend between 1998 and 2012 measured in the unit-less metric "optical depth". Reproduced from Smith et al. (2016)

A changing ratio of CO_2-attributable forcing to total forcing shows that having a flexible and scenario-based approach which includes non-CO_2 forcing will be crucial and necessary to adjust the estimates of the RCBs. an estimate shows that on average for the CMIP5 models, the ratio between non-CO2 forcing factors and the total forcing in 2015 is 0.86 (Meinshausen et al., 2011). This estimate is also consistent for RCP2.6, RCP4.5 and RCP8.5. Since there are such apparent differences in the ratio (0.23 vs 0.14), it suggests that there are uncertainties about the impact of non-CO_2 forcing and especially the negative forcing effect from aerosols. There is a consensus in the literature that the net aerosol forcing effect is negative, but the question is in which magnitude. Matthews et al. (2017) point out that difference between CMIP5 and IPCC estimates comes from a more notable negative aerosol effect in the CMIP5 estimates, which in turn leads to a smaller net non-CO_2 forcing factor and thus a larger fraction of the total forcing coming from CO_2 as illustrated (Figure 2.4).

A way of accounting for a changing forcing ratio is to make the TCRE directly dependent on it. Matthews et al. (2017) uses the CMIP5 models best estimate of 1.6°C/1000 GtC and then scales it by dividing it by a moving forcing ratio. As previously mentioned, this ratio estimate is 0.86 in 2015, leading to an effective model-based TCRE of 1.6°C/1000 GtC *1/0.86=1.86°C/1000 GtC. The relation is then tested by looking at the estimated global temperature change for this TCRE, through cumulative CO_2 emissions from the industrial revolution in 1870 until 2015 of 555 GtC. 1.86°C/1000GtC*555GtC = 1.03°C, which is well within

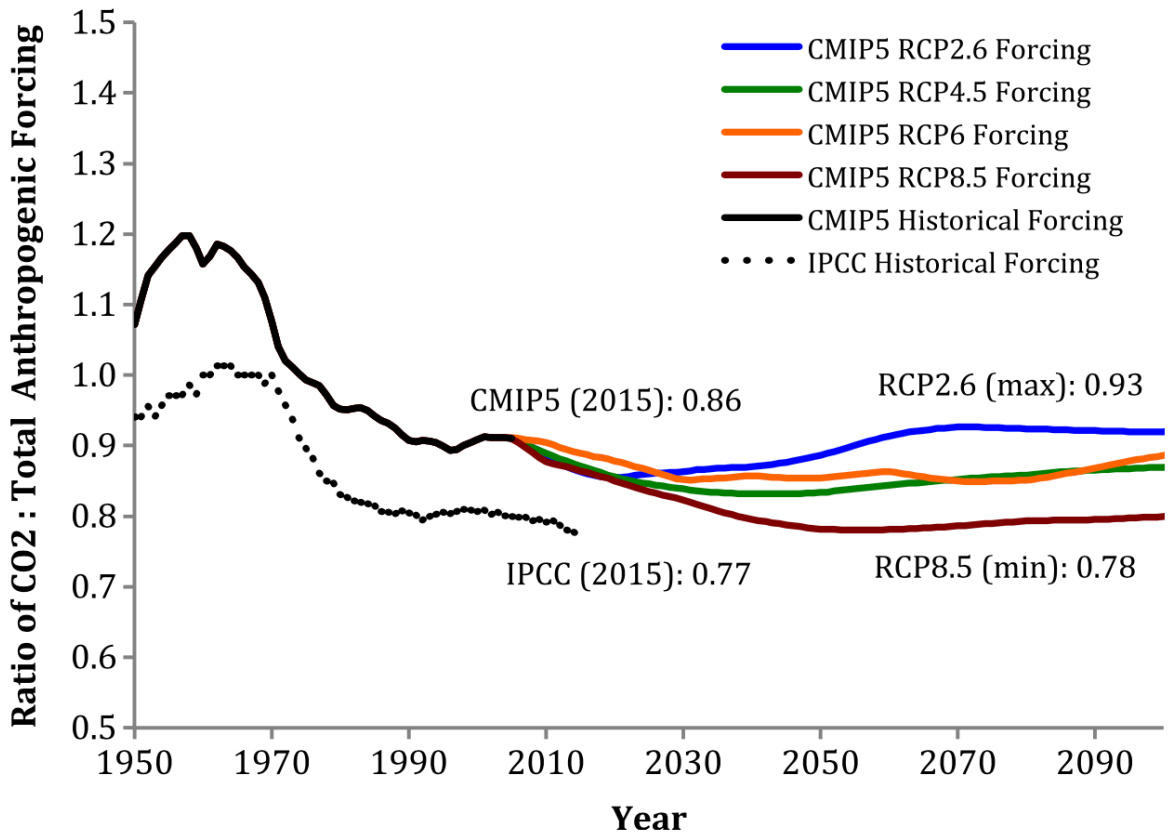

Figure 2.4: Ratio between human-induced CO_2 forcing and the total anthropogenic forcing. From 1950 until 2015 they consist of historically estimated data, while the ratios from 2015-2100 follow different RCP's in the CMIP5 model, as shown in the figure legend. CMIP5 models estimate a more substantial aerosol effect than the IPCC, leading to a larger negative forcing. Hence the fraction for non-CO_2 forcing is smaller for CMIP5 estimates (0.14) than for the IPCC (0.23) in 2015. Reproduced from (Matthews et al., 2017)

the Global Warming Index's 90% CI of 0.85°C-1.23°C and thus consistent with the observed warming (Haustein et al., 2017).

The difference between the effective estimates (1.78 vs 1.86) is much smaller compared to the CO_2-only TCRE's (1.6 vs 1.35). Associated RCB estimates will have quite similar outcomes but with differences due to their differing estimates of the non-CO_2 forcing factors.

Figure 2.5 illustrates the TCRE with a direct dependency on the moving forcing ratio through different concentration pathways and their respective carbon budgets per degree of global temperature warming. It also shows the linked carbon budgets for previously estimated observational- and model-based CO_2-only TCREs. Figure 2.5 clearly demonstrates the need for a flexible and path-dependent estimate method and that using a strictly linear TCRE is problematic. The more optimistic scenario RCP2.6, which is relevant for temperature targets of 1.5-2°C shows a considerable change in the forcing ratio due to the drastic mitigation regimes in the

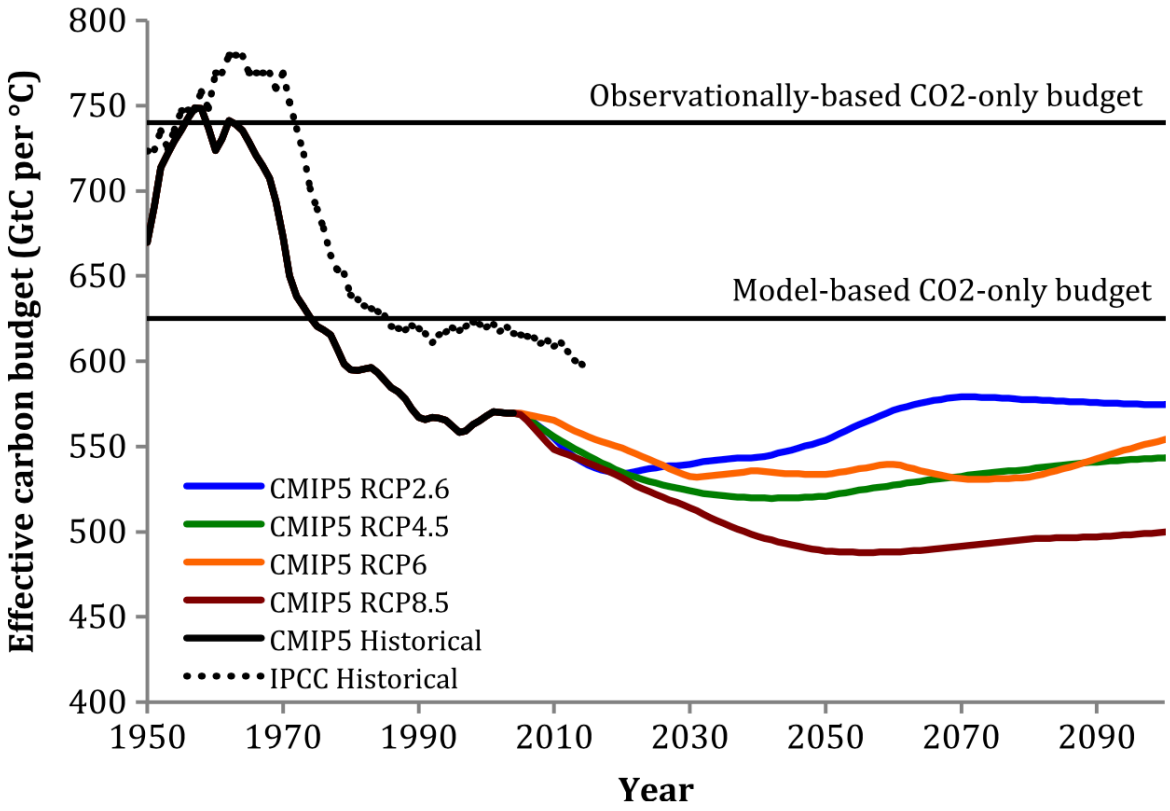

Figure 2.5: The effective carbon budget (GtC/°C) from related emission scenarios, as in Figure 2.4. The figure underlines the need for a flexible carbon budget estimation framework that can account for a changing forcing ratio over time. Reproduced from (Matthews et al., 2017)

scenario. Due to the different lifetimes of the forcing agents, where CO_2, in general, has the longest, the ratio will likely change closer towards 1. Looking at CO_2, the critical factor for atmospheric concentration is the cumulative emissions (due to its long lifetime), while it for methane (with a lifetime of 9 years) is much more linked to the emissions. Thus, carbon budgets, in general, should be considered to be dependent on the time when considering the different mitigation policies.

2.4.3 TCRE limitations and assumptions

Section 2.4.1-2.4.2 discusses four different ways to estimate carbon budgets through the TCRE. Some of them follow the traditional way of using an approximately linear relation, and one of them uses estimated TCRE and scale it with a moving forcing ratio which thus indirectly removes the linearity. A common feature is their wide CIs which add uncertainties to the estimate of the carbon budget. AR5 states that a TCRE with at least a 66% probability is within 0.2-0.7°C/1000GtCO$_2$ (0.73-2.57°C/1000GtC) and is robust up to 7300 GtCO$_2$. This relation would be robust up to 1990 GtC through the factor 44/12 due to the molecular weight of the CO_2

molecule in comparison to the carbon atom (Collins et al., 2013). All realistic temperature goals (1.45°C-5.11°C) are well within when considering the estimates robust-limit of 1990 GtC.

The TCRE robustness range estimated by IPCC is, however, only valid if the assumption about the linearity and the carbon-cycle systems stationarity is valid. Moreover, using at least 66% as a metric is not necessarily an exact science. As previously mentioned, adding numerous different forcing agents adds uncertainty to the estimate since several factors like, e.g. thawing of permafrost. Another example of uncertainty is that the interaction effects between greenhouse gases are not well understood. In (Rypdal, 2016) he mentions that as long as the climate system is far away from a tipping point, this assumption thought to be valid. There are several potential tipping points for the carbon-cycle climate system, e.g. the runaway melting of the West-Antarctic ice sheet (WAIS) (more detailed explanation in Section 2.5).

In (Comyn-Platt et al., 2018) they mention that the release of methane in wetlands and carbon dioxide and methane from the thawing of permafrost will inflict a non-linear effect on the global temperature. According to their model simulations, the release would be more substantial between 1.0-1.5°C than for 1.5-2.0°C, which implies that the tipping point might be closer than previously thought. Currently, too few climate models incorporate the thawing of permafrost and its feedback mechanism, leading to an inadequate understanding of its impact on the carbon-cycle climate system and the effect on the TCRE assumptions of linearity and stationarity. The results from (MacDougall, Zickfeld, Knutti, & Matthews, 2015) states that it does not invalidate the linearity assumption.

The global carbon-cycle climate system could however be so affected by tipping points that it stops working in the way as it does now. The TCRE stationarity assumption claims that the climate system will work the same way now as it will in the future. Even if the climate system is not close to any tipping points, the assumption might already be wrong, as mentioned in (Rypdal, 2016), due to saturation effects in the land biosphere and in the ocean mixed layer that may lead to a reduction of fluxes in a different climate.

2.4.4 Scenario types

Given a specific temperature threshold like, e.g., the 2.0°C target from the Paris Agreement, the corresponding emission scenarios can be classified as exceedance-, avoidance- or overshoot-scenarios. As illustrated in Figure 2.6, an exceedance scenario is a scenario with cumulative anthropogenic emissions of CO_2 and its temperature response that exceed a set temperature target. In Gasser et al. (2018), they define an avoidance scenario as a scenario where the cumulative emissions keep below a given threshold for the temperature target. An overshoot scenario does, on the other hand, surpass the threshold for cumulative emissions of a given temperature target, and thus has a peak warming above the temperature target. Due to negative emissions through, e.g. CCS, the emissions and thus temperature decreases and hits the temperature target over time.

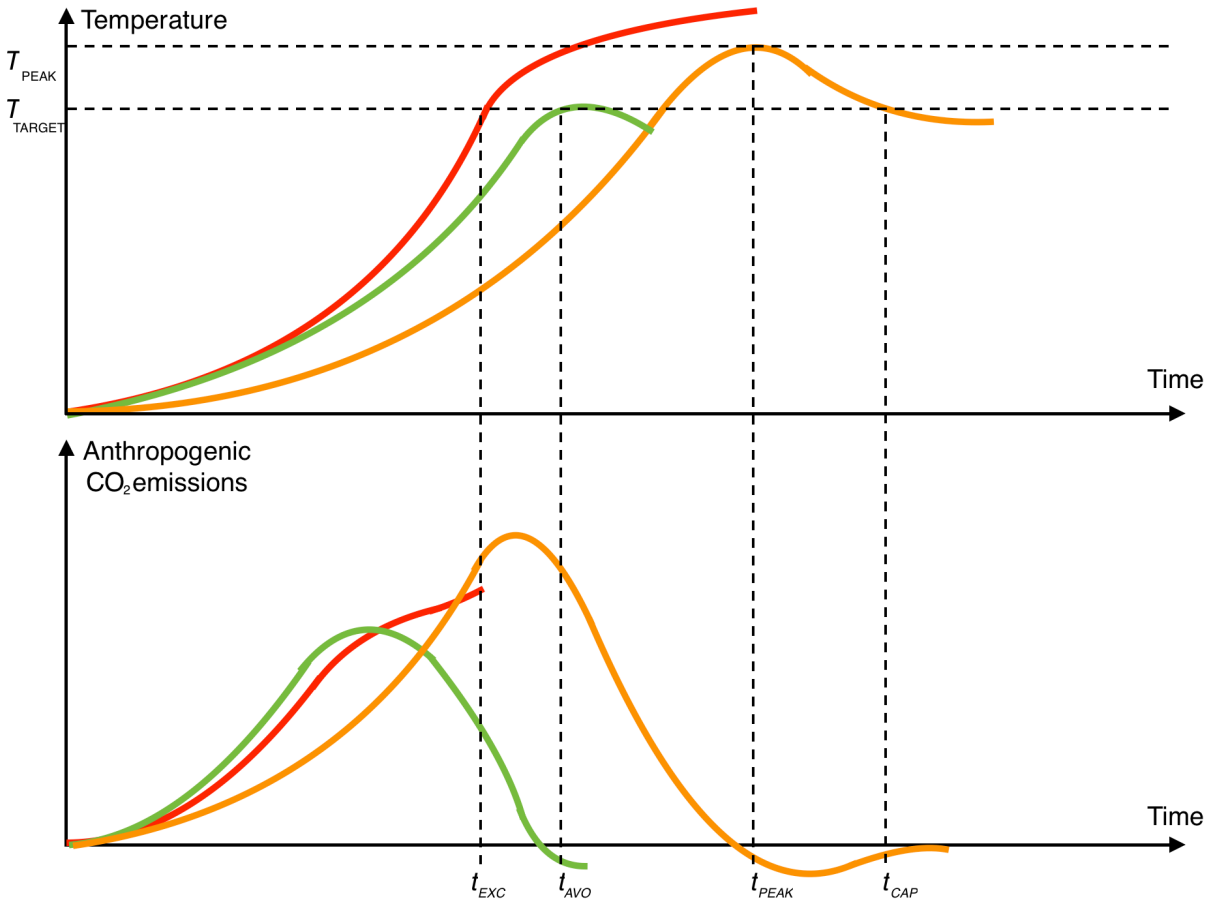

Figure 2.6: Avoidance-, overshoot- and exceedance emission scenarios. The red curves illustrate an exceedance scenario showing a given emission scenario exceeding the temperature target. The green curves illustrate an avoidance scenario and its temperature response, where the peak temperature has to be equal to or lower than the temperature target. The orange curves represent the overshoot scenario, where the emissions peak leading to a peak temperature before it declines to a point colder than the temperature target.

2.5 Tipping points

In the climate system, there may exist certain critical thresholds where a small perturbation can lead to the system transitioning from one stable state to another one. These changes are either global or regional, non-linear of nature and lead to irreversible transitions (Collins et al., 2019). In the case of potential global tipping points, they are often referred to as large-scale singular events that will lead to or be linked with extreme changes in the climate system. Examples are changes in the thermohaline circulation, runaway melting of the WAIS and Greenland ice sheet (GIS), or a shift in the El Niño-Southern Oscillation (Hoegh-Guldberg et al., 2018).

Assessments in SR15 indicate that for the large-scale singular events, there has been an evident increase in the associated risk of occurrence since AR5. The estimates show the changes can happen at much lower temperatures, with a moderate and high risk for events happening at 1°C (1.6°C) and 2.5°C (4°C), respectively (Hoegh-Guldberg et al., 2018). The assessments of risk bases on model results and new observations of the WAIS show a possible acceleration in the ice retreat that supports the marine ice sheet instability (MISI) hypothesis (Meredith et al., 2019).

Climate change can also trigger regional tipping points, with examples being the collapse of the Asian monsoon system, the dieback of boreal forests, a deforestation threshold in the world's rainforests and large scale thawing of permafrost and the linked release of carbon di-oxide and methane (Hoegh-Guldberg et al., 2018). Due to our focus on Arctic amplification, we focus on the integration of permafrost as a factor in our model and will thus discuss it in more detail.

2.5.1 Permafrost

Recent estimates show that around 60% of the world's soil carbon is stored in the northern permafrost regions, with a total of about 1460-1600 GtC. Permafrost occurs in areas where the ground temperature rarely reaches above 0°C and cover around 18 million km^2, which accounts for about 15% of the global soil area. Most of this area is in the Northern Hemisphere, in areas such as Siberia, Northern Canada and the Tibetan Plateau. However, there is also permafrost on the Southern Hemisphere in, e.g., Antarctica. The surface permafrost carbon pool that is shallower than 3 meters is estimated to 1035 ± 150 GtC (95% CI). This estimate is about half

of the remaining Earth biomes, containing 2050 GtC, when not including the Arctic and Boreal regions (E. Schuur et al., 2015; E. A. G. Schuur, McGuire, Romanovsky, Schädel, & Mack, 2018).

These permafrost carbon pools have been accumulating over hundreds to thousands of years. However, due to the increasing air and soil temperatures in the Arctic and high latitudes, the permafrost is thawing, leading to an accelerating decomposition of the soils organic matter and increasing microbial respiration. These processes lead to increased emissions of GHGs such as CO_2 and CH_4 into the atmosphere. In the case of microbial respiration, which is known to occur in conditions as low as -20°C, estimates from Natali et al. show that it is the main contributor on the winter emissions of CO_2 (Lawrence, Koven, Swenson, Riley, & Slater, 2015; Natali et al., 2019).

With the Arctic amplification (Section 3.7), partial thawing of the 18 million km^2 of permafrost is inevitable. Thus, through increased warming, the seasonally thawed active layer will increase both its thickness and lead to changes in the hydrological state. However, emissions are also occurring from abrupt permafrost thaw through different processes such as thermokarst, in areas where there is excess ground ice. Where gradual thawing is a slower process that happens over periods from a couple of years to decades, abrupt thaw happens severely quicker over a period between a few days to years (E. A. G. Schuur et al., 2018).

Due to varying soil temperatures, the stability of the different permafrost zones will vary. Newer model estimates show that around 55% of the total permafrost region is continuous, with a classification that need a probability of presence in over 90% of a 1 km_2 area. In general, the most susceptible permafrost lies where the soil temperatures is warmer. However, because a single weather extreme can trigger abrupt thaw, it means that areas with a colder mean temperature still are vulnerable. The estimate of the mean annual ground temperature in the boundary point between the discontinuous and sporadic zones shows is -0.01 ± 0.37°C. In contrast, in between the sporadic and isolated zones, the estimate is 1.46 ± 0.44°C. If only considering the sporadic and isolated patches, they still account for about 34% of the estimated permafrost region (see Figure 2.7), underlining the vulnerability of the permafrost carbon pool (Obu et al., 2019).

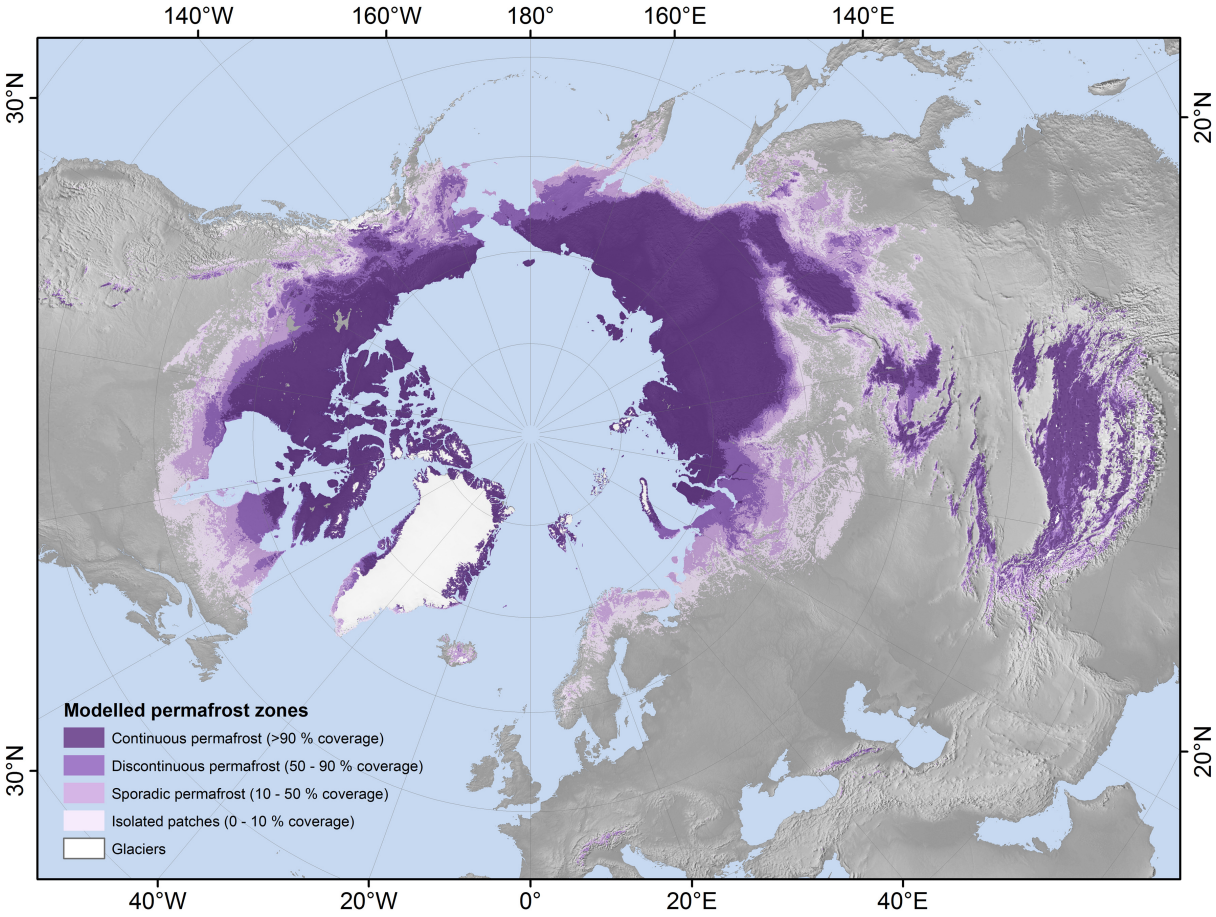

Figure 2.7: Estimated probability of permafrost zones in the Northern Hemisphere. The estimated permafrost distribution was based on the probability of modelled mean annual ground temperatures at the top of permafrost zones below 0°C for the period between 2000-2016. The zonal differences were classified through the modelled fraction of coverage of permafrost within a 1 km^2 area. Reproduced from (Obu et al., 2019).

At present date, estimates show that around 20% of the northern permafrost region is vulnerable to or has already experienced abrupt thaw. Most of these changes will likely happen, which in turn can lead to self-reinforcing feedbacks affecting about half of the total permafrost soil carbon through, e.g. increasing water depth, ground subsidence and erosion (Turetsky et al., 2020). A single weather extreme can trigger abrupt thaw, which with record-breaking temperatures the last decade (as discussed in Section 2.1) emphasises why abrupt thaw is already happening. The fear is that through these and other feedbacks, abrupt thaw can end up becoming more independent from the external climate factors. Indications that this might already be happening is visible through the increasing number of thermokarst lakes in the colder areas of the northern permafrost region (Lewkowicz & Way, 2019).

SROCC estimates show that by the year 2100 under an RCP2.6 scenario, there is at least a 90% probability that the near-surface permafrost area will decrease by 2-66%. This decrease leads to the release of vast amounts of soil carbon, with about 40-70% of the related forcing accountable to methane emissions. The estimates are uncertain, with emissions between ten to several hundred gigatons carbon for a conservative scenario of RCP2.6 (Meredith et al., 2019). With estimates from 2014 that there is 217±12 GtC (95% CI) located in just the top 30 cm of the surface soil carbon pools in the northern circumpolar permafrost region, it underlines the implications these potential emissions can have on the climate system as a whole (Hugelius et al., 2014).

With abrupt changes in thermokarst lake areas, there is, in general, low confidence in the ability to estimate the impact abrupt thaw will have on the regional permafrost and total permafrost region. It is found to be the central mechanism in rapid landscape change and hence a crucial part of permafrost estimates, emphasising the reason to research the area further (Kokelj, Lantz, Tunnicliffe, Segal, & Lacelle, 2017).

Increased frequency and area burned from forest-fires in the northern permafrost region are other, not frequently included factors that lead to the underestimating of the warming effect of permafrost. Some indications show future drying of the Arctic soil through changes in temperature and decreasing snow and permafrost cover, which seems to lead to a higher likelihood for forest fires (Meredith et al., 2019). A pulse disturbance such as forest fires can work as a feedback effect, further drying the soil and inducing more degradation of permafrost (Gibson et al., 2018).

Another uncertainty factor comes from excluding parts of the global permafrost such as the submerged permafrost in the East Siberian Sea, due to the uncertainty in quantification (E. Schuur et al., 2015). As of 2019, most CMIP5 models do not include a permafrost component at all, which is critical to improving the carbon cycle simulations for the Arctic, which underlines the possible estimate uncertainties and need to address them (Natali et al., 2019).

2.6 Iteration process in the non-linear framework

As a part of our research project, a non-linear forcing framework is implemented in the SRM. The non-linear forcing framework is constructed in such a manner, that any relation can be researched (detailed explanation in Section 3.6). The temperature response estimate in the non-linear forcing framework consists of a fixed-point iteration loop. The following section validates the iteration process for a linear model, including a non-linear forcing.

We start with a proof that validates the system when not including non-linear forcing, $F(t)$. Due to simplicity reasons, the following calculations is performed on a 1-box model on the form:

$$C\frac{dT}{dt} = -\lambda T + f(t).$$

Through the differential operator, $\mathcal{L}$, the equation can be rewritten as:

$$\mathcal{L}T = f(t). \tag{1}$$

Where $\mathcal{L} = C\, dT/dt + \lambda$. This leads the original equation to the following form:

$$(\mathcal{L}T)(t) = C\frac{dT}{dt} + \lambda T.$$

As long as the differential operator, $\mathcal{L}$, is a linear differential operator, any generic model such as an n-box or 1-box model is applicable. Hence, our climate models follow the form described in Equation 1. To solve this problem, a Green's function $\tilde{G}(t)$ is found on the form such that

$$\left(\mathcal{L}\tilde{G}\right)(t) = \delta(t),$$

Which leads to:

$$T(t) = \int_0^t \tilde{G}(t-s)\, f(s) ds.$$

Hence $T(t)$ is a solution to Equation 1. The proof of this solution's validity follows:

$$\begin{aligned}(\mathcal{L}T)(t) &= \mathcal{L}\int_0^t \tilde{G}(t-s)\, f(s) ds \\ &= \int_0^t (\mathcal{L}\tilde{G})(t-s)\, f(s) ds \\ &= \int_0^t \delta(t-s)\, f(s) ds \\ &= f(t).\end{aligned}$$

As briefly discussed in Section 3.2, it is worth noting that the Green's function $\widetilde{\mathrm{G}}(t)$, used in the greenhouse gas concentration estimates does not include the step-function, $\theta(t)$, while it in this proof does, where, $\widetilde{\mathrm{G}}(t) = G(t)\theta(t)$.

When including a non-linear forcing factor, $F(T)$, the system's equation follows the form:

$$\mathcal{L}T = f(t) + F(T) \tag{2}$$

This relation is solvable through a $T(t)$ given as,

$$T(t) = \int_0^t \tilde{G}(t-s)\big[f(s) + F\big(T(s)\big)\big]\, ds.$$

The proof follows:

$$(\mathcal{L}T)(t) = \mathcal{L}\int_0^t \tilde{G}(t-s)\,\big[f(s) + F\big(T(s)\big)\big] ds$$

$$= \int_0^t (\mathcal{L}\tilde{G})(t-s)\left[f(s) + F\big(T(s)\big)\right]ds$$

$$= \int_0^t \delta(t-s)\left[f(s) + F\big(T(s)\big)\right]ds$$

$$= f(t) + F\big(T(t)\big).$$

We then define an integral operator, $\mathcal{R}$, such that,

$$\mathcal{R}T = \int_0^t \tilde{\mathrm{G}}(t-s)\left[f(s) + F\big(T(s)\big)\right]ds.$$

Hence, through the relation $\mathcal{R}T$, Equation 2 is equivalent to Equation 3:

$$\mathcal{R}T = T \tag{3}$$

Where $\mathcal{R}T$ is solvable through fixed-point iteration:

$$T_{\mathrm{n}+1} = \mathcal{R}(T_{\mathrm{n}}).$$

In the SRM we check for convergence numerically. However, one can also check the convergence analytically even if it is not necessary in this case. The Contraction Mapping Principle is a theorem that states that the iterations of $\mathcal{R}(T_{\mathrm{n}})$ will converge if

$$\|\mathcal{R}(T) - \mathcal{R}(T')\| \leq c\|T - T'\|, \qquad \forall T, T'$$

For a constant, $c\epsilon(0,1)$. Hence, a c close to 0 leads to a rapid convergence. Here, $\|\cdot\|$ can be any norm for functions of T, e.g.,

$$\|T\| = \sup_{0\leq t\leq t_{\max}} \|T(t)\|.$$

2.7 Climate models

2.7.1 Energy balance models

Through simplifications of the Earth's radiative balance, one can still gain an understanding of the impacts on our climate system. By using simple climate models like energy balance models (EBMs) this can be done with simple, physical relations through a simple differential equation. Equation 4 describes the change in global storage of heat relative to the incoming and outgoing energy from the climate system, which in effect is the climate system's forcing:

$$C\frac{dT}{dt} = E_{\text{in}} - E_{\text{out}} = (1-\alpha)\frac{S_0}{4} - \varepsilon\sigma T^4. \tag{4}$$

The left-hand side of the equation represents the change in surface temperature. The global average heat capacity is denoted C, while E_{in} and E_{out} denotes the incoming and outgoing energy. Thus, the equation describes the radiative balance of the system. The only source of energy is the incoming solar radiation, represented with the solar constant S_0, the total solar irradiance per m^2. From the Sun's point of view, Earth is a disc. Thus, only a quarter is accessible to incoming solar energy. Only parts of this energy will reach the surface due to reflections back into space from, e.g. cloud cover, surface ice and the atmospheric composition, accounted to by the Earth's average co-albedo, $(1-\alpha)$, where the albedo, α is the factor of reflected energy. Most of the outgoing radiation from Earth is infrared. Thus the Earth is assumed to work as an adjusted black body to account for the greenhouse effect, with the factor for emissivity ε, a number between 0 and 1. The average amount of emitted energy per m^2 is represented using the Stefan-Boltzmann law, where σ is the Stefan-Boltzmann constant and T is the global mean surface temperature (Goosse, Barriat, Lefebvre, Loutre, & Zunz, 2010).

In an equilibrium where $C\frac{dT}{dt} = 0$, Equation 1 yields an estimated surface temperature as illustrated, in Equation 5:

$$T = \left(\frac{(1-\alpha)\frac{S_0}{4}}{\varepsilon\sigma}\right)^{\frac{1}{4}}. \tag{5}$$

This example is a zero-dimensional model, but energy balance models can, however, be of varying complexity. For instance with vertical layers in the atmosphere leading to a one-dimensional model, where each layer would interact with each other with different factors due to the composition in each atmospheric layer (Gettelman & Rood, 2016).

2.7.2 Reduced complexity models

As our understanding of the global carbon-cycle climate system has improved, more and more factors have been added to climate models. Some models are so complex that there exists a natural cap on the number of scenarios the models can run due to the runtime. The increasing number of factors also increases the number of uncertainties to the carbon budget estimates. Minimising these uncertainties is essential to improve the RCB. This can be done by going for a more scenario-based approach where reducing the model complexity decreases the runtime, which increases its capability of running a larger number of scenarios.

A possible approach is to use a reduced complexity model. The climate model MAGICC is one of the most used models of that complexity level. When comparing it to the very complex models ESMs in the CMIP5 model ensemble, it includes considerably fewer forcing factors. However, it still incorporates the essential gas- and carbon cycles, climate feedback-mechanisms and radiative forcing. As previously mentioned, the strength of these models lies in their flexibility, so they can mimic the more complexed models without compromising the geophysical relations. Since it can run a more substantial number of scenarios without using a supercomputer, it has become the baseline for less complex models and widely used. However, there is a shortage of different models in this category. This has led to MAGICC being used in such an extensive manner that it is hard to cross-check and validate the estimates. By focusing research on models in this category, one could considerably increase the ability to run scenarios and hence likely increase our understanding of the climate system (MAGICC, 2015; Wigley, 1995).

3 The Simple Response Model

This section describes the developed SRM, produced in a team effort as a part of our research project leading up to the master thesis. The research partners were Andreas Johansen, Andreas Rostrup Martinsen, Endre Falck Mentzoni and our supervisor Martin Rypdal. The following sub-sections describes and explains the process and results for each of the steps and components.

3.1 Emission scenarios

The emission scenarios used as input consists of anthropogenic emissions of CO_2 in the unit $GtCO_2$, given as $E(t)$. Our CO_2 emission scenarios consist of observed temperature data from a dataset from Boden, Marland, and Andres (2015), including data from 1751 until 2011, consisting of CO_2 emissions from fossil-fuel, burning, cement manufacture and gas-flaring. Given estimated global emissions of 37.1 $GtCO_2$ in 2018, we performed an interpolation on the dataset from 2011 to 2018 (Le Quéré et al., 2018). We then merged the historical emissions with emission scenarios from 86 of 127 different Shared Socioeconomic Pathways (SSP) made from IAMs, collected from the SSP database, as illustrated in Figure 3.1 (Riahi et al., 2017; Joeri Rogelj et al., 2018).

All of the discarded scenarios were exceedance scenarios with increasing emissions until 2100. To implement the other forcing factors, methane and aerosol emissions, we use the CO_2 emission scenario and convert it to their respective emissions using a scaling method. Multiplying the emissions with two different factors forces the emissions to match observed emissions in 2019 for both of the forcing factors. The emission scenario for methane is $E_{\mathrm{METHANE}}(t) = aE(t)$, while it for aerosol emissions is scaled by a different and much smaller factor, $E_{\mathrm{AERO}}(t) = bE(t)$. Both factors are assumed to be constants.

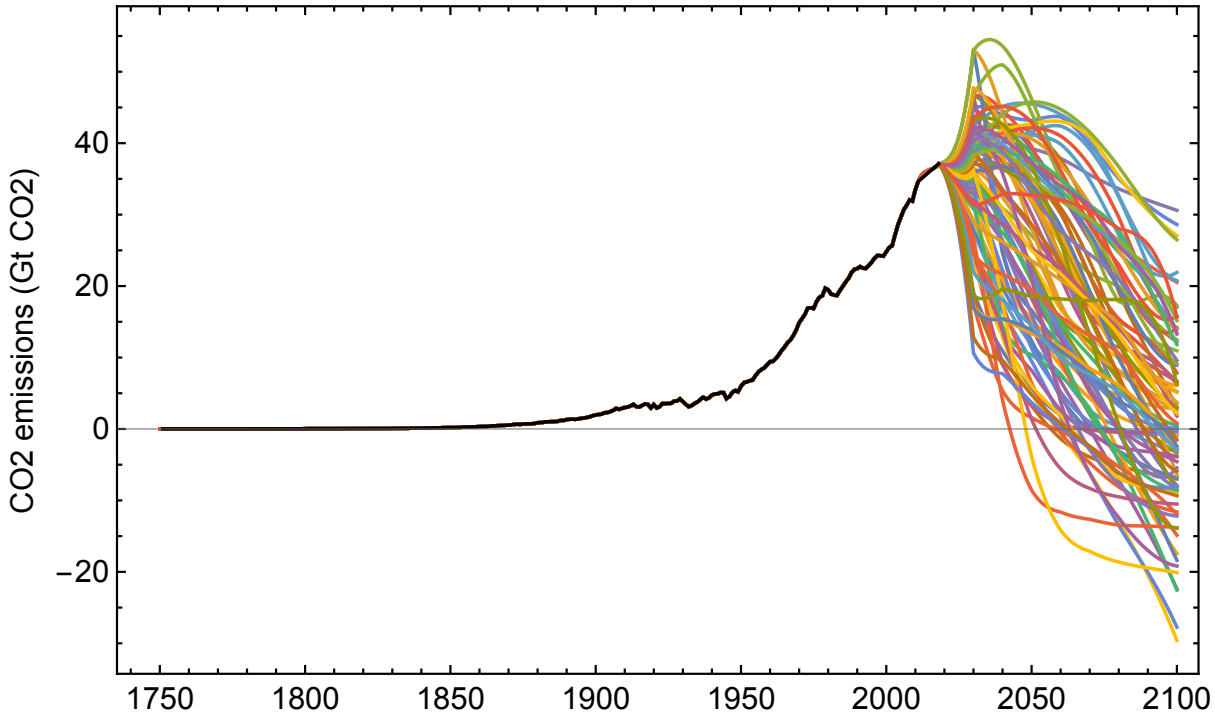

Figure 3.1: Shows the 86 emission scenarios used in our climate model. In the period from the year 1750 until 2018 the data is observed, global CO_2 emissions from fossil-fuel burning, cement manufacture and gas-flaring. From the year 2019 until 2100, the historical data merges with 86 different SSPs from IAMs, leading to a total of 81 different emission scenarios. Code to reproduce the plot is provided in Appendix C.

Since the 86 emission- (and thus forcing scenarios) are widely different (Figure 3.1), their respective temperature response will also vary substantially. In the same manner, the mitigation pathways for the different forcing factors will also likely be quite different. In the present situation with a BAU, the methane and aerosol emissions are directly proportional to the CO_2 emissions with factors a, and, b. Consequently, without any conditions to the relation, if carbon dioxide emissions became zero, so would the methane and aerosol emissions. That is, however, not true, since there are plenty of natural sources for methane emissions as, e.g. livestock and wetlands.

In the more optimistic emission scenarios, this relation would likely become a problem, where emissions also become net negative in the simulation. Hence, the relation can only persist until a certain emission threshold in a given scenario. An analysis of the relation between estimated global annual methane and carbon dioxide emissions from IAMs is illustrated in Figure 3.2 (see code in Appendix C (Johansen, 2020)).

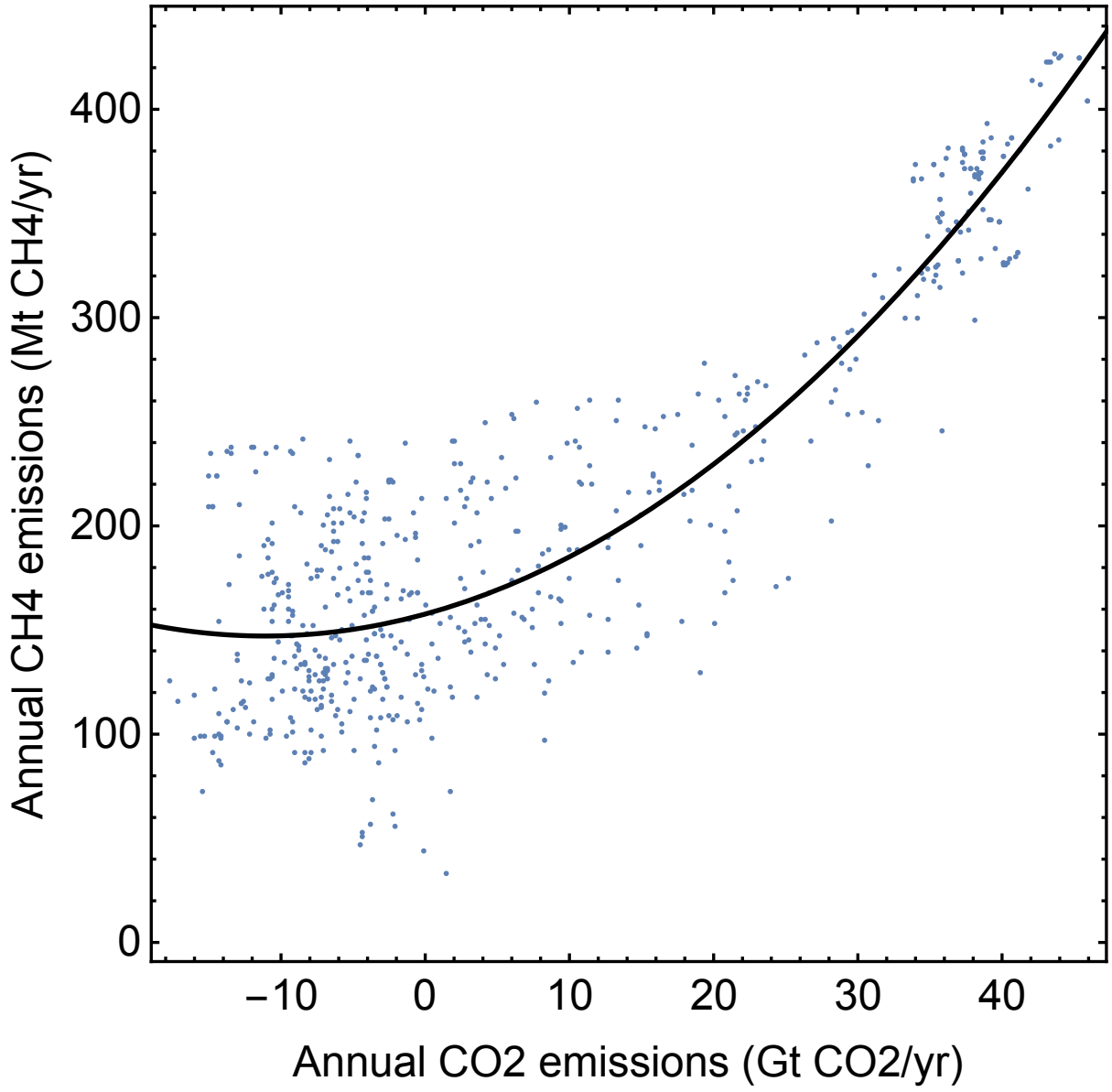

Figure 3.2: The relationship between global, annual CO_2- and CH_4 emissions per year estimated through IAMs. The scatterplot illustrates a relatively linear trend for CO_2 and CH_4 emissions between 30-50 Gt CO_2/yr, with a worsening linearity approximation for lower magnitudes. Produced plot with data from (Huppmann et al., 2018; J. Rogelj et al., 2018). Code to reproduce the plot is found in Appendix C.

The analysed data consists of different IAMs scenarios for annual, global emissions of CO_2 and CH_4 per year, between 2010-2100 (Huppmann et al., 2018; J. Rogelj et al., 2018). Figure 3.2 illustrates that if the CO_2 emissions decline towards zero and even go negative, the CH_4 emissions stall the decline and remain at a positive forcing rate of about 100-200 Mt CH_4/yr. Which also is the case for the scenarios in AR5. The scatterplot confirms the assumption about the natural sources of methane emissions. It also shows that a constant proportionality factor, a will stop being a good approximation at a point between 20-30 Gt CO_2/yr.

The same issues apply to anthropogenic aerosol emissions. There will likely always exist sources for emissions to occur such as through, e.g. the burning of biomass or sulphur dioxide (SO_2) from volcano emissions. Due to the already negative forcing, a lower emission rate would lead to a smaller negative magnitude (see Figure 3.3).

We have assumed an asymptotic behaviour when the forcing meets -0.4 W/m² as illustrated in Figure 3.3, which is relatively consistent to the best estimate of the direct aerosol effect of -0.35 W/m² in AR5. However, because of the more limited knowledge and level of accuracy for the measurements of the aerosol emissions, it is the most uncertain forcing factor in the model (Myhre et al., 2013).

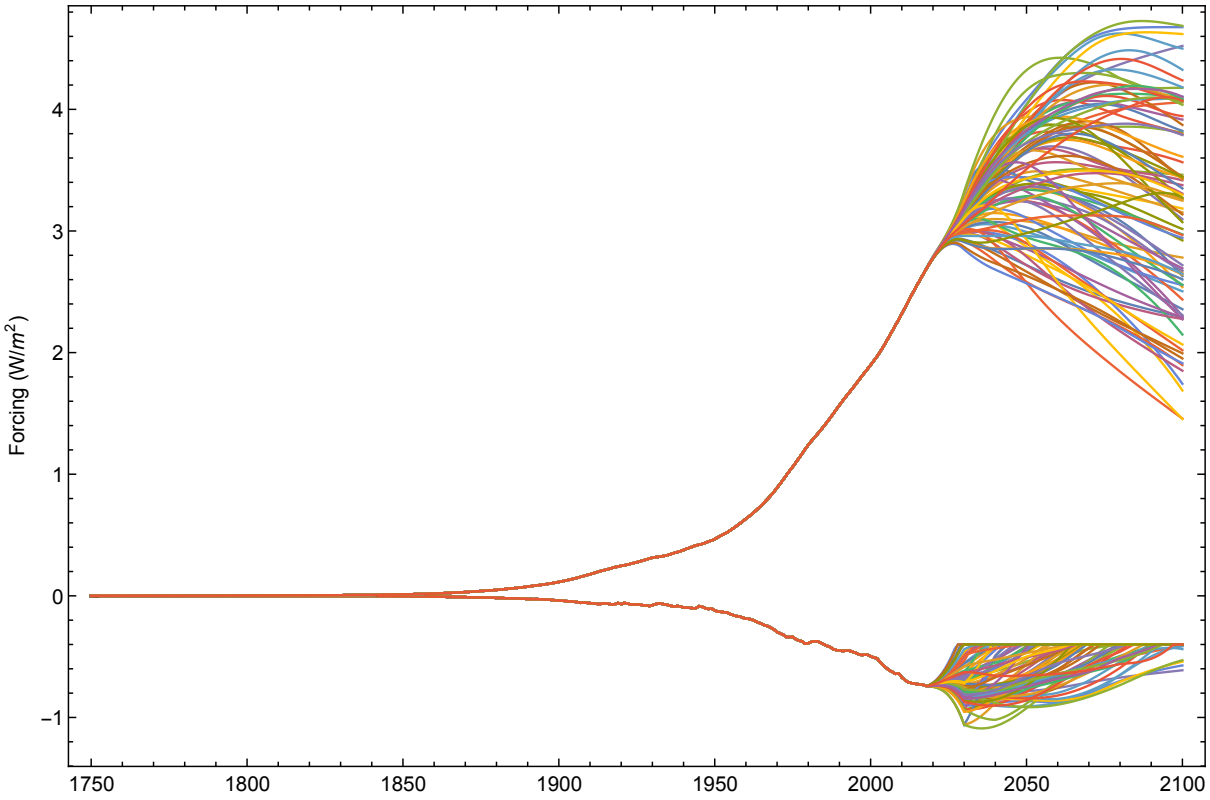

Figure 3.3: Simulation of the forcing from the 86 emission scenarios using our best estimate carbon model. The GHG forcing from CO_2 and CH_4 is denoted by the 86 pathways with positive forcing, while 86 pathways with a negative magnitude denotes the aerosol forcing. Each of the scenarios thus shows a pathway for both the combined GHG- and the aerosol forcing. The flat top illustrates the assumed asymptotic behaviour for the aerosol forcing of -0.4W/m². Code to reproduce the figure is found in Appendix C.

3.2 Concentration estimate

When the emission scenarios for the greenhouse gases are known, we can estimate the atmospheric concentration for the greenhouse gases, as shown in Equation 6 and 7. By using the pre-industrial atmospheric concentrations as a baseline, we integrate our carbon response model

and a given emission scenario from a baseline year to a specified year. The pre-industrial atmospheric concentration for carbon dioxide is 280 ppm (parts per million), while it for methane is 700 ppb (parts per billion). Factor u is a conversion factor that is either 44/12 or 1 if the emission scenario is given in GtC or $GtCO_2$, respectively:

$$[\mathrm{CO_2}] = 280\ \mathrm{ppm} + u\int_{-\infty}^{t} G_{\mathrm{CAR}}(t-s)E(s)ds \tag{6}$$

$$[\mathrm{CH_4}] = 700\ \mathrm{ppb} + u\int_{-\infty}^{t} G_{\mathrm{CAR-M}}(t-s)aE(s)ds. \tag{7}$$

The general carbon model, as illustrated in Equation 8, is an exponential response function that in this case, consists of four exponential functions with differing timescales, τ and a constant. In general, a Green's function also consists of a step-function, where $\widetilde{\mathrm{G}}(t) = G(t)\theta(t)$. The step-function is in our case is implemented in the SRM code, such that, e.g. Equation 8 is an approximated Green's function. The estimate of the constants c_1, c_2, c_3, c_4 and c_5 was done through mathematical approximation, as illustrated below. In contrast, the constant 0.47 is equivalent to the mean atmospheric change to a 100 GtC pulse from a background concentration of 389 ppm (Joos et al., 2013). The constant c_3 works as a constraint to force the sum of constants equal to 1, leading to $c_3 = 1 - c_1 - c_2 - c_4 - c_5$. The timescales are 1, 10, 100 and 1000 years and supposed to represent different components of the carbon-cycle system. Where, e.g. the thermohaline circulation in large part is represented through the slowest exponential function, compared to much more rapid parts of the carbon-cycle climate system represented through the shorter timescales like one year in our model:

$$G_{\mathrm{CAR}}(t) = 0.47\left(c_1 e^{-\frac{t}{\tau_1}} + c_2 e^{-\frac{t}{\tau_2}} + c_3 e^{-\frac{t}{\tau_3}} + c_4 e^{-\frac{t}{\tau_4}} + c_5\right). \tag{8}$$

The response function is obtained from a carbon pulse experiment with a magnitude of 100 GtC in an ESM. The actual carbon cycle in the ESM is a non-linear emission, but the exponential response function provides a linear approximation. Joos et al. (2013) performed a multi-model analysis to see the reaction of the different models to a 100 GtC carbon pulse to the present atmospheric background concentration at the time of 389 ppm. As illustrated in Figure 3.4, they estimated a multi-model mean from the different Earth System Models and the related ± 2 standard deviations.

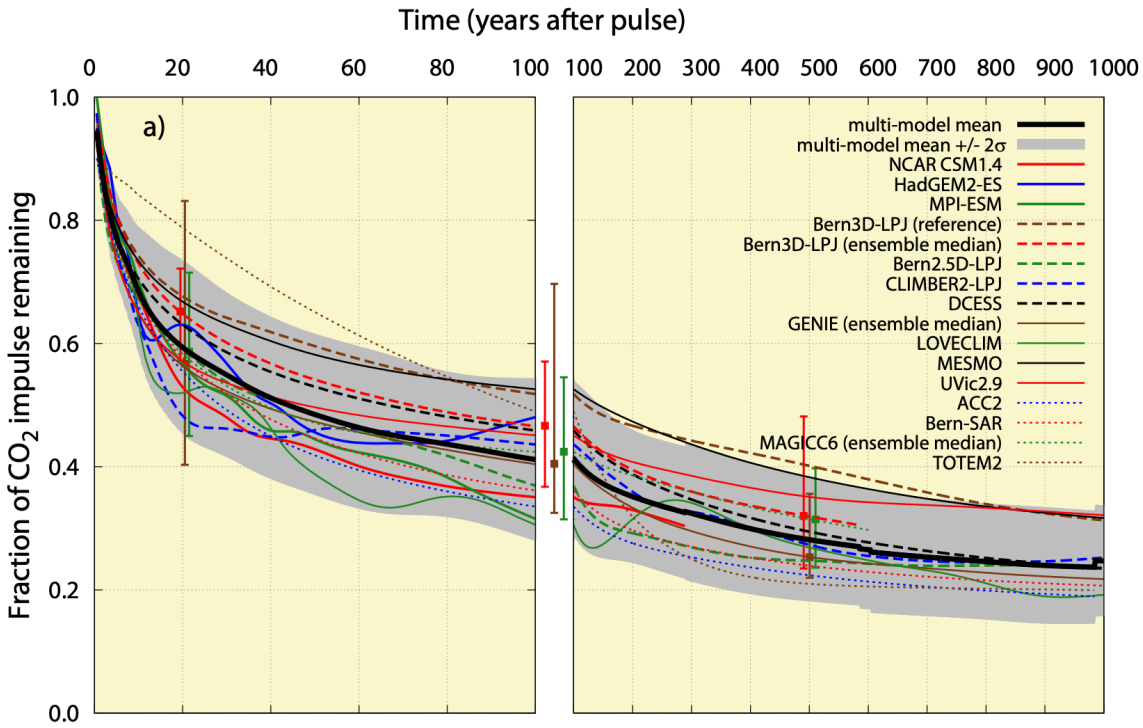

Figure 3.4: The impulse response function for the greenhouse gas CO_2 illustrated by the remainder of a 100 GtC emission pulse for 16 different models over 1000 years. The atmospheric baseline concentration of carbon dioxide was 389 ppm. The solid lines represent the ESMs, while thin solid and dashed lines illustrate Earth system Models with Intermediate Complexity (EMIC). Illustrated by the dotted lines, are the reduced complexity models. Each model had the same weight, leading to a multi-model mean. The multi-model mean was used to estimate the carbon model $G_{CAR\text{-}M}(t)$ in our research project, while a modification of the ± 2 standard deviations produced carbon model 2 and 3. The used code lies in the Appendix. Reproduced from (Joos et al., 2013).

We fitted our four exponential functions from Equation 8 to find the constants c_1, c_2, c_3, c_4 and c_5 for both the mean and ± 2 standard deviations. Afterwards, we halved it to ± 1 standard deviation to look at a narrower range. The fit to the mean became our best estimate carbon model, while ± 1 standard deviation is our carbon model alternatives as carbon model number 2 and 3. Table 1 presents the estimated parameters.

Since the methane lifetime is much shorter than the carbon dioxide lifetime, there needs to be a different carbon response model for the estimate of the CH_4 concentration. The best estimate of the total perturbation lifetime of methane was in AR5 estimated to be τ_m = 12.4 years (Myhre et al., 2013). Due to this, we made a methane carbon model that only consisted of one exponential function. The estimate of the factor c_m (see Table 1) is done by tuning exponential response function to the methane concentration of 1880 ppb in the year 2019, leading to $G_{CAR\text{-}M}(t)$ as shown in Equation 9:

$$G_{\mathrm{CAR-M}}(t) = c_{\mathrm{m}} e^{-\frac{t}{\tau_{\mathrm{m}}}}. \quad (9)$$

Table 1: Summary of estimated parameters for the produced SRM carbon models. The column, Carbon response model denotes the four different carbon response models, with the best estimate, ± 1 standard deviation (σ) and the methane carbon response models. The implementation of the parameters c_1, c_2, c_3, c_4 and c_5 takes place through Equation 8. Parameter c_m tunes the methane concentration to a 2019 concentration of 1880 ppb.

Carbon response model	c_1	c_2	c_3	c_4	c_5	c_{m}
-1σ	0.180	0.296	0.254	0.122	0.148	
Best estimate	0.152	0.246	0.274	0.134	0.194	
+1σ	0.110	0.212	0.310	0.106	0.262	
Methane						0.34

3.3 Forcing estimates

In the case of aerosol concentrations, we made a qualified assumption that due to the short lifetime of aerosols in the scale of days, the concentration of aerosols is in general proportional to the emissions of anthropogenic aerosols into the atmosphere. Thus, the anthropogenic radiative forcing from aerosols is also proportional to the aerosol emission scenario, as shown in Equation 10:

$$F_{\mathrm{AERO}}(t) \propto [Aerosol] \propto E_{\mathrm{AERO}}(t) = bE(t). \quad (10)$$

When it comes to the two GHGs, the anthropogenic radiative forcing is computed using well-known relations from the literature. Equation 11 shows the estimate of the CO2 forcing (Myhre, Highwood, Shine, & Stordal, 1998). The estimated concentration is denoted as $[\mathrm{CO}_2]$, where 280 ppm is the pre-industrial revolution baseline concentration:

$$F_{\mathrm{CO}_2} = (5.35\ \mathrm{Wm}^{-2}) \ln\left(1 + \frac{[\mathrm{CO}_2] - 280\ \mathrm{ppm}}{280\ \mathrm{ppm}}\right). \quad (11)$$

The calculation of the radiative forcing from anthropogenic emissions of methane uses a power-law relation, as shown in Equation 12 (Myhre et al., 1998). The estimated concentration is as

previously denoted as $[CH_4]$, 700 ppb is the pre-industrial revolution baseline concentration while the constant p, incorporates the potency of methane as a greenhouse gas:

$$F_{CH_4} = p\left(\sqrt{[CH_4]} - \sqrt{700\ \text{ppb}}\right). \tag{12}$$

The total anthropogenic radiative forcing from the three included forcing agents are then assembled to one collected forcing factor, as shown in Figure A.3 and Equation 13:

$$F_{TOT}(t) = F_{CO_2}(t) + F_{CH_4}(t) + F_{AERO}(t). \tag{13}$$

3.4 Temperature response function

To estimate the temperature response for a given climate model we calculate it in a similar way as for the estimate of the concentrations, by convolving the climate models exponential response function and the estimated forcing scenario as shown in Equation 14:

$$T(t) = \int_{-\infty}^{t} G_{CLI}(t-s)F_{TOT}(s)ds. \tag{14}$$

The climate model consists of a similar framework as the carbon response model, with an exponential response function. For the research project, we included 14 of the ESMs in CMIP5 model ensemble, where CNRM-CM5 and IPSL-CM5A-LR (Figure A.4 shows included ESMs) were considered irrelevant due to our focus on avoidance and overshoot carbon budgets (see Section 2.4.4). The constants and timescales for each of the CMIP5 ESMs use the parameters as advised in (Cummins, Stephenson, & Stott, 2020). These parameters were estimated using multi-box energy-balance models fitted to 4×CO_2-runs for each of the selected models CMIP5 ensemble. The resulting climate model framework is thus 14 ESM emulators through their parameters, executed through Equation 14. As illustrated in Figure A.4, the simulated temperature response for a given scenario widely differs for each of the 14 ESMs from CMIP5. This uncertainty underlines the reason to construct the RCB framework discussed in Section 3.5 with varying carbon and climate models. Figure 3.5 illustrates the estimated temperature response for each of the 86 emissions scenarios using a single CMIP5 ESM.

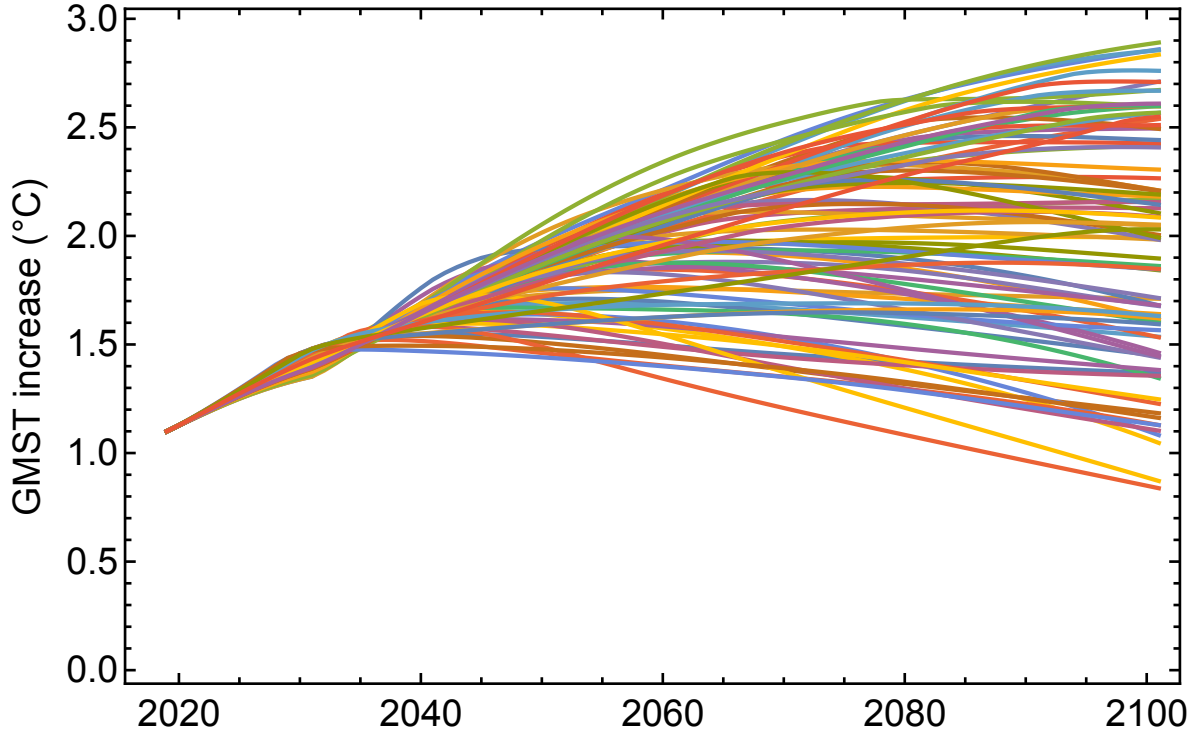

Figure 3.5: The estimated temperature responses for the SRM for each of the 86 emission scenarios. Time is on the first axis (in years), and the associated temperature response on the second axis. The plot is reproducible through code in Appendix C.

3.5 Estimating the RCB

Each of the 14 included CMIP5 ESMs estimated different temperature responses for given scenarios, as illustrated in Figure A.4. As previously mentioned, each of the model combinations with, e.g. our best estimate carbon response model, grant a particular TCRE relation when looking at the temperature responses of scenarios with widely varying magnitudes. The TCRE's can differ considerably, as illustrated in Figure 2.2, where we looked at CO_2-only TCRE's for observed temperature data and the best estimate using the CMIP5 model ensemble. Thus, to do a thorough analysis of the impact each different model has on the RCB, a systematic review of their impacts on these estimates is needed. Since climate budgets are the main instrument for the guiding of climate policies around the world (as mentioned in Section 2.4), these estimates should be as accurate and understandable as possible.

3.5.1 Likelihood estimate

By assigning likelihoods to the estimated carbon budgets for a linked temperature target, it becomes simpler for policymakers and politicians to make more qualified decisions for future mitigation policies. As previously mentioned, it will with a small conceptual climate model, such as our SRM be significantly easier to process a higher number of scenarios. The simplicity and lower computing times enable the opportunity to more effortlessly compare the resulting temperature response for many different carbon and climate models.

As illustrated in Figure 3.1, the most optimistic scenarios end up with net negative emissions, and some of them do so for several decades until 2100. To be able to go to negative emissions of CO_2, the technology development in areas such as CCS has to thrive in such a manner that what is now relatively successful in small scale, is scalable to large-scale (J. Rogelj et al., 2018). To account for the possibility that the technology does not reach its theoretical potential in time, we have as a precaution for our simulations removed the scenarios that turn net negative from the simulation.

In the same way, as technology development incorporates uncertainty to carbon budget estimates, so does human mitigation choices and the possible errors in the models themselves. Hence, by systematically looking at the impact the different carbon and climate models has on the RCB for a temperature target, one can account for a more comprehensive rundown of the included uncertainties.

Assigning a likelihood to carbon budgets was a goal of the research project. In IPCC's AR5, the assumption was a normal distribution (J. Rogelj et al., 2018; Stocker et al., 2013), however recent studies have found that a log-normal distribution of the TCRE might be the case (Millar et al., 2018). Since there is still no broad consensus on a log-normal distribution, a normal distribution of the TCRE was assumed.

Since our interest lies in the risk of reaching higher temperatures, we use maximum temperatures when estimating the TCRE's due to its link with the RCB estimate (see code in Appendix

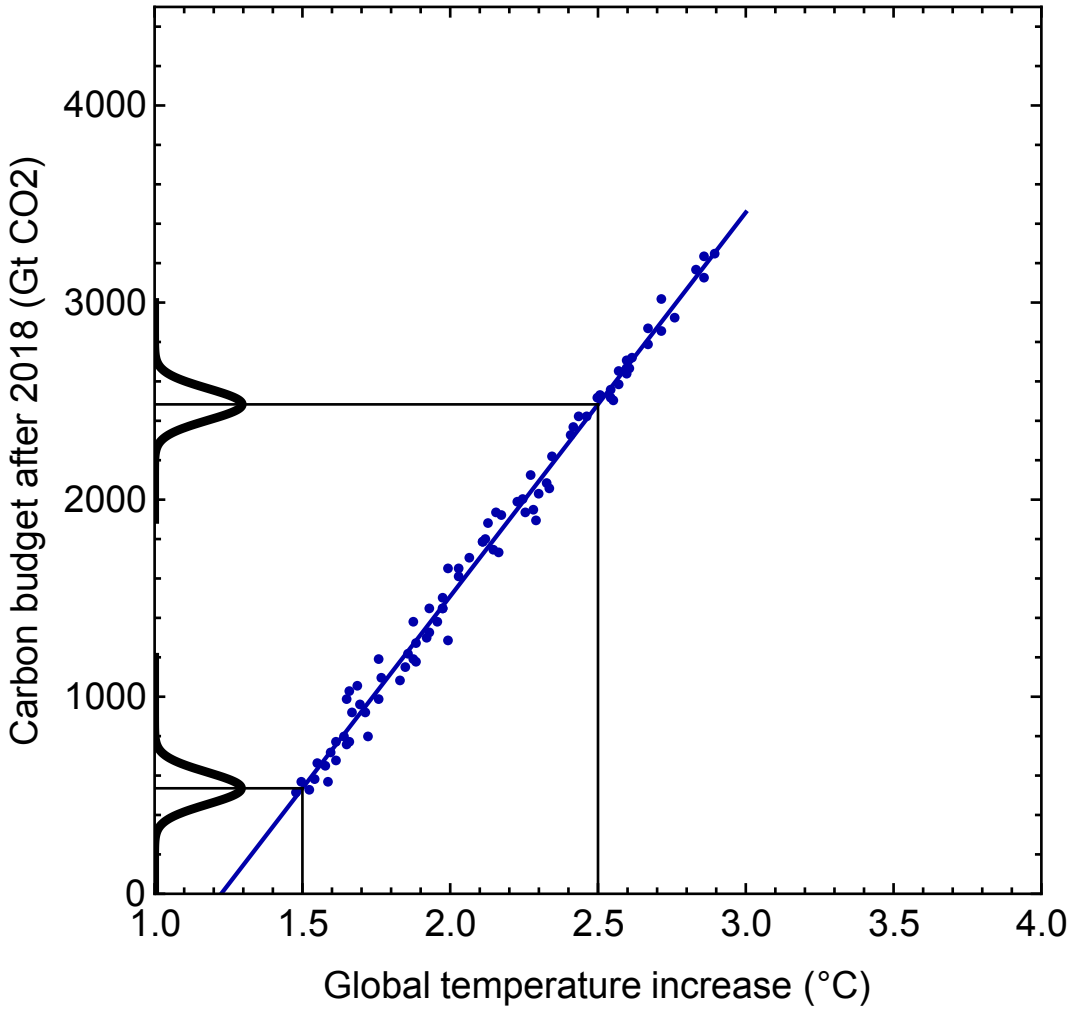

Figure 3.6: Plot of the TCRE for a single climate model and our best-estimate carbon model. Each dot is an emission scenario. The pdfs on the y-axis show the probability distributions for the RCBs for temperature targets of 1.5°C and 2.5°C. Code to reproduce the plot is provided in Appendix C.

C). Figure 3.6 illustrates the remaining positive emission pathways with their estimated maximum temperature, associated carbon budget and probability distribution for given temperature targets, through estimating with a single climate- and our best estimate carbon response model.

The carbon budgets appear to have an approximately linear relation to the temperature response for a single carbon and climate model. Thus, the linearity assumption for the TCRE seems to be valid for this simulation. The calculation of the probability density function illustrated on the y-axis in Figure 3.6 was done in the same manner as in the paper by Cox, Huntingford, and Williamson (2018).

By systematically changing the model combinations, we produced likelihood plots for the RCBs between 200-4000 GtC with steps of 100 GtC, for a temperature target between 1.0-

4.0°C with steps of 0.01°C, as illustrated in Figure 3.7. By estimating the likelihoods with combinations of the 14 different ESM's from the CMIP5 ensemble, our best estimate and ±1 standard deviation carbon models and an added internal variability illustrate the uncertainty in the carbon budget estimates well. In general, it is worth noting that the higher the RCB, the higher the uncertainty becomes as demonstrated by the heteroscedastic nature of the likelihood lines in Figure 3.7(a,d).

In Figure 3.7(a) the likelihood simulation for the RCBs is run with our best estimate carbon model $G_{\text{CAR-M}}(t)$, and each of the included 14 earth system models in the CMIP5 model ensemble. The plot illustrates that for lower temperature targets, the uncertainty is lower, while it for higher temperature targets increases.

In Figure 3.7(b) the simulation was done with a mean of the 14 ESM's from CMIP5 and the ±1 standard deviation carbon models estimated in Section 3.2. The narrow uncertainty range in comparison to Figure 3.7(a), makes it clear that the uncertainty does not come from our constructed carbon models.

We then added internal variability to emulate seasonal variabilities in the temperature response. The implementation involved adding a forcing as an additive white Gaussian noise with a variance of 1 and scaling it to the estimated temperature response for each of the 86 emission scenarios in the CMIP5 models. Through scaling the temperature output to the internal variance in the 14 earth system models from CMIP5, we emulate the short-term temperature variation. Our interest lies in the decadal trends, thus to remove the noise from more considerable temperature variations, a simple moving average with a sample window of 10 was added. Figure A.2 illustrates the estimated seasonal temperature variations.

The inclusion of the internal variability to the RCB estimate when including our best estimate carbon model and the mean of the 14 included ESM's from the CMIP5 model ensemble exhibited a linear trend. As assumed and illustrated in Figure 3.7(c), the internal variability has little impact on the estimate of the RCB, with an approximately linear relation as a TCRE. This plot underlines that the uncertainty lies in the spread between ESMs. Hence, in the process in Equation 14, where we convolve the forcing scenarios with the exponential response functions for the CMIP5 models.

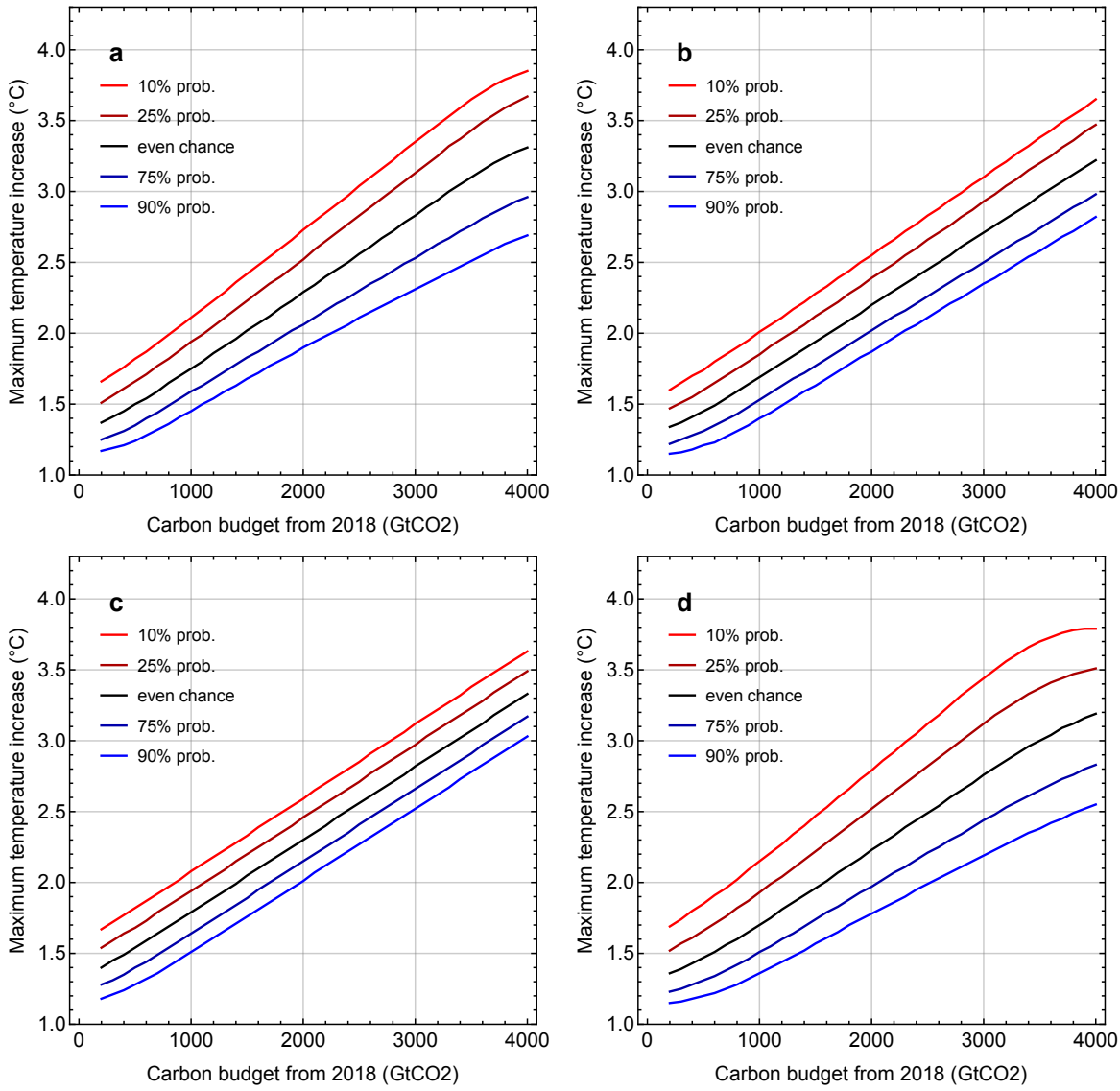

Figure 3.7: Likelihood plots for the RCB for a continuum of temperature targets. **(a)** Using our best estimate carbon model, and the 14 emulators of ESMs from the CMIP5 ensemble. **(b)** Using our ±1 standard deviation carbon models and the mean of the 14 ESM emulators. **(c)** Using our best estimate carbon model, the mean of the 14 ESM emulators and added internal variability. **(d)** Taking combinations of both the ±1 standard deviation carbon models, all of the 14 ESM's and the internal variability. The probabilities are as indicated in the figure legends, where there is, e.g. a 90% probability that a temperature response will stay below the blue line for a given carbon budget. The temperature targets range from 1.0-4.0°C. Code to reproduce the figure is provided in Appendix C.

When combining both of our ±1 standard deviation carbon models, all of the chosen CMIP5 ESM emulators and the added internal variability we see in Figure 3.7(d), that the uncertainty in the estimate increases drastically. This gives a broader, and heavier-tailed probability distribution which is indicated by, in general, both a higher maximum and minimum estimate of the temperature response for a range of carbon budget sizes when comparing Figure 3.7(d) to Figure 3.7(a).

The main result from this likelihood estimate is that through including all of the model combinations and internal variability, the risk of higher temperature responses increases for almost the entirety of the carbon budget range. As illustrated in Figure 3.7(d), we also see a lowered 90% probability line, which underlines the considerable increase in uncertainty for both higher and lower temperature responses. Estimates from SR15 state that an RCB of 580 GtCO2 and 420 GtCO2 to limit warming to 1.5°C gives a probability of 50% and 66%, respectively (IPCC, 2018). Figure 3.7(d) illustrates that the SRM is consistent with the SR15 estimates. Through varying the models, we even out the different climate sensitivities from the CMIP5 climate models, which illustrated through the TCRE's in Figure A.5 and Figure B.1, can be quite considerable.

3.6 Non-linear forcing framework

Our SRM does not include any non-linear effects, feedback-mechanisms or potential tipping points. To expand the complexity of the SRM, we wanted to construct a simple framework in the RCB estimate that could add non-linear forcing through both linear and non-linear equations, as illustrated through a generic relation in Figure 3.8. Since the whole notion of an RCB depends on the concept of an approximately linear relationship in a TCRE, this non-linear forcing cannot be too prominent in comparison to the linear part, too continue to overhold the linearity assumption. As an assumption, we started with an extension of the temperature response in Equation 14, where we include a non-linear forcing factor, $\tilde{F}(T)$ that depends on the global mean surface temperature, T, as illustrated in Equation 15:

$$T(t) = \int_{-\infty}^{t} G_{\mathrm{CLI}}(t-s)\left(F_{\mathrm{TOT}}(s) + \tilde{F}(T)\right) ds. \tag{15}$$

Through fixed-point iteration, we can illustrate that the non-linear forcing cannot be too prominent. First, we need to translate Equation 15 to vector form, as shown in Equation 13:

$$\underline{T}_{\mathrm{n}}(s) = G\left(\underline{F}_{\mathrm{TOT}}(s) + \underline{\tilde{F}}(\underline{T}_{n-1})\right). \tag{16}$$

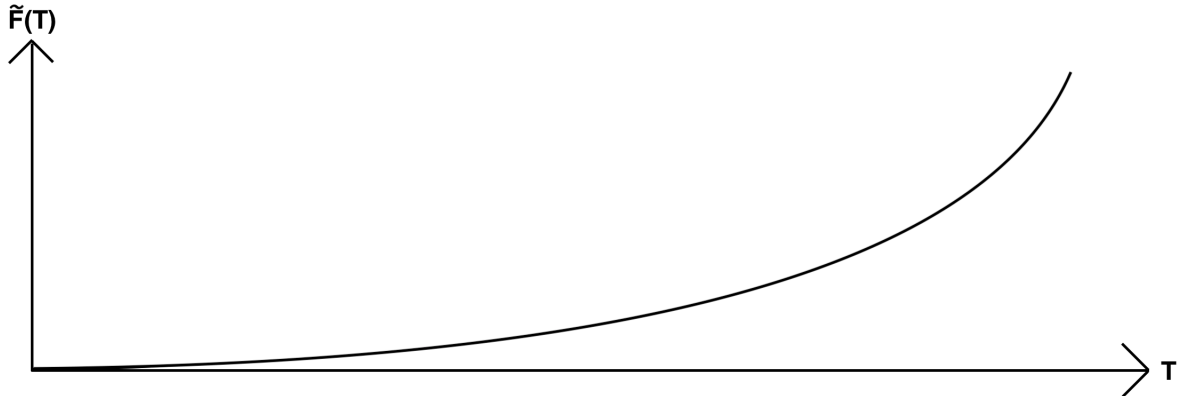

Figure 3.8: Illustration of a hypothetical non-linear temperature-dependent forcing, i.e. the forcing is directly dependent on the temperature. The temperature is given on the x-axis, while the temperature-dependent non-linear forcing, $\tilde{F}(T)$ is shown on the y-axis.

Thus, the only way for the approximately linearity assumption to still hold is through treating $\underline{\tilde{F}}(T)$ as a constant. Which only is true if the rate of change is slow compared to $\underline{F}_{\mathrm{TOT}}(s)$, and hence leading to a non-linearity of a relatively small magnitude, as illustrated in Equation 17 and 18:

$$\underline{T}_{\mathrm{n+1}}(s) = G\big(\underline{F}_{\mathrm{TOT}}(s) + \underline{\tilde{F}}(\underline{T}_n)\big) \tag{17}$$

$$\underline{T}_{\mathrm{n+1}}(s) - \underline{T}_{\mathrm{n}}(s) = G\left(\underline{F}_{\mathrm{TOT}}(s) + \underline{\tilde{F}}(\underline{T}_n)\right) - \underline{T}_{\mathrm{n}}(\mathrm{s}) = \mathrm{G}\left(\underline{\tilde{F}}(\underline{T}_n) - \underline{\tilde{F}}(\underline{T}_{n-1})\right). \tag{18}$$

The implementation of the non-linear forcing comes through a fixed-point iteration loop with a specific number of iterations inside the temperature response estimates (for details, see Section 2.6 and code in Appendix C). The construction of the non-linear framework is flexible, such that one can test any hypothetical equation for accounting for a collected or specific non-linear forcing effect or feedback mechanism. In this research project, we focused on the non-linear forcing effect from GHG emissions from warming of wetlands and permafrost thaw due to the Arctic amplification factor as a part of Andreas Johansen's thesis (Johansen, 2020). However, since there is no broad consensus for any specific relation for the added non-linear forcing effect from permafrost emissions, we looked at a relatively likely scenario with a hyperbolic tangent relation. We also tested a linear relation to show that any generic equation can apply non-linear forcing.

We started the analysis by looking at TCRE's for all the examined forcing equations summarised in Table B.1 in the Appendix. With a magnitude of 2 W/m^2 some of the computations led

to broken linearity assumptions, as illustrated in Figure A.24. In one of the cases, the forcing was so significant that it practically removed the difference between the two climate models TCRE's, as shown in Figure A.23, which led to the discarding of both Equation B6 and B7 from Table B.1.

With a higher temperature threshold of 3°C, the linearity assumptions became increasingly poor. The worsening most likely happens due to our focus on overshoot- and avoidance emission scenarios where e.g. several of the scenarios never reach as much as 2°C warming above pre-industrial levels (1850-1900). Each of the different CMIP5 ESM emulators exhibits a differing forcing sensitivity, leading to very different TCRE estimates as illustrated in Figure 3.9(a).

The CSIRO model appears to be more sensitive to forcing, leading to temperature responses far above 3°C, which in effect induces a convex trend since it for the more aggressive scenarios generate higher temperature responses. On the other hand, for the more conservative scenarios, the non-linear forcing effect is essentially absent, which leads to a lower temperature response. The explanation reverses for the GFDL model. With what seems to be a smaller forcing sensitivity, none of the scenarios meets the temperature threshold of 3°C, thus leading to a concave trend. Since none of the deviating scenarios has high residuals or leverage, they do not have a substantial influence on the TCRE. Still, however, it does impact the RCB estimate, leading to large uncertainties as illustrated in Figure 3.9(b).

We also found that changing the number of iterations between 5 and 50 had a minimal impact on the estimated RCBs for the different equations, illustrated with appendix Figure A.29. To force an impact, we had to use one of the hyperbolic tangent equations with a magnitude of 2 W/m^2, Equation B5 from Table B.1.

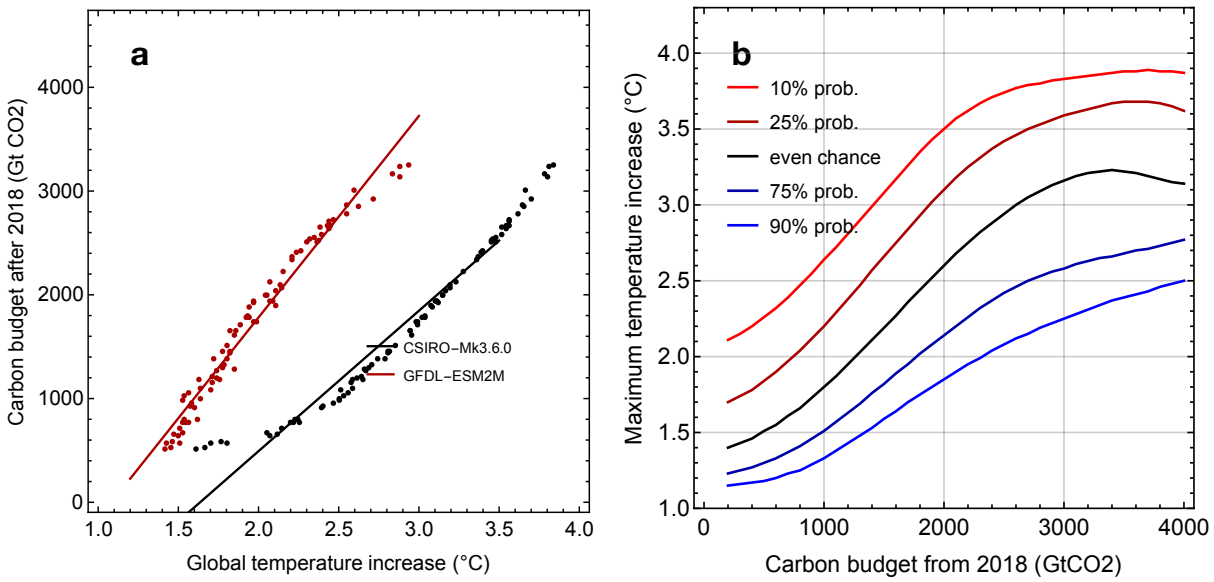

Figure 3.9: The effect of non-linear temperature-dependent forcing on our RCB estimates (using Equation B3). **(a)** The TCRE for two (emulators of) climate models in the CMIP5 model ensemble, and our best estimate carbon model. Each dot is one of the 86 emission scenarios. **(b)** Likelihood plots for the estimated RCB using combinations of both the ±1 standard deviation carbon models, all of the 14 ESM's from the CMIP5 ensemble and the internal variability. The probabilities are as indicated in the figure legends, where there is, e.g. a 90% probability that a temperature response will stay below the blue line given a distinct carbon budget. The temperature targets range from 1.0-4.0°C. Code to reproduce the plot is provided in Appendix C.

According to findings in SR15, there is a greater risk of passing through tipping points when scenarios exceed a maximum temperature of 1.5°C. Several tipping points are estimated to be impacted dramatically in this temperature area. An example of this is the GIS that has an existing and well-documented instability with a best estimate of 1.6°C (95% CI: 0.8-3.2°C) (Hoegh-Guldberg et al., 2018; Robinson, Calov, & Ganopolski, 2012). Thus, in line with our conservative line of assumptions, we made a "best guess" equation with a lower temperature threshold of 2°C. Figure 3.10 illustrates the RCBs using Equation B1 from Table B.1 and the linear SRM (see Appendix A for more plots for Equation B1). Other complementary plots and the produced plots from examined equations such as Equation B10 from Table B.1 are found in Appendix A.

Including the non-linear forcing effect impacts the RCB estimate in comparison to the linear SRM. With a feasible RCB of 600 $GtCO_2$, corresponding to limiting warming in line with the 2°C target of the Paris accord, the 10% and 90% probability line increase about 0.6°C and 0.15°C, respectively. Once again, this underlines the dramatic consequences using traditional RCBs that does not include a linked likelihood can have on the result for Earth's climate.

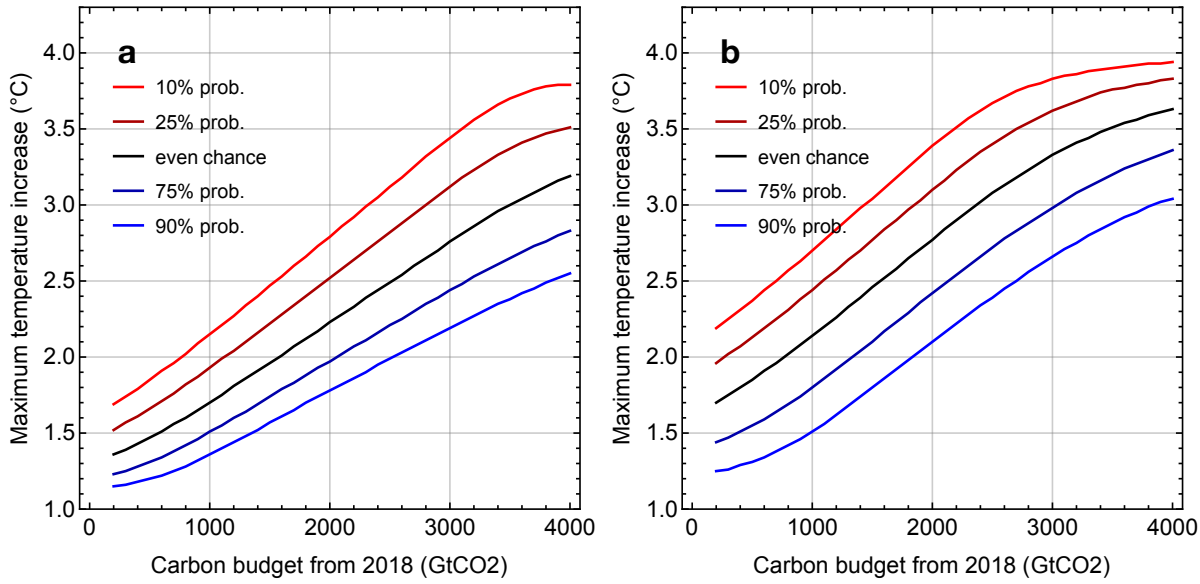

Figure 3.10: Likelihood plots for estimated RCBs given a mitigation target. Both plots were produced using combinations of both the ±1 standard deviation carbon models, all of the 14 ESM's and the internal variability. **(a)** The RCB estimate using the linear SRM, found in Figure 3.7(d). **(b)** The RCB estimate for the SRM, including the non-linear temperature-dependent forcing according to Equation B1 (Table B.1). Illustration of the probabilities is in the figure legends, where there is, e.g. a 90% probability that a temperature response will stay below the blue line given a distinct carbon budget. The temperature targets range from 1.0-4.0°C. Code to reproduce the figure is provided in the Appendix.

3.7 Arctic amplification

Another part of our collaborative research project was to estimate the temperature response in the Arctic region in comparison to a global GMST. A standard way to do this is through analysing the Arctic amplification factor, which is an estimate of the rate of change in Arctic temperatures compared to typically global temperatures (Dai et al., 2019).

(Johansen, 2020) took a look at how to implement this issue into our SRM. Through using the dataset of observed global annual mean surface temperatures and Arctic annual mean temperatures, a linear best fit was estimated, finding the equation for the Arctic amplification factor on the form $T_{\mathrm{ARC}} = v + w \times T_{\mathrm{GLO}}$, leading to Equation 19 (Lenssen et al., 2019; Team, 2020):

$$T_{\mathrm{ARC}} = 0.100 + 2.23 \times T_{\mathrm{GLO}}. \qquad (19)$$

T_{ARC} denotes the Arctic temperature anomaly, T_{GLO} denotes the global temperature anomaly, while v and w were estimated to be 0.100 and 2.23, respectively (See illustration in Figure A.30 and estimation in Appendix C).

After estimating the Arctic amplification factor, the estimate of a linked Arctic RCB followed the same manner as in Section 3.5.1. If we aim to stay below global warming of a 2°C GMST increase in relation on pre-industrial levels, a global RCB of 600 $GtCO_2$ could be the target as illustrated in Figure 3.7(d). Regional temperature responses in the Arctic will be different due to the Arctic amplification factor, thus increasing the likeliness of very severe temperature responses.

Figure 3.11 illustrates the dramatic effect the Arctic amplification factor has on the estimated temperature response. For a global RCB of 600 $GtCO_2$, the linked temperature response for the 50% probability line increases by approximately 2°C, from around 1.6°C to 3.5°C. These extreme regional temperature responses could induce tipping points such as the abrupt thaw of permafrost, and other Arctic regional tipping point leading to a possible feedback loop. Findings in SR15 does, however, show that there is about a 50% chance that warming to a GMST of 2°C would not be sufficient to reach a permafrost tipping point. However, a GMST increase of 3°C could reach a tipping point through soil warming, leading to a change in the hydrological state of the permafrost (Hoegh-Guldberg et al., 2018). The fulfilment of these conditions might happen when considering extreme weather events in record-breaking years or through, e.g. forest fires, possibly leading to local tipping point events.

Figure 3.11(b) also shows that there with a 90% probability for a 200 $GtCO_2$ RCB estimates a temperature anomaly compared to the pre-industrial revolution of around 2.7°C. This estimate is also backed up by the estimated temperature between 64°N-90°N in 2019 of 2.71°C (Lenssen et al., 2019; Team, 2020).

By combining the result from the non-linear effects from Section 3.6, we assumed that the estimated temperature response would worsen when including the Arctic amplification factor but were unsure about the magnitude.

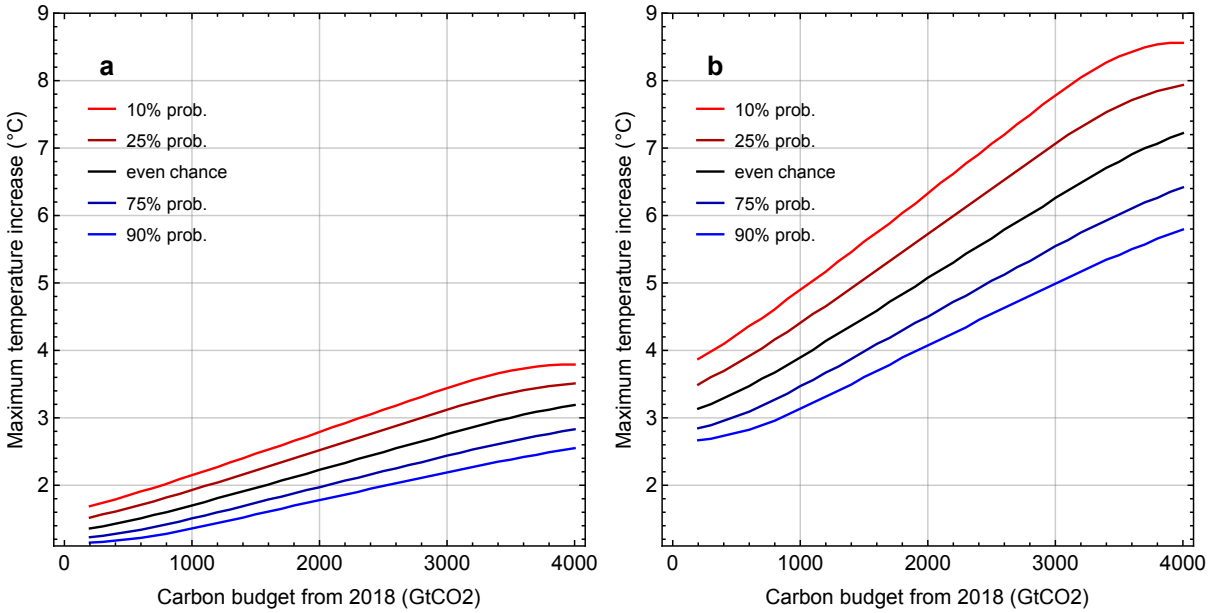

Figure 3.11: The estimated RCBs given a temperature target, ranging from 0.0-9.0°C. The estimates use combinations of both the ±1 standard deviation carbon models, all of the 14 ESM's and the internal variability. **(a)** is the same plot as in Figure 3.7(d), while **(b)** includes the Arctic amplification factor from equation 16. The figure legend indicate the probabilities associated with each coloured curve, where there is, e.g. a 90% probability that a temperature response will be on the blue line given a distinct carbon budget. Reproducible through code found in Appendix C (Johansen, 2020).

The implementation of non-linear forcing resulted in a widening of the likelihood plots with generally, higher estimated temperatures. Johansen (2020) looked at our "best guess" for the non-linear forcing effect, Equation B1 and an additional relation in Equation B10. Figure 3.12 illustrates that the non-linear effect on the estimate of the Arctic amplification factor RCBs, show the same, widening trend mentioned above, indicated primarily through increasing temperature responses in the upper bounds as indicated by the red 10% probability line.

When considering the more moderate non-linear forcing effect from Equation B10, there are apparent differences, as illustrated in Figure 3.12(c). Using the example global RCB of 600 $GtCO_2$, the temperature responses for the 50% and 10% probability line, increases from around 3.5°C and 4.4°C to 3.7°C and 4.9°C, respectively. These somewhat small differences can have drastic results when considering different Arctic tipping points. As illustrated in Figure 3.12(b), a more considerable non-linear forcing effect from Equation B1 will dramatically worsen the estimated temperature response. The 50% likelihood line indicates an increase of 0.9°C, to 4.4°C in comparison to the non-linear Arctic RCB of 600 $GtCO_2$.

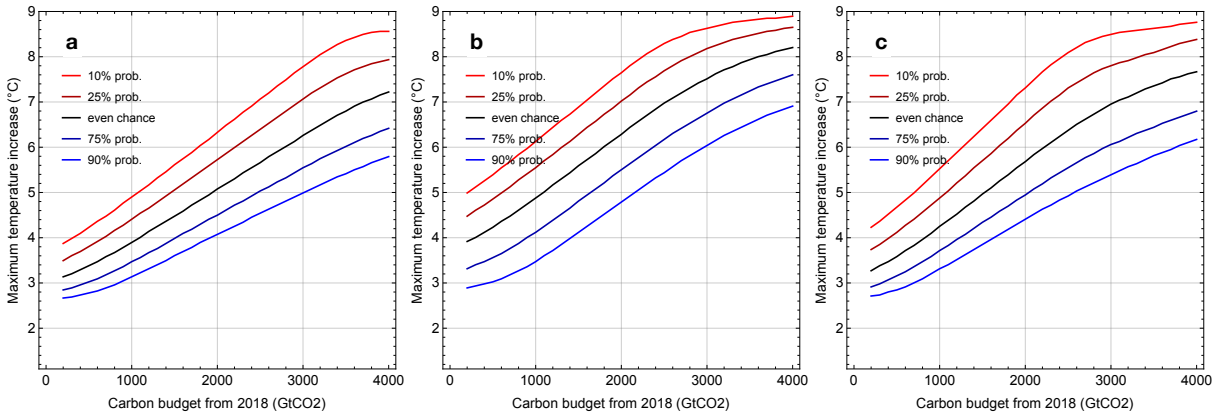

Figure 3.12: Likelihood plots for the estimated RCBs when including the Arctic amplification factor, given a temperature target, ranging from 0.0-9.0°C. The estimates use combinations of both the ±1 standard deviation carbon models, all of the 14 ESM's and the internal variability. **(a)** The RCB estimate of the linear SRM when including the Arctic amplification factor, illustrated in Figure 3.11(b). **(b)** includes the non-linear forcing from Equation B1. **(c)** includes the non-linear forcing from Equation B10. The figure legend explain the probabilities, where there is, e.g. a 90% probability that a temperature response will be on the blue line given a distinct carbon budget Johansen (2020). Reproducible through code and non-linear forcing equations found in Appendix C.

3.8 MAGICC comparison

To compare the SRM performance with MAGICC, Martinsen (2020) extracted temperature simulations from MAGICC6 simulations in the SSP dataset, as seen in Figure A.33 (Riahi et al., 2017; Joeri Rogelj et al., 2018). It includes estimated global mean surface temperatures for each of the nine decades from 2020-2100 in all of the 86 included scenarios, leading to a total of 774 data points. These temperatures were compared in a scatterplot to the related estimates from our SRM. As illustrated in Figure 3.13(a), our model is very consistent with MAGICC, lightly underestimating it as shown by the black dashed line. Pinpointing which factors lead to this underestimate has not been done in this research project, but there are several principal differences in the model frameworks. Amongst these differences are the inclusion of other greenhouses gases such as ozone (O_3) and N_2O, and a changing forcing ratio between CH_4/CO_2 (more detailed explanation of the forcing ratio in Section 3.1). Martinsen (2020) reviewed these and other factors, with a more comprehensive review of the differences located in his thesis.

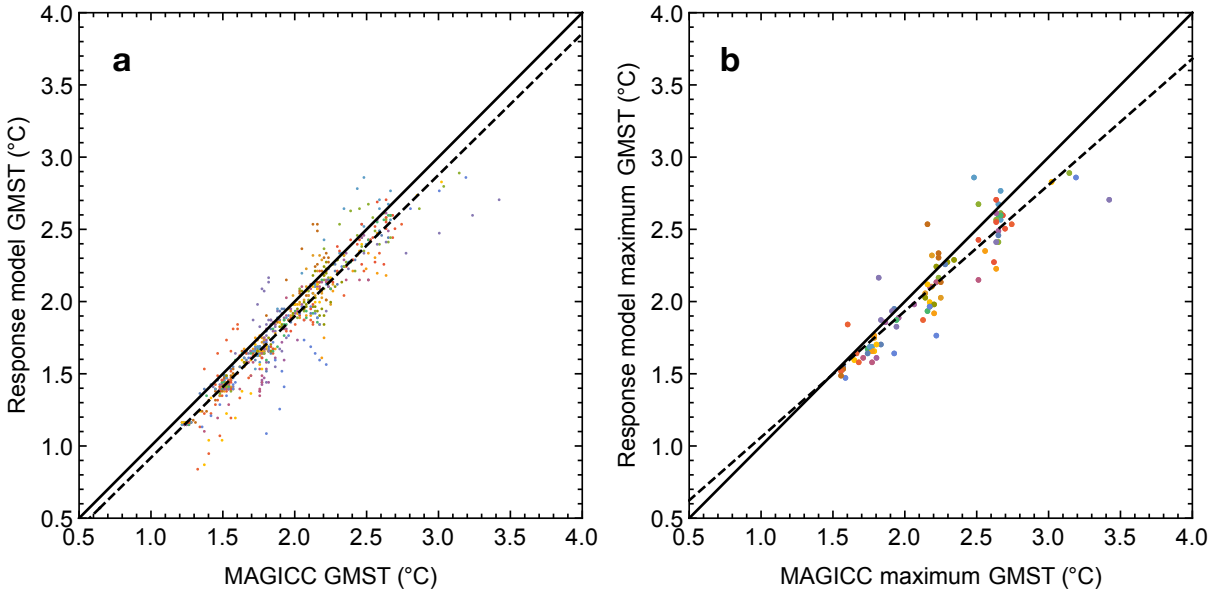

Figure 3.13: Estimated GMSTs for the SRM and MAGICC6 using 86 SSP scenarios (Riahi et al., 2017; Joeri Rogelj et al., 2018). The MAGICC and SRM estimates for all scenarios are shown on the x-axis and y-axis, respectively. **(a)** illustrates estimated GMST responses for each of the nine decades between 2020-2100, resulting in 774 data points. **(b)** illustrates the estimated maximum GMST for each of the SSP scenarios. Plot produced by Martinsen (2020). Reproducible through code in Appendix C.

Due to our use of maximum temperatures in the RCB estimates (see Section 3.5.1) we analysed the maximum GMSTs for all of the scenarios, regardless of at what point in time that maximum GMST took place. As illustrated in Figure 3.13(b), it seems like the SRM is consistent with the more conservative SSP scenarios, while there is an increasing underestimation for the higher temperatures.

There are several possible explanations for the underestimate, as mentioned above. Even though it was not a part of this research project, the difference might be accounted to a lower climate sensitivity for the SRM in comparison to MAGICC6. Figure 3.13(b) illustrates that with an estimated SRM temperature of 2.5°C, the linked MAGICC temperature lies around 2.7°C, leading to an underestimate of around 8%. However, there are only 86 data points clustered between about 1.5-2.7°C with a few outliers, leading to a limited conclusion basis.

When including a non-linear forcing effect, we assumed that the SRM estimates would overestimate in comparison to MAGICC6. MAGICC does not include strong non-linear feedbacks or forcing factors that exhibit a non-linear forcing effect like, e.g. abrupt permafrost thaw, as discussed in Section 3.6.

In this example, we included a non-linear effect from Equation B1 (see Table B.1 in Appendix B), with a maximum added forcing magnitude of 1 W/m² and a temperature threshold of 2°C. Figure 3.14 illustrates these estimates.

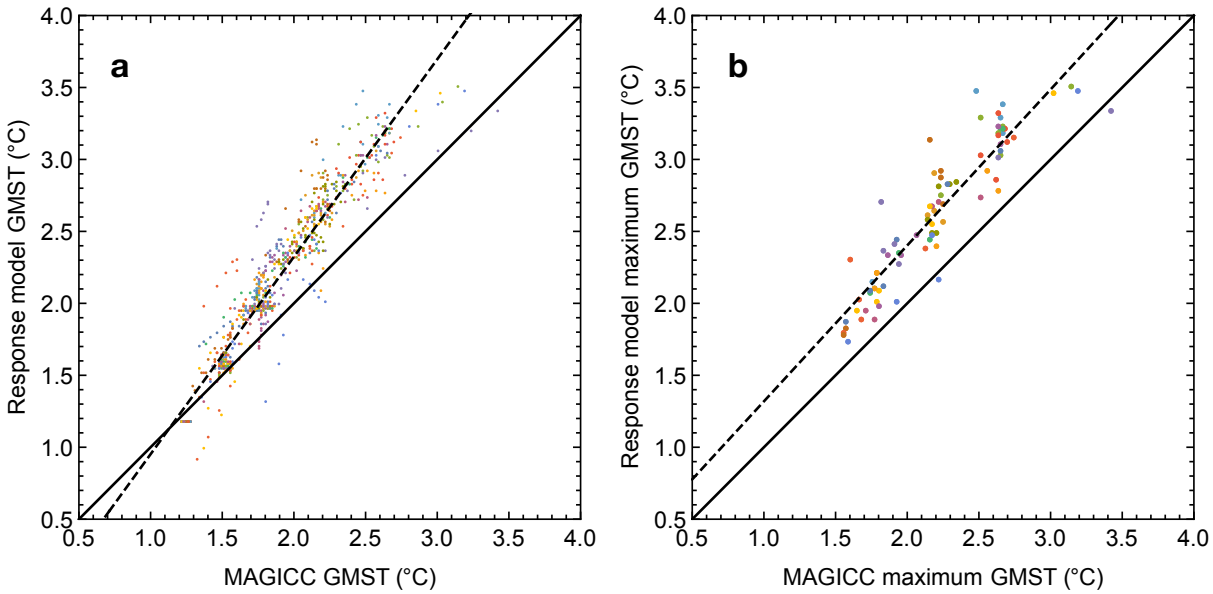

Figure 3.14: Estimated GMSTs for MAGICC6 and the SRM when including non-linear forcing from Equation B1, using 86 SSP scenarios (Riahi et al., 2017; Joeri Rogelj et al., 2018). The MAGICC and non-linear SRM estimates for all scenarios are shown on the x-axis and y-axis, respectively. **(a)** illustrates estimated GMST responses for each of the nine decades between 2020-2100, resulting in 774 data points. **(b)** illustrates the estimated maximum GMST for each of the SSP scenarios. Reproducible through code in Appendix C (Martinsen, 2020).

Figure 3.14(a) illustrates that with the inclusion of a non-linear forcing effect, there is an increasing temperature trend for the SRM temperature response. Due to the moderately high-temperature threshold of 2°C in Equation B1, when considering the risks for large-scale singular events found in SR15 (see Section 2.5), we see that most of the non-linear effect kicks in at higher temperatures in the SRM estimates. This leads to an increasing deviation from the approximately 1:1 linear relation for higher SRM temperatures, compared to Figure 3.13(a).

The maximum temperature estimates in Figure 3.14(b) show a relatively similar picture, with a general increase in the estimated temperature response. However, there is an approximately linear relation, starting at a higher base maximum temperature of about 0.8°C for the SRM temperature response.

Martinsen (2020) also looked at the non-linear forcing impact from Equation B10, found in Table B.1. Equation B10 illustrated a much more moderate temperature response from the non-

linear forcing effect, for both the GMST and maximum GMST estimates, as illustrated in Figure A.34. However, there is a definite impact on the estimates, for even a relatively weak non-linear forcing, easily visualised in Figure A.35. These results underline the reason to implement non-linear effects in climate modelling, in a similar way as just using CO_2-only RCBs only sheds light on the part of the truth in comparison to an effective RCB as discussed in Section 2.4.

4 Conclusion

In relation to many of the very complex ESMs used by, e.g. CMIP5, the developed Simple Response Model may seem very elementary. However, the resulting simulations for temperature responses seem to be very consistent with the literature. For instance, through interpolation of Figure B.1, an estimate of the mean TCRE for the SRM show a TCRE of 1.83°C/1000GtC (see calculation in Appendix B) in comparison to 1.86°C/1000GtC estimated by (Matthews et al., 2017). The SRM TCRE is also well within the 66% CI for the TCRE in AR5 of 0.2-0.7°C/1000GtCO$_2$ (0.5°C/1000GtCO$_2$) (Collins et al., 2013). The SRM estimate is, however, an approximation, without adding a variation of carbon models and the internal variability.

Due to the simplicity and flexibility of the SRM, it is considered to be a reasonable alternative to other simple- and reduced-complexity models, such as the benchmark model, MAGICC. The analysis conducted by Martinsen (2020) reinforced this by finding approximately perfect linearity when comparing the estimated temperature responses between the SRM and MAGICC, as seen in Figure 3.13. Through implementing likelihood estimate plots for the RCB, we believe that the results are easily comprehendible, such that policymakers without scientific background knowledge can make effective mitigation policies. For instance, policymakers in the Arctic region could easily be exposed to the potentially extreme regional impact global climate change can inflict on the regional temperatures, through the Arctic amplification factor, as illustrated in Figure 3.11.

The effect of non-linear forcing on the estimate of the RCB appears to be severe, as illustrated in Figure 3.10. The inclusion of the non-linear forcing framework enables the possibility of studying any possible non-linear forcing effect, which in this case ended up with the warming of wetlands and abrupt permafrost thaw. Since there is no consensus on any specific non-linear temperature relation to, e.g. abrupt permafrost thaw, a range of relations were studied (see Table B.1), all underlining the drastic effect on the RCB. With further research of the non-linear components leading to more knowledge and understanding of their ability to impact the carbon cycle-climate system, a specific non-linear forcing effect or a combined effect, in general, could be studied through the SRM.

One of the principal findings from the RCB estimates is that generally, the larger the emissions of GHGs, the larger the uncertainty in the temperature response becomes. Thus, with less ambitious mitigation targets, there is an increasing possibility for extreme impacts both on the climate-, ecosystems and higher adaptation costs. AR5 also expects that the limits of climate change adaptation will intensify due to findings in AR5, that suggests that there is a finite capacity of adaptation efforts because of the underlying regional and sectoral vulnerability in climate change (Klein et al., 2014).

With such an uncertain future, planning for adaptation efforts can be very difficult, where bad decision-making can lead to maladaptation. Choosing the wrong adaptive measure can lead to taking problematically high chances both for the climate system and the financial burden these impacts can have on the global economy (Klein et al., 2014; Mimura et al., 2014). With estimates for yearly adaptation costs in 2030 already in the range of USD$ 140-300 billion, the global economy would gain from increasing the more cost-effective, mitigation efforts relative to climate change adaptation (Sánchez et al., 2016; UNEP, 2018). As briefly discussed in Section 2.2, to substantially impact the RCB, the used efforts has to be of a large magnitude. By combining forces from both the adaptation-, mitigation efforts and transforming the energy sector towards a lower fossil fuel ratio, these changes can lead to the realisation of effective mitigation policies.

4.1 Further work

SRM performance can improve, and there are several possibilities for further work. First and foremost, repeating the study with the CMIP6 model ensemble can lead to more accurate findings since it includes updated state-of-the-art science. The inclusion of other ESMs or EMICs not included in CMIP5 or CMIP6 would likely also strengthen the SRM without increasing its complexity.

As mentioned in Section 3.5.1, new research debates that the probability distribution for the TCRE might be log-normal and not normal (Millar et al., 2018). Repeating the RCB estimates with varying probability distribution functions could thus be done to review the impact from a possibly wrong assumption.

In relation to ESMs, EMICs and reduced complexity models, the SRM includes quite few forcing factors. Through the implementation of, e.g. climate feedback-mechanisms and other forcing factors, the SRM could likely improve the replication of the carbon-cycle climate system. Forcing factors such as nitrous oxide (N_2O) and chlorofluorocarbons (CFCs) with possible greenhouse gas interactions are additions that could equate the SRM to MAGICC.

However, including too many forcing factors might also remove the simplicity of the SRM framework. A possibility is to incorporate a time dependency in the factors *a* and *b* such that the forcing ratios for methane and aerosols are non-constant until the conditions for stalling decline for methane emissions and the asymptotic behaviour in the case of aerosols are met. Due to the uncertainty in aerosols as a forcing factor, complicating it without further research and background might as well worsen the SRM performance.

Bibliography

Allen, M. R., Dube, O. P., Solecki, W., Aragón-Durand, F., Cramer, W., Humphreys, S., . . . Zickfeld, K. (2018). Framing and Context. In V. Masson-Delmotte, P. Zhai, H.-O. Pörtner, D. Roberts, J. Skea, P. R. Shukla, A. Pirani, W. Moufouma-Okia, C. Péan, R. Pidcock, S. Connors, J. B. R. Matthews, Y. Chen, X. Zhou, M. I. Gomis, E. Lonnoy, T. Maycock, M. Tignor, & T. Waterfield (Eds.), *Global Warming of 1.5°C. An IPCC Special Report on the impacts of global warming of 1.5°C above pre-industrial levels and related global greenhouse gas emission pathways, in the context of strengthening the global response to the threat of climate change, sustainable development, and efforts to eradicate poverty*: In Press.

Aye, G. C., & Edoja, P. E. (2017). Effect of economic growth on CO2 emission in developing countries: Evidence from a dynamic panel threshold model. *Cogent Economics & Finance, 5*(1), 1379239. doi:10.1080/23322039.2017.1379239

Blake, E. S., & Zelinsky, D. A. (2018). Tropical Cyclone Report: Hurricane Harvey. Retrieved from https://www.nhc.noaa.gov/data/tcr/AL092017_Harvey.pdf

Boden, T. A., Marland, G., & Andres, R. J. (2015). *Global, Regional, and National Fossil-Fuel CO2 Emissions*.

Bruhwiler, L., Michalak, A. M., Birdsey, R., Fisher, J. B., Houghton, R. A., Huntzinger, D. N., & Miller, J. B. (2018). Chapter 1: Overview of the global carbon cycle. In N. Cavallaro, G. Shrestha, R. Birdsey, M. A. Mayes, R. G. Najjar, S. C. Reed, P. Romero-Lankao, & Z. Zhu (Eds.), *Second State of the Carbon Cycle Report (SOCCR2): A Sustained Assessment Report* (pp. pp. 42-70). Washington, DC, USA: U.S. Global Change Research Program.

Burnett, R., Chen, H., Szyszkowicz, M., Fann, N., Hubbell, B., Pope, C. A., . . . Spadaro, J. V. (2018). Global estimates of mortality associated with long-term exposure to outdoor fine particulate matter. *Proceedings of the National Academy of Sciences, 115*(38), 9592-9597. doi:10.1073/pnas.1803222115

Coady, D., Parry, I., Le, N.-P., & Shang, B. (2019). Global Fossil Fuel Subsidies Remain Large: An Update Based on Country-Level Estimates. *IMF Working Papers, 2019*(89). doi:http://dx.doi.org/10.5089/9781484393178.001

Collins, M., Knutti, R., Arblaster, J., Dufresne, J.-L., Fichefet, T., Friedlingstein, P., . . . Wehner, M. (2013). Long-term climate change: Projections, commitments and irreversibility. *Climate Change 2013: The Physical Science Basis. Contribution of Working Group I to the Fifth Assessment Report of the Intergovernmental Panel on Climate Change*, 1029-1136. doi:10.1017/CBO9781107415324.024

Collins, M., Sutherland, M., Bouwer, L., Cheong, S.-M., Frölicher, T., Combes, H. J. D., . . . Tibig, L. (2019). Extremes, Abrupt Changes and Managing Risk. In H.-O. Pörtner, D. C. Roberts, V. Masson-Delmotte, P. Zhai, M. Tignor, E. Poloczanska, K. Mintenbeck, A. Alegría, M. Nicolai, A. Okem, J. Petzold, B. Rama, & N. M. Weyer (Eds.), *IPCC Special Report on the Ocean and Cryosphere in a Changing Climate*: In press.

Comyn-Platt, E., Hayman, G., Huntingford, C., Chadburn, S. E., Burke, E. J., Harper, A. B., . . . Sitch, S. (2018). Carbon budgets for 1.5 and 2 °C targets lowered by natural wetland and permafrost feedbacks. *Nature Geoscience, 11*(8), 568-573. doi:10.1038/s41561-018-0174-9

Cox, P. M., Huntingford, C., & Williamson, M. S. (2018). Emergent constraint on equilibrium climate sensitivity from global temperature variability. *Nature, 553*(7688), 319-322. doi:10.1038/nature25450

Cummins, D. P., Stephenson, D. B., & Stott, P. A. (2020). Optimal Estimation of Stochastic Energy Balance Model Parameters. *Journal of Climate*. doi:10.1175/jcli-d-19-0589.1

Dai, A., Luo, D., Song, M., & Liu, J. (2019). Arctic amplification is caused by sea-ice loss under increasing CO2. *Nature Communications, 10*(1), 121. doi:10.1038/s41467-018-07954-9

de Coninck, H., Revi, A., Babiker, M., Bertoldi, P., Buckeridge, M., Cartwright, A., . . . Sugiyama, T. (2018). Strengthening and Implementing the Global Response. In V. Masson-Delmotte, P. Zhai, H.-O. Pörtner, D. Roberts, J. Skea, P. R. Shukla, A. Pirani, W. Moufouma-Okia, C. Péan, R. Pidcock, S. Connors, J. B. R. Matthews, Y. Chen, X. Zhou, M. I. Gomis, E. Lonnoy, T. Maycock, M. Tignor, & T. Waterfield (Eds.), *Global Warming of 1.5°C. An IPCC Special Report on the impacts of global warming of 1.5°C above pre-industrial levels and related global greenhouse gas emission pathways, in the context of strengthening the global response to the threat of climate change, sustainable development, and efforts to eradicate poverty*: In Press.

Frölicher, T. L., Fischer, E. M., & Gruber, N. (2018). Marine heatwaves under global warming. *Nature, 560*(7718), 360-364. doi:10.1038/s41586-018-0383-9

Gasser, T., Kechiar, M., Ciais, P., Burke, E., Kleinen, T., Zhu, D., . . . Obersteiner, M. (2018). Path-dependent reductions in CO2 emission budgets caused by permafrost carbon release. *Nature Geoscience, 11*. doi:10.1038/s41561-018-0227-0

Gettelman, A., & Rood, R. B. (2016). Simulating the Atmosphere. In A. Gettelman & R. B. Rood (Eds.), *Demystifying Climate Models: A Users Guide to Earth System Models* (pp. 61-85). Berlin, Heidelberg: Springer Berlin Heidelberg.

Gibson, C. M., Chasmer, L. E., Thompson, D. K., Quinton, W. L., Flannigan, M. D., & Olefeldt, D. (2018). Wildfire as a major driver of recent permafrost thaw in boreal peatlands. *Nature Communications, 9*(1), 3041. doi:10.1038/s41467-018-05457-1

Gillett, N. P., Arora, V. K., Matthews, D., & Allen, M. R. (2013). Constraining the Ratio of Global Warming to Cumulative CO_2 Emissions Using CMIP5 Simulations. *Journal of Climate, 26*(18), 6844-6858. Retrieved from www.jstor.org/stable/26192829

Goosse, H., Barriat, P. Y., Lefebvre, W., Loutre, M. F., & Zunz, V. (2010). Introduction to climate dynamics and climate modeling. 59-86. Retrieved from http://www.climate.be/textbook/pdf/Chapter_3.pdf

Haustein, K., Allen, M. R., Forster, P. M., Otto, F. E. L., Mitchell, D. M., Matthews, H. D., & Frame, D. J. (2017). A real-time Global Warming Index. *Scientific Reports, 7*(1), 15417. doi:10.1038/s41598-017-14828-5

Hoegh-Guldberg, O., Jacob, D., Taylor, M., Bindi, M., Brown, S., Camilloni, I., . . . Zhou, G. (2018). Impacts of 1.5ºC Global Warming on Natural and Human Systems. In V. Masson-Delmotte, P. Zhai, H.-O. Pörtner, D. Roberts, J. Skea, P. R. Shukla, A. Pirani, W. Moufouma-Okia, C. Péan, R. Pidcock, S. Connors, J. B. R. Matthews, Y. Chen, X. Zhou, M. I. Gomis, E. Lonnoy, T. Maycock, M. Tignor, & T. Waterfield (Eds.), *Global Warming of 1.5°C. An IPCC Special Report on the impacts of global warming of 1.5°C above pre-industrial levels and related global greenhouse gas emission pathways, in the context of strengthening the global response to the threat of climate change, sustainable development, and efforts to eradicate poverty*: In press.

Hugelius, G., Strauss, J., Zubrzycki, S., Harden, J. W., Schuur, E. A. G., Ping, C. L., . . . Kuhry, P. (2014). Estimated stocks of circumpolar permafrost carbon with quantified uncertainty ranges and identified data gaps. *Biogeosciences, 11*(23), 6573-6593. doi:10.5194/bg-11-6573-2014

Huppmann, D., Kriegler, E., Krey, V., Riahi, K., Rogelj, J., Rose, S. K., . . . Zhang, R. (2018). IAMC 1.5°C Scenario Explorer and Data hosted by IIASA (Publication no. 10.22022/SR15/08-2018.15429). from Integrated Assessment Modeling Consortium &

International Institute for Applied Systems Analysis https://data.ene.iiasa.ac.at/iamc-sr15-explorer

Hurlbert, M., Krishnaswamy, J., Davin, E., Johnson, F. X., Mena, C., Morton, J., . . . Zommers, Z. (2019). Risk management and decision-making in relation to sustainable development. In P. Shukla & J. Skea (Eds.), *Climate Change and Land: an IPCC special report on climate change, desertification, land degradation, sustainable land management, food security, and greenhouse gas fluxes in terrestrial ecosystems* (pp. 673-800): IPCC.

IPCC. (2014). Summary for policymakers. In C. B. Field, V. R. Barros, D. J. Dokken, K. J. Mach, M. D. Mastrandrea, T. E. Bilir, M. Chatterjee, K. L. Ebi, Y. O. Estrada, R. C. Genova, B. Girma, E. S. Kissel, A. N. Levy, S. MacCracken, P. R. Mastrandrea, & L.L.White (Eds.), *Climate Change 2014: Impacts,Adaptation, and Vulnerability. Part A: Global and Sectoral Aspects. Contribution of Working Group II to the Fifth Assessment Report of the Intergovernmental Panel on Climate Change* (pp. 1-32). Cambridge, United Kingdom and New York, NY, USA: Cambridge University Press.

IPCC. (2018). Summary for Policymakers. In V. Masson-Delmotte, P. Zhai, H.-O. Pörtner, D. Roberts, J. Skea, P. R. Shukla, A. Pirani, W. Moufouma-Okia, C. Péan, R. Pidcock, S. Connors, J. B. R. Matthews, Y. Chen, X. Zhou, M. I. Gomis, E. Lonnoy, T. Maycock, M. Tignor, & T. Waterfield (Eds.), *Global Warming of 1.5°C. An IPCC Special Report on the impacts of global warming of 1.5°C above pre-industrial levels and related global greenhouse gas emission pathways, in the context of strengthening the global response to the threat of climate change, sustainable development, and efforts to eradicate poverty*: In Press.

Johansen, A. (2020). Assessment of the Remaining Carbon Budget: Incorporating Arctic Amplification in a Simple Response Model

Joos, F., Roth, R., Fuglestvedt, J. S., Peters, G. P., Enting, I. G., von Bloh, W., . . . Weaver, A. J. (2013). Carbon dioxide and climate impulse response functions for the computation of greenhouse gas metrics: a multi-model analysis. *Atmos. Chem. Phys., 13*(5), 2793-2825. doi:10.5194/acp-13-2793-2013

KC, S., & Lutz, W. (2017). The human core of the shared socioeconomic pathways: Population scenarios by age, sex and level of education for all countries to 2100. *Global Environmental Change, 42*, 181-192. doi:https://doi.org/10.1016/j.gloenvcha.2014.06.004

Klein, R. J. T., Midgley, G. F., Preston, B. L., Alam, M., Berkhout, F. G. H., Dow, K., & Shaw, M. R. (2014). Adaptation opportunities, constraints, and limits. In C. B. Field, V. R. Barros, D. J. Dokken, K. J. Mach, M. D. Mastrandrea, T. E. Bilir, M. Chatterjee, K. L. Ebi, Y. O. Estrada, R. C. Genova, B. Girma, E. S. Kissel, A. N. Levy, S. MacCracken, P. R. Mastrandrea, & L.L.White (Eds.), *Climate Change 2014: Impacts, Adaptation, and Vulnerability. Part A: Global and Sectoral Aspects. Contribution of Working Group II to the Fifth Assessment Report of the Intergovernmental Panel on Climate Change* (pp. 899-943). Cambridge, United Kingdom and New York, NY, USA: Cambridge University Press.

Kokelj, S., Lantz, T., Tunnicliffe, J., Segal, R., & Lacelle, D. (2017). Climate-driven thaw of permafrost preserved glacial landscapes, northwestern Canada. *Geology, 45*, G38626.38621. doi:10.1130/G38626.1

Lawrence, D. M., Koven, C. D., Swenson, S. C., Riley, W. J., & Slater, A. G. (2015). Permafrost thaw and resulting soil moisture changes regulate projected high-latitude CO 2 and CH 4 emissions. *Environmental Research Letters, 10*(9), 094011. doi:10.1088/1748-9326/10/9/094011

Le Quéré, C., Andrew, R. M., Friedlingstein, P., Sitch, S., Hauck, J., Pongratz, J., . . . Zheng, B. (2018). Global Carbon Budget 2018. *Earth Syst. Sci. Data, 10*(4), 2141-2194. doi:10.5194/essd-10-2141-2018

Le Quéré, C., Jackson, R. B., Jones, M. W., Smith, A. J. P., Abernethy, S., Andrew, R. M., . . . Peters, G. P. (2020). Temporary reduction in daily global CO2 emissions during the COVID-19 forced confinement. *Nature Climate Change*. doi:10.1038/s41558-020-0797-x

Le Quéré, C., Moriarty, R., Andrew, R. M., Peters, G. P., Ciais, P., Friedlingstein, P., . . . Zeng, N. (2015). Global carbon budget 2014. *Earth System Science Data, 7*, 47-85. doi:10.5194/essd-7-47-2015

Lenssen, N. J. L., Schmidt, G. A., Hansen, J. E., Menne, M. J., Persin, A., Ruedy, R., & Zyss, D. (2019). Improvements in the GISTEMP Uncertainty Model. *Journal of Geophysical Research: Atmospheres, 124*(12), 6307-6326. doi:10.1029/2018jd029522

Lewkowicz, A. G., & Way, R. G. (2019). Extremes of summer climate trigger thousands of thermokarst landslides in a High Arctic environment. *Nature Communications, 10*(1), 1329. doi:10.1038/s41467-019-09314-7

MacDougall, A. H., Zickfeld, K., Knutti, R., & Matthews, H. D. (2015). Sensitivity of carbon budgets to permafrost carbon feedbacks and non-CO2 forcings. *Environmental Research Letters, 10*(12), 125003. doi:10.1088/1748-9326/10/12/125003

MAGICC. (2015, 30.08). Model Description. Retrieved from http://wiki.magicc.org/index.php?title=Model_Description

Martinsen, A. R. (2020). Assessment of the Remaining Carbon Budget: A Comparison of a Simple Response Model and the MAGICC model.

Matthews, H. D., Landry, J.-S., Partanen, A.-I., Allen, M., Eby, M., Forster, P. M., . . . Zickfeld, K. (2017). Estimating Carbon Budgets for Ambitious Climate Targets. *Current Climate Change Reports, 3*(1), 69-77. doi:10.1007/s40641-017-0055-0

Meinshausen, M., Smith, S. J., Calvin, K., Daniel, J. S., Kainuma, M. L. T., Lamarque, J.-F., . . . van Vuuren, D. P. P. (2011). The RCP greenhouse gas concentrations and their extensions from 1765 to 2300. *Climatic Change, 109*(1), 213. doi:10.1007/s10584-011-0156-z

Meredith, M., Sommerkorn, M., Cassotta, S., Derksen, C., Ekayki, A., Hollowed, A., . . . Schuur, E. A. G. (2019). Polar Regions. In H.-O. Pörtner, D. C. Roberts, V. Masson-Delmotte, P. Zhai, M. Tignor, E. Poloczanska, K. Mintenbeck, A. Alegría, M. Nicolai, A. Okem, J. Petzold, B. Rama, & N. M. Weyer (Eds.), *IPCC Special Report on the Ocean and Cryosphere in a Changing Climate*: In press.

Messner, D., Schellnhuber, J., Rahmstorf, S., & Klingenfeld, D. (2010). The budget approach: a framework for a global transformation toward a low-carbon economy. *J. Renew. Sustain. Energy, 2*. doi:10.1063/1.3318695

Millar, R. J., Fuglestvedt, J. S., Friedlingstein, P., Rogelj, J., Grubb, M. J., Matthews, H. D., . . . Allen, M. R. (2018). Author Correction: Emission budgets and pathways consistent with limiting warming to 1.5 °C. *Nature Geoscience, 11*(6), 454-455. doi:10.1038/s41561-018-0153-1

Mimura, N., Pulwarty, R. S., Duc, D. M., Elshinnawy, I., Redsteer, M. H., Huang, H. Q., . . . Rodriguez, R. A. S. (2014). Adaptation planning and implementation. In C. B. Field, V. R. Barros, D. J. Dokken, K. J. Mach, M. D. Mastrandrea, T. E. Bilir, M. Chatterjee, K. L. Ebi, Y. O. Estrada, R. C. Genova, B. Girma, E. S. Kissel, A. N. Levy, S. MacCracken, P. R. Mastrandrea, & L.L.White (Eds.), *Climate Change 2014: Impacts,Adaptation, and Vulnerability. Part A: Global and Sectoral Aspects. Contribution of Working Group II to the Fifth Assessment Report of the Intergovernmental Panel on Climate Change* (pp.

869-898). Cambridge, United Kingdom and New York, NY, USA: Cambridge University Press.
Myhre, G., Highwood, E. J., Shine, K. P., & Stordal, F. (1998). New estimates of radiative forcing due to well mixed greenhouse gases. *Geophysical Research Letters, 25*(14), 2715-2718. doi:10.1029/98GL01908
Myhre, G., Shindell, D., Bréon, F.-M., Collins, W., Fuglestvedt, J., Huang, J., . . . Zhang, H. (2013). Anthropogenic and Natural Radiative Forcing. *Climate Change 2013: The Physical Science Basis. Contribution of Working Group I to the Fifth Assessment Report of the Intergovernmental Panel on Climate Change*, 659-740. doi:10.1017/CBO9781107415324.018
NASA Earth Observatory. (2020). 2019 Was the Second Warmest Year on Record. Retrieved from https://earthobservatory.nasa.gov/images/146154/2019-was-the-second-warmest-year-on-record
Natali, S., Watts, J., Rogers, B., Potter, S., Ludwig, S., Selbmann, A.-K., . . . Zona, D. (2019). Large loss of CO2 in winter observed across the northern permafrost region. *Nature Climate Change*. doi:10.1038/s41558-019-0592-8
National Research Council. (2020). *Climate Change: Evidence and Causes: Update 2020*. Washington, DC: The National Academies Press.
Newman, P. (2017). Decoupling Economic Growth from Fossil Fuels. *Modern Economy, 08*, 791-805. doi:10.4236/me.2017.86055
Obu, J., Westermann, S., Bartsch, A., Berdnikov, N., Christiansen, H., Avirmed, D., . . . Zou, D. (2019). Northern Hemisphere permafrost map based on TTOP modelling for 2000–2016 at 1 km2 scale. *Earth-Science Reviews, 193*. doi:10.1016/j.earscirev.2019.04.023
Peterson, E. W. F. (2017). The Role of Population in Economic Growth. *SAGE Open, 7*(4), 2158244017736094. doi:10.1177/2158244017736094
Riahi, K., van Vuuren, D. P., Kriegler, E., Edmonds, J., O'Neill, B. C., Fujimori, S., . . . Tavoni, M. (2017). The Shared Socioeconomic Pathways and their energy, land use, and greenhouse gas emissions implications: An overview. *Global Environmental Change, 42*, 153-168. doi:https://doi.org/10.1016/j.gloenvcha.2016.05.009
Robinson, A., Calov, R., & Ganopolski, A. (2012). Multistability and critical thresholds of the Greenland ice sheet. *Nature Climate Change, 2*(6), 429-432. doi:10.1038/nclimate1449
Rogelj, J., Forster, P. M., Kriegler, E., Smith, C. J., & Seferian, R. (2019). Estimating and tracking the remaining carbon budget for stringent climate targets. *Nature, 571*(7765), 335-342. doi:10.1038/s41586-019-1368-z
Rogelj, J., Popp, A., Calvin, K. V., Luderer, G., Emmerling, J., Gernaat, D., . . . Tavoni, M. (2018). Scenarios towards limiting global mean temperature increase below 1.5 °C. *Nature Climate Change, 8*(4), 325-332. doi:10.1038/s41558-018-0091-3
Rogelj, J., Shindell, D., Jiang, K., Fifita, S., Forster, P., Ginzburg, V., . . . Vilariño, M. V. (2018). Mitigation Pathways Compatible with 1.5°C in the Context of Sustainable Development. In V. Masson-Delmotte, P. Zhai, H.-O. Pörtner, D. Roberts, J. Skea, P. R. Shukla, A. Pirani, W. Moufouma-Okia, C. Péan, R. Pidcock, S. Connors, J. B. R. Matthews, Y. Chen, X. Zhou, M. I. Gomis, E. Lonnoy, T. Maycock, M. Tignor, & T. Waterfield (Eds.), *Global Warming of 1.5°C. An IPCC Special Report on the impacts of global warming of 1.5°C above pre-industrial levels and related global greenhouse gas emission pathways, in the context of strengthening the global response to the threat of climate change, sustainable development, and efforts to eradicate poverty*: In Press.
Rypdal, K. (2016). Global warming projections derived from an observation-based minimal model. *Earth System Dynamics, 7*(1), 51-70. doi:10.5194/esd-7-51-2016
Sánchez, B., Iglesias, A., McVittie, A., Álvaro-Fuentes, J., Ingram, J., Mills, J., . . . Kuikman, P. J. (2016). Management of agricultural soils for greenhouse gas mitigation: Learning

from a case study in NE Spain. *J Environ Manage, 170*, 37-49. doi:10.1016/j.jenvman.2016.01.003

Schuur, E., McGuire, A. D., Schädel, C., Grosse, G., Harden, J., Hayes, D. J., . . . Vonk, J. (2015). Climate change and the permafrost carbon feedback. *Nature, 2015*, 171-179. doi:10.1038/nature14338

Schuur, E. A. G., McGuire, A. D., Romanovsky, V., Schädel, C., & Mack, M. (2018). Chapter 11: Arctic and boreal carbon. *Second State of the Carbon Cycle Report (SOCCR2): A Sustained Assessment Report* 428-468. doi: https://doi.org/10.7930/SOCCR2.2018.Ch11

Smith, D. M., Booth, B. B. B., Dunstone, N. J., Eade, R., Hermanson, L., Jones, G. S., . . . Thompson, V. (2016). Role of volcanic and anthropogenic aerosols in the recent global surface warming slowdown. *Nature Climate Change, 6*(10), 936-940. doi:10.1038/nclimate3058

Stocker, T. F., Qin, D., Plattner, G.-K., Alexander, L. V., Allen, S. K., Bindoff, N. L., . . . Xie, S.-P. (2013). Technical Summary. *Climate Change 2013: The Physical Science Basis. Contribution of Working Group I to the Fifth Assessment Report of the Intergovernmental Panel on Climate Change*, 33-115.

Team, G. (2020). GISS Surface Temperature Analysis (GISTEMP), version 4. *NASA Goddard Institute for Space Studies.* Retrieved from https://data.giss.nasa.gov/gistemp/

The World Bank. (2020). Country Profile. Retrieved from https://databank.worldbank.org/views/reports/reportwidget.aspx?Report_Name=CountryProfile&Id=b450fd57&tbar=y&dd=y&inf=n&zm=n&country=NOR

Turetsky, M. R., Abbott, B. W., Jones, M. C., Anthony, K. W., Olefeldt, D., Schuur, E. A. G., . . . McGuire, A. D. (2020). Carbon release through abrupt permafrost thaw. *Nature Geoscience, 13*(2), 138-143. doi:10.1038/s41561-019-0526-0

UNEP. (2018). *The Adaptation Gap Report 2018*. Retrieved from Nairobi, Kenya: https://unepdtu.org/wp-content/uploads/2019/04/agr-final-version-2018.pdf

Wigley, T. M. L. (1995). MAGICC and SCENGEN: Integrated models for estimating regional climate change in response to anthropogenic emissions. In S. Zwerver, R. S. A. R. van Rompaey, M. T. J. Kok, & M. M. Berk (Eds.), *Studies in Environmental Science* (Vol. 65, pp. 93-94): Elsevier.

World Meteorological Organization. (2020). *WMO statement on the status of the global climate in 2019*. doi:10.13140/RG.2.2.13705.19046

Zhang, Q., Zheng, Y., Tong, D., Shao, M., Wang, S., Zhang, Y., . . . Hao, J. (2019). Drivers of improved PM_{2.5} air quality in China from 2013 to 2017. *Proceedings of the National Academy of Sciences, 116*(49), 24463-24469. doi:10.1073/pnas.1907956116

Appendix A

Additional plots illustrating supplementary results found in the SRM, as discussed in Section 3.

Additional figures estimated from the linear SRM code discussed in Section 3.1-3.5.

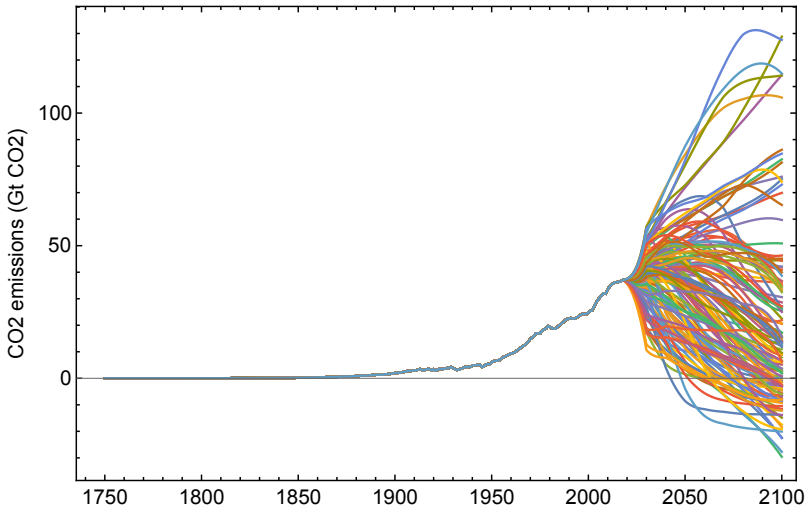

Figure A.1: Estimate of 127 emission scenarios before removal of exceedance scenarios.

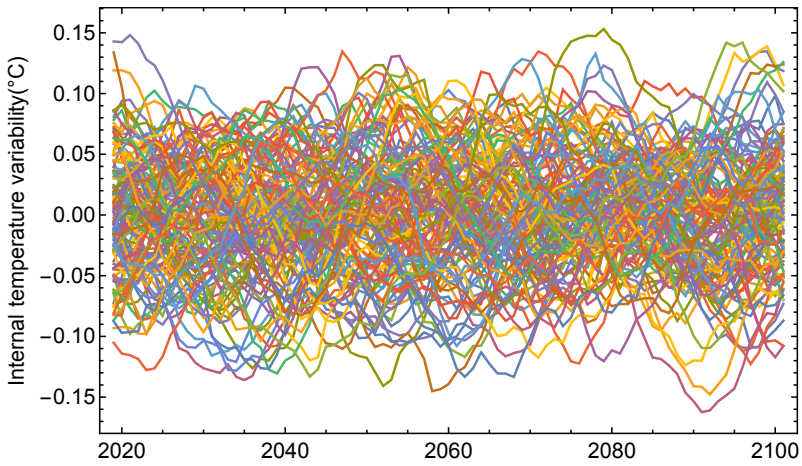

Figure A.2: Internal temperature variabilities for each of the original 127 emission scenarios.

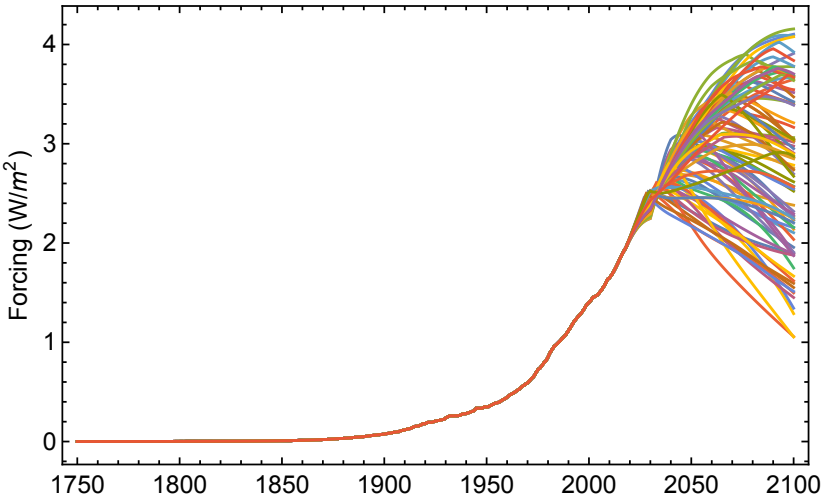

Figure A.3: Combined forcing from both the GHGs and the aerosols, for each of the 86 emission scenarios.

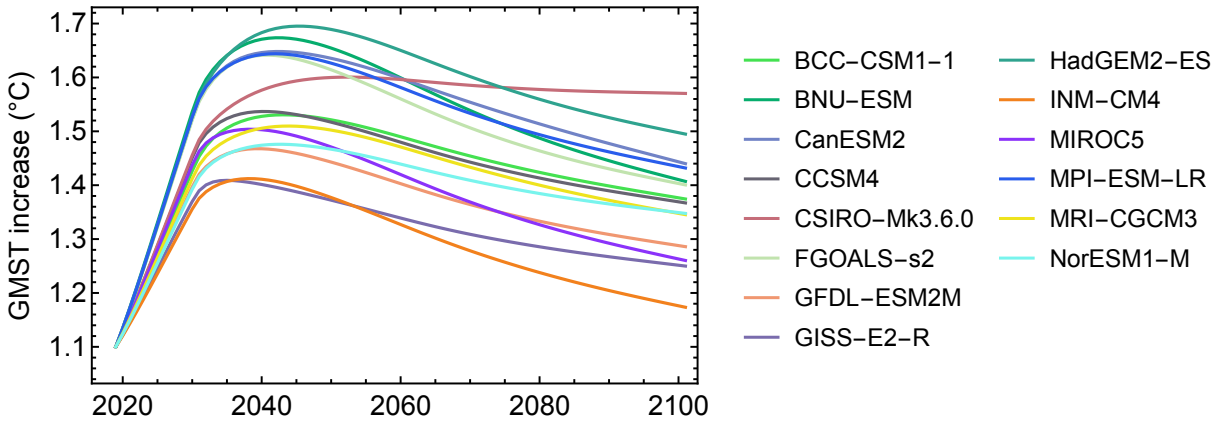

Figure A.4: Estimated temperature response for an emission scenario for each of the 14 ESMs from CMIP5 (see figure legend) using the best estimate carbon model.

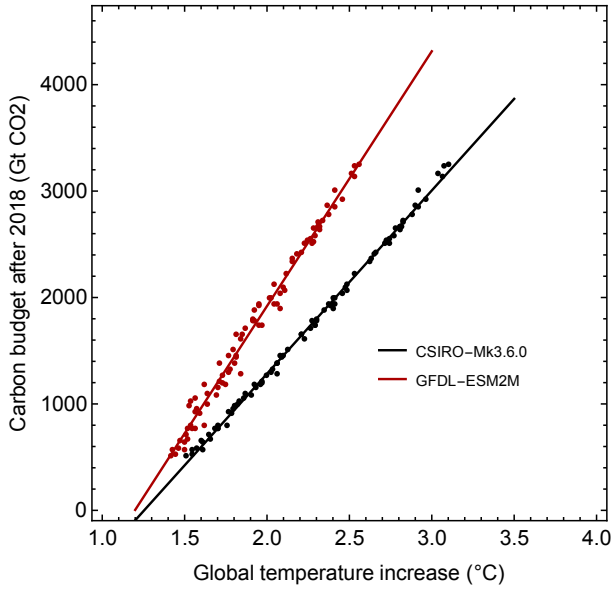

Figure A.5: TCRE for two climate models from the CMIP5 model ensemble, and our best estimate carbon model. Neither the internal variability or the non-linear forcing framework was included. The figure legend denotes the TCRE for the CSIRO and GFDL models from the CMIP5 model ensemble. Each dot is one of the 86 emission scenarios. Produced through code in Appendix C.

Additional figures (Figure A.6-A.29) estimated through the non-linear framework in the SRM, as discussed in Section 3.6.

Figure A.6-A.11 were produced with the non-linear forcing relation Equation B1 found in Table B.1.

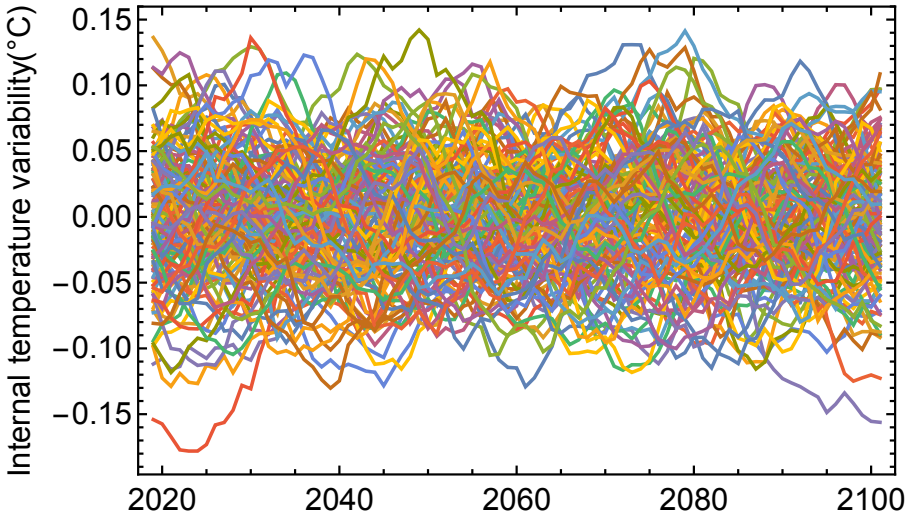

Figure A.6: Internal temperature variabilities for each of the original 127 emission scenarios when including the non-linear forcing from Equation B1.

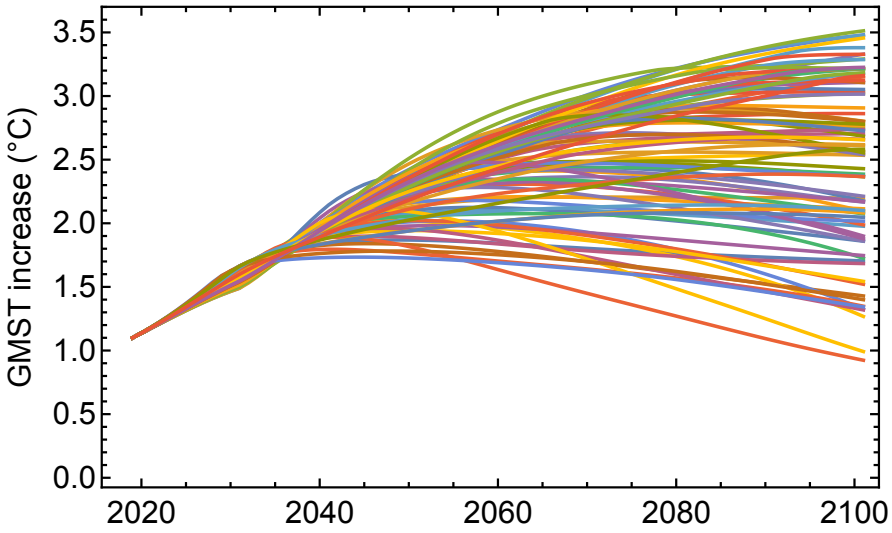

Figure A.7: Estimated temperature response for the SRM when including non-linear forcing from Equation B1. Each line is one of the 86 emission scenarios.

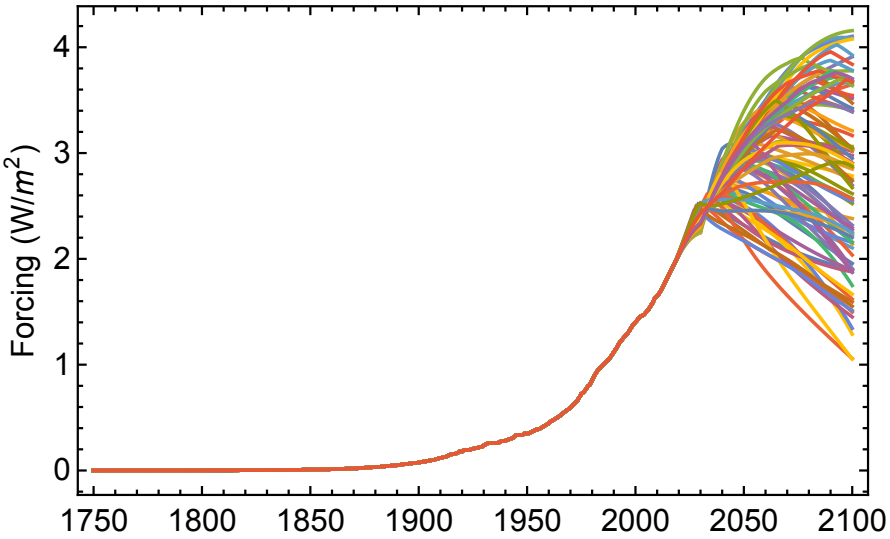

Figure A.8: Combined forcing from both the GHGs and the aerosols, for each of the 86 emission scenarios. Includes non-linear forcing from Equation B1.

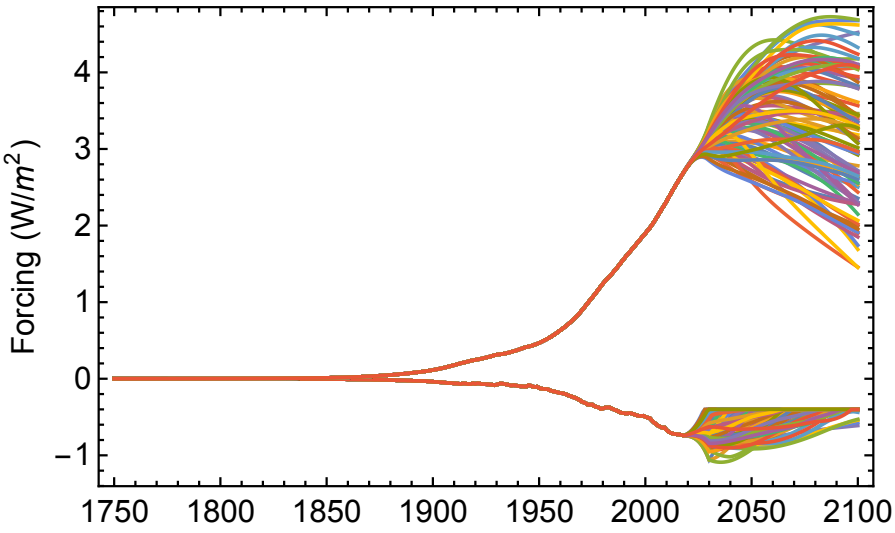

Figure A.9: Forcing estimates for aerosols and the GHGs, for each of the 86 emission scenarios. Includes non-linear forcing from Equation B1. See further explanation in figure text for Figure 3.3.

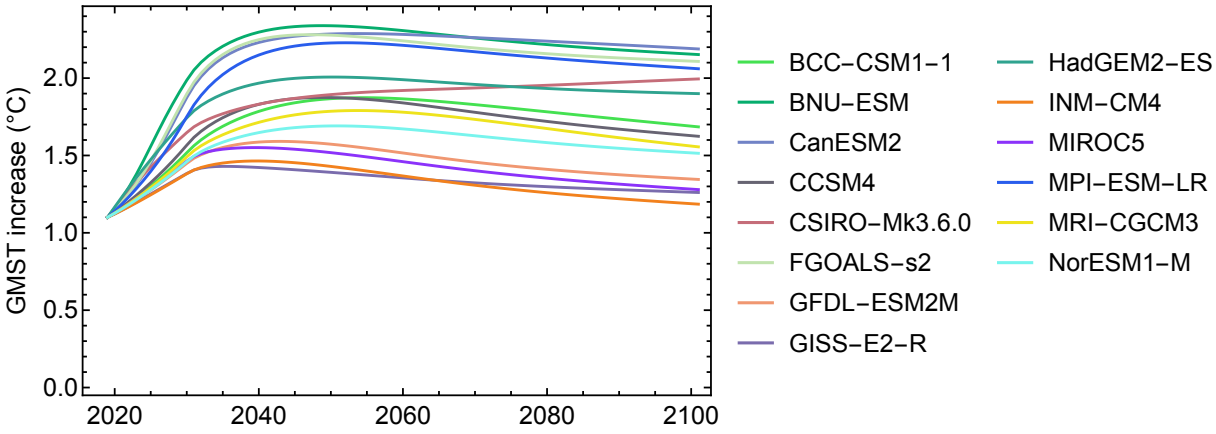

Figure A.10: Estimated temperature response for an emission scenario for each of the 14 ESMs from CMIP5 (see figure legend) using the best estimate carbon model. The estimates includes non-linear forcing from Equation B1.

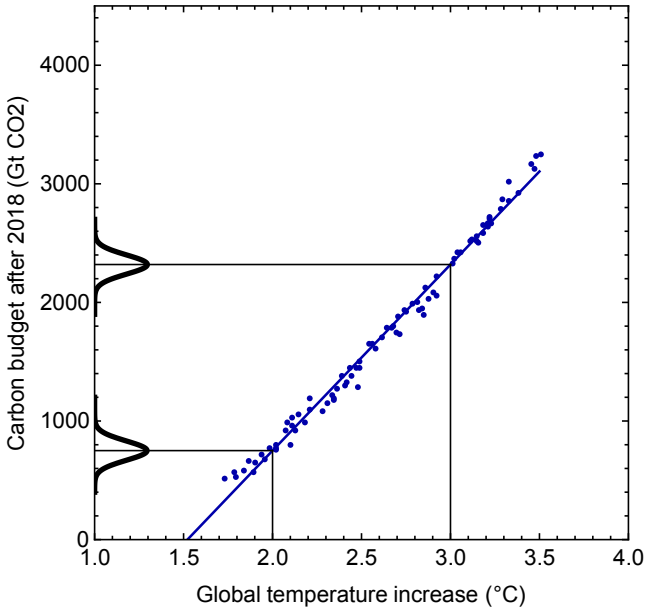

Figure A.11: Estimated TCRE in same manner as Figure 3.6, with an included non-linear forcing relation from Equation B1. Probability distribution for RCBs for a 2°C and 3°C mitigation target on y-axis.

Figure A.12-A.17 were produced with the non-linear forcing relation Equation B10 found in Table B.1.

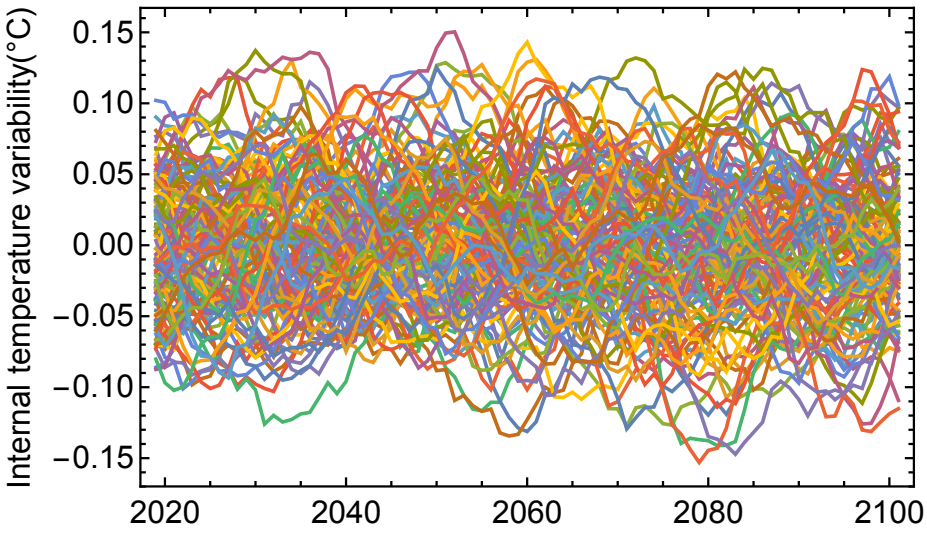

Figure A.12: Internal temperature variabilities for each of the original 127 emission scenarios when including the non-linear forcing from Equation B10.

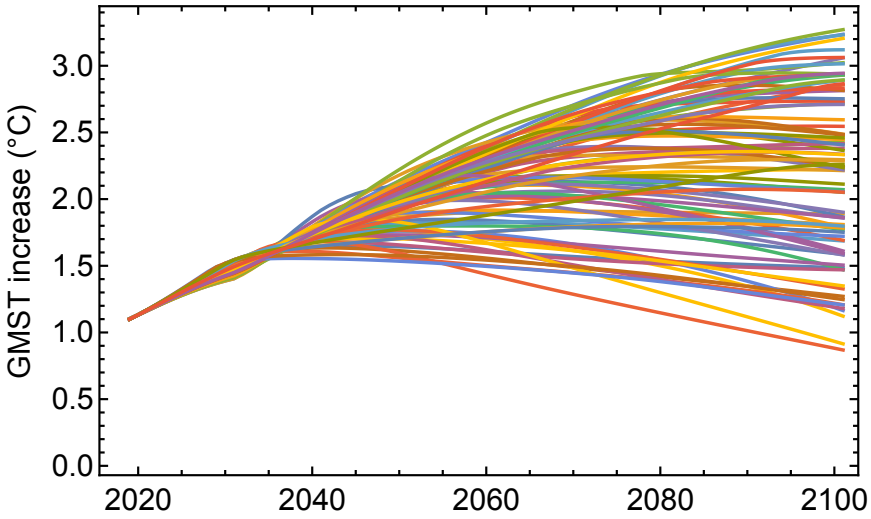

Figure A.13: Estimated temperature response for the SRM when including non-linear forcing from Equation B10. Each line is one of the 86 emission scenarios.

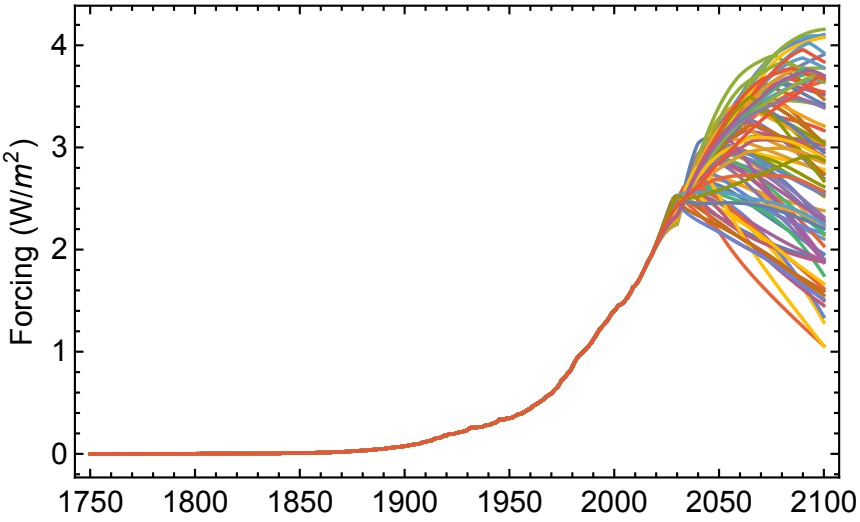

Figure A.14: Combined forcing from both the GHGs and the aerosols, for each of the 86 emission scenarios. Includes non-linear forcing from Equation B10.

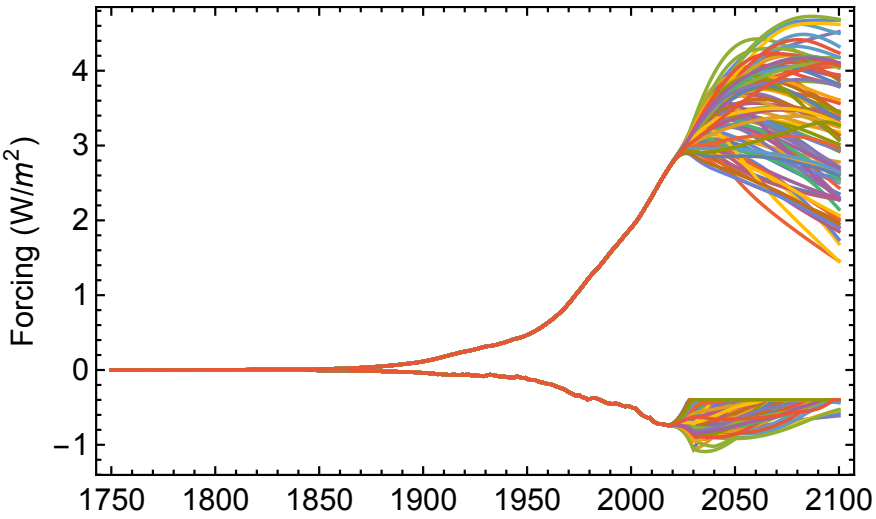

Figure A.15: Forcing estimates for aerosols and the GHGs, for each of the 86 emission scenarios. Includes non-linear forcing from Equation B1. See further explanation in figure text for Figure 3.3.

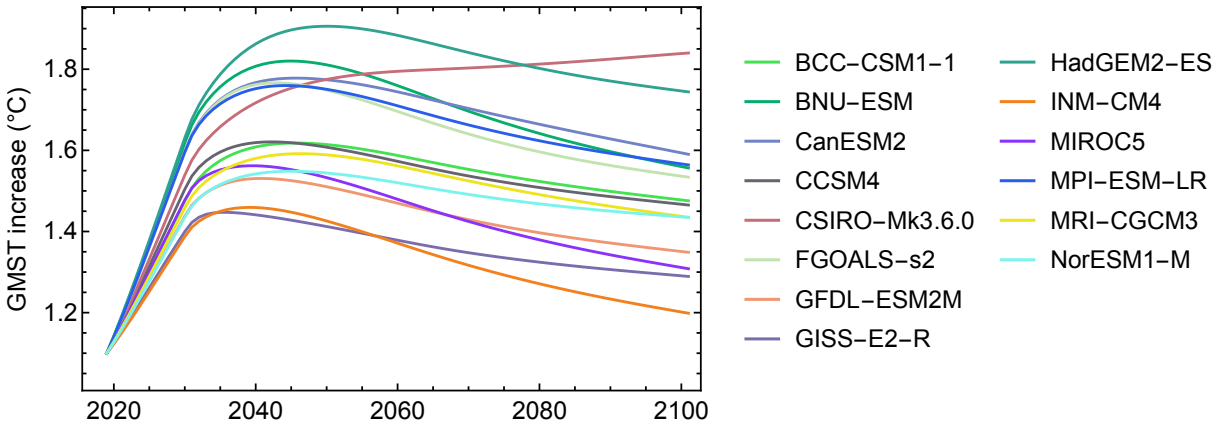

Figure A.16: Estimated temperature response for an emission scenario for each of the 14 ESMs from CMIP5 (see figure legend) using the best estimate carbon model. The estimate includes non-linear forcing from Equation B10.

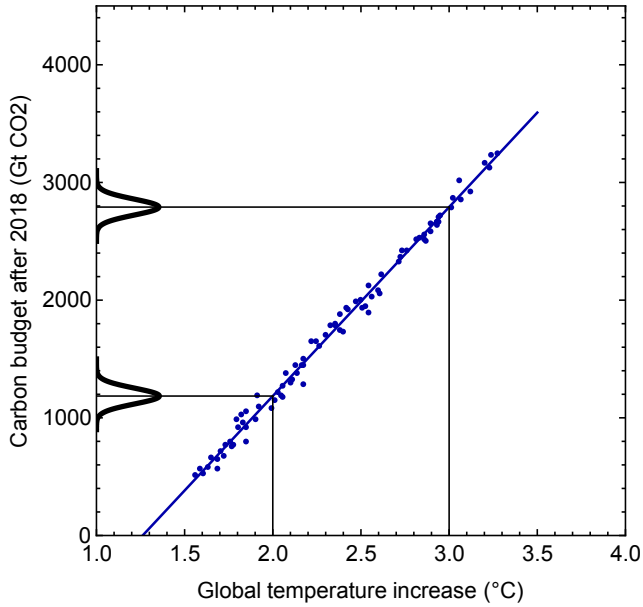

Figure A.17: Estimated TCRE in same manner as Figure 3.6, with an included non-linear forcing relation from Equation B10. Probability distribution for RCBs for a 2°C and 3°C mitigation target on y-axis.

Figure A.18-A.28 are RCB estimates for all of the examined equations in Table B.1. All figures were estimated in the exactly same manner, where Figure A.18-A28(a) shows a TCRE plot in same manner as Figure A.5 (see figure text for more detailed explanation). Figure A.18-A.28(b) show RCB estimates in same manner as Figure 3.7(d) (see figure text for more detailed explanation).

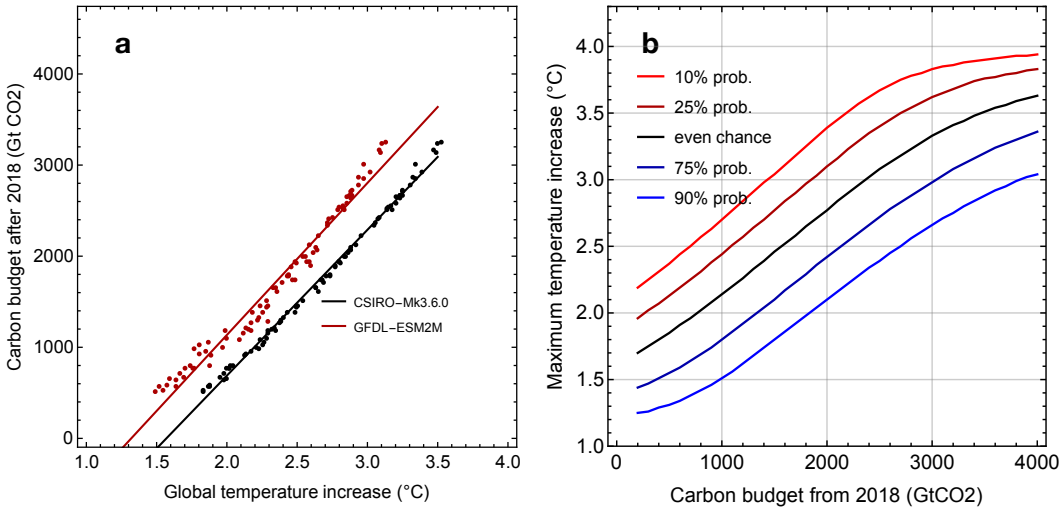

Figure A.18: Plots produced with non-linear forcing from Equation B1 from Table B.1.

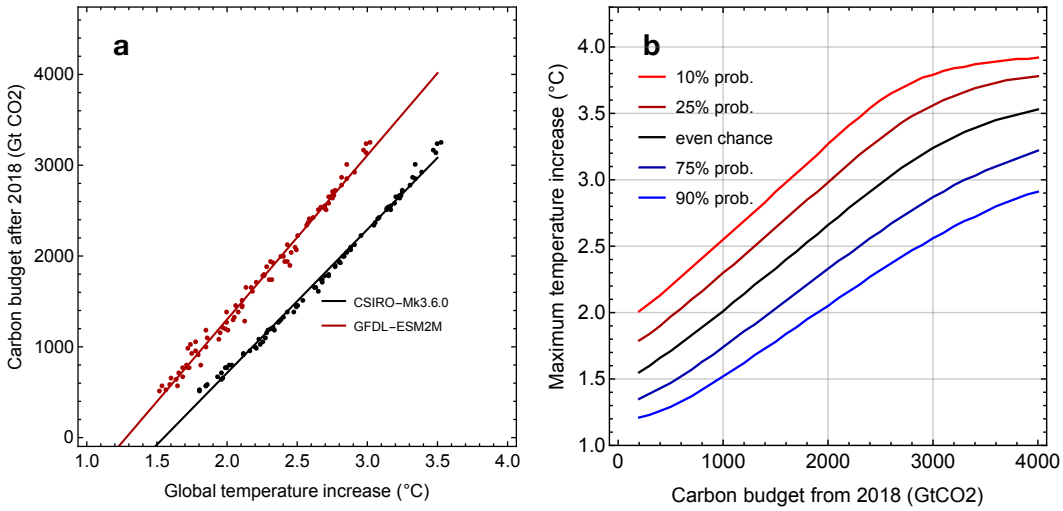

Figure A.19: Plots produced with non-linear forcing from Equation B2 from Table B.1.

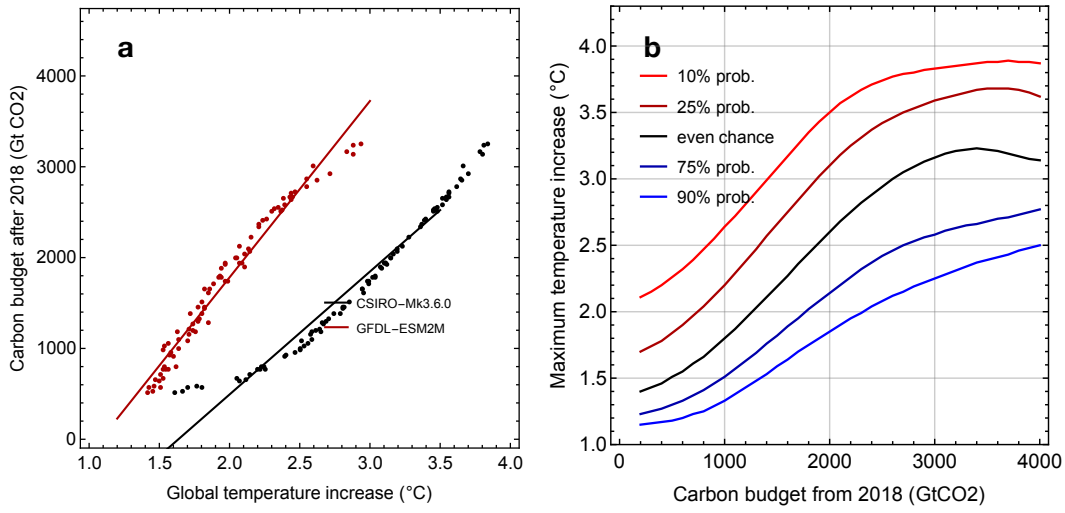

Figure A.20: Plots produced with non-linear forcing from Equation B3 from Table B.1.

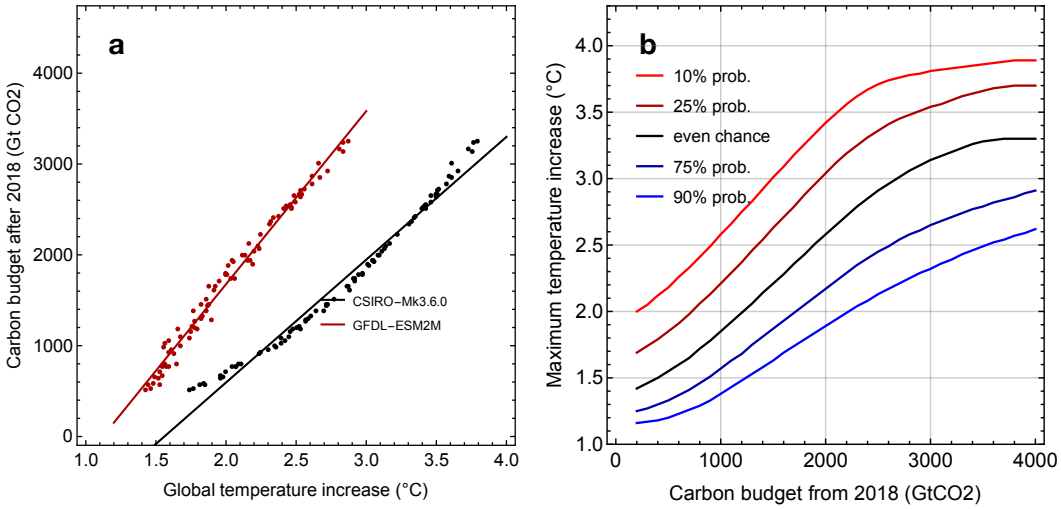

Figure A.21: Plots produced with non-linear forcing from Equation B4 from Table B.1.

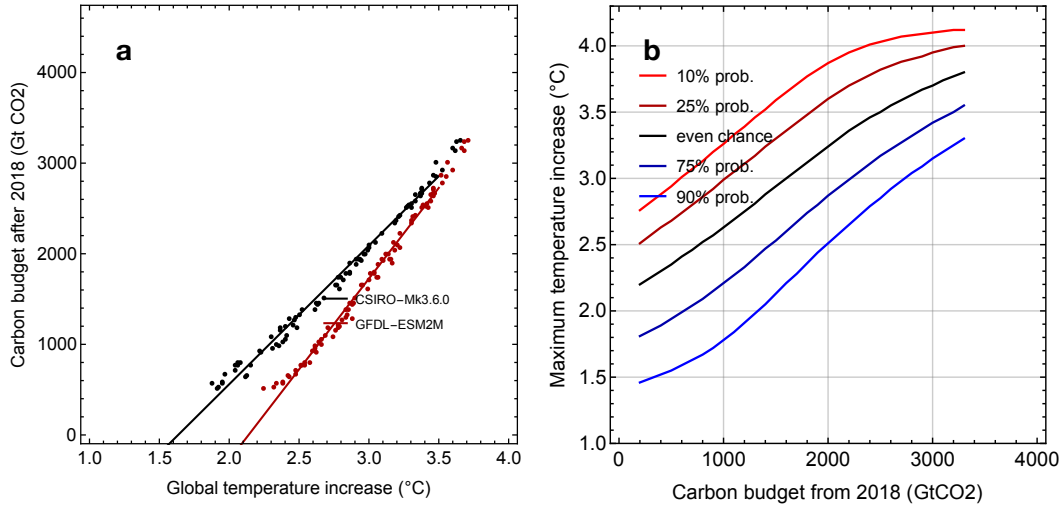

Figure A.22: Plots produced with non-linear forcing from Equation B5 from Table B.1.

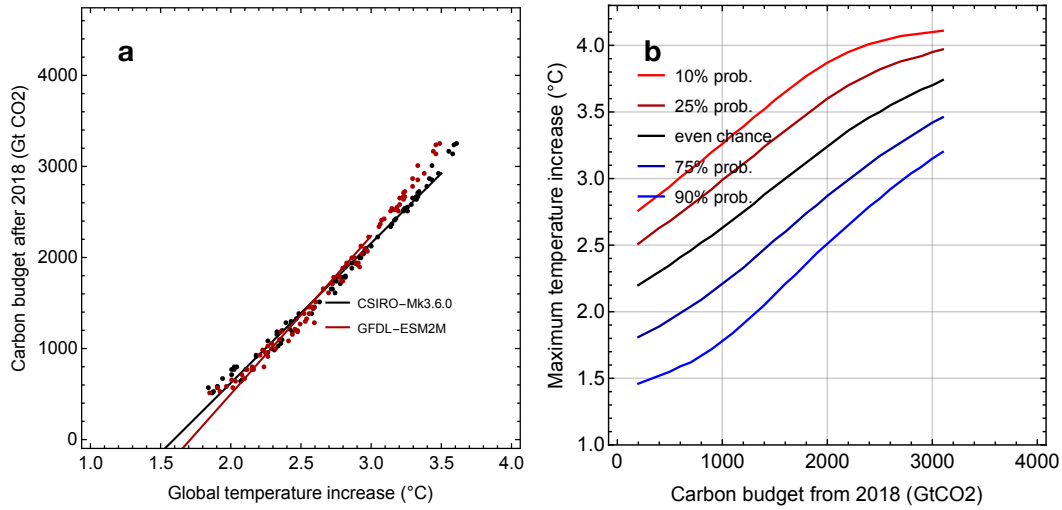

Figure A.23: Plots produced with non-linear forcing from Equation B6 from Table B.1.

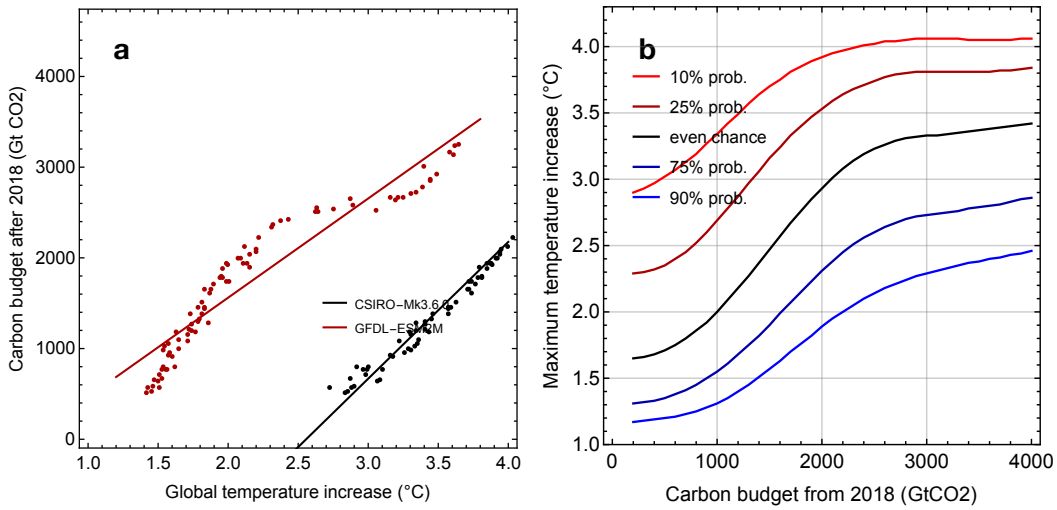

Figure A.24: Plots produced with non-linear forcing from Equation B7 from Table B.1.

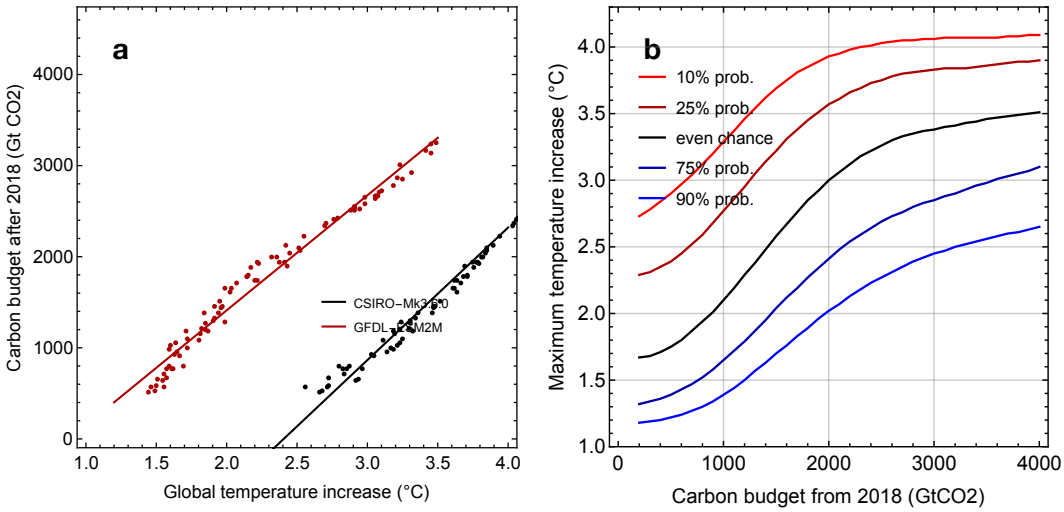

Figure A.25: Plots produced with non-linear forcing from Equation B8 from Table B.1.

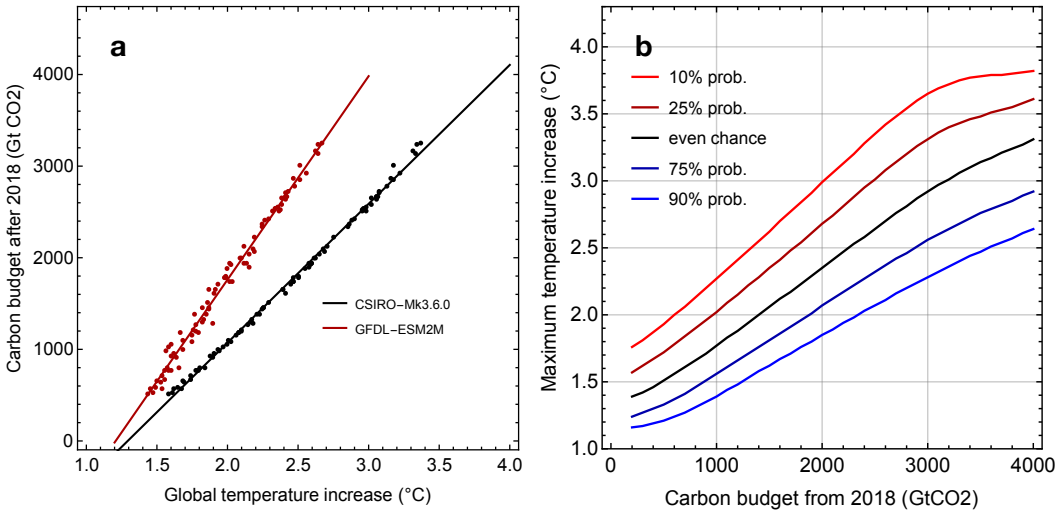

Figure A.26: Plots produced with non-linear forcing from Equation B9 from Table B.1.

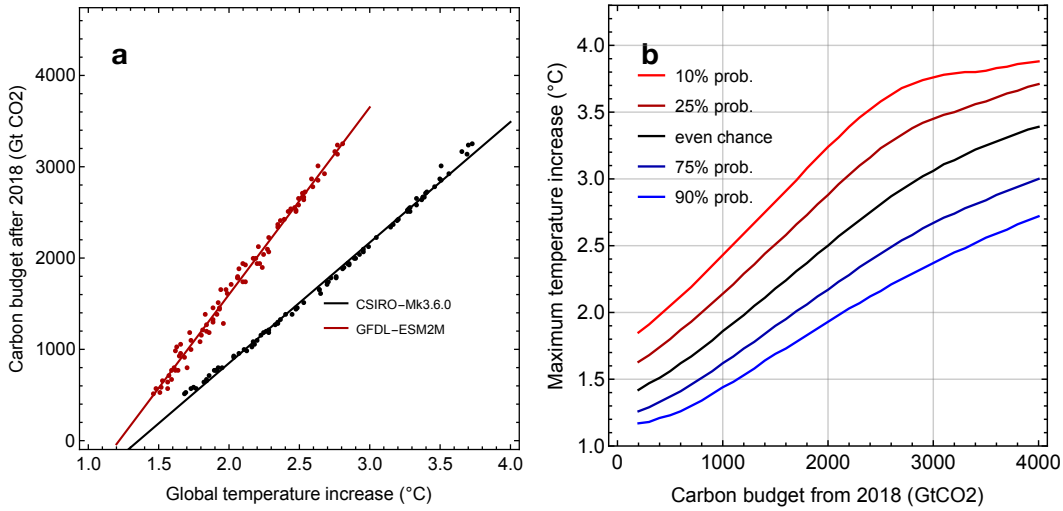

Figure A.27: Plots produced with non-linear forcing from Equation B10 from Table B.1.

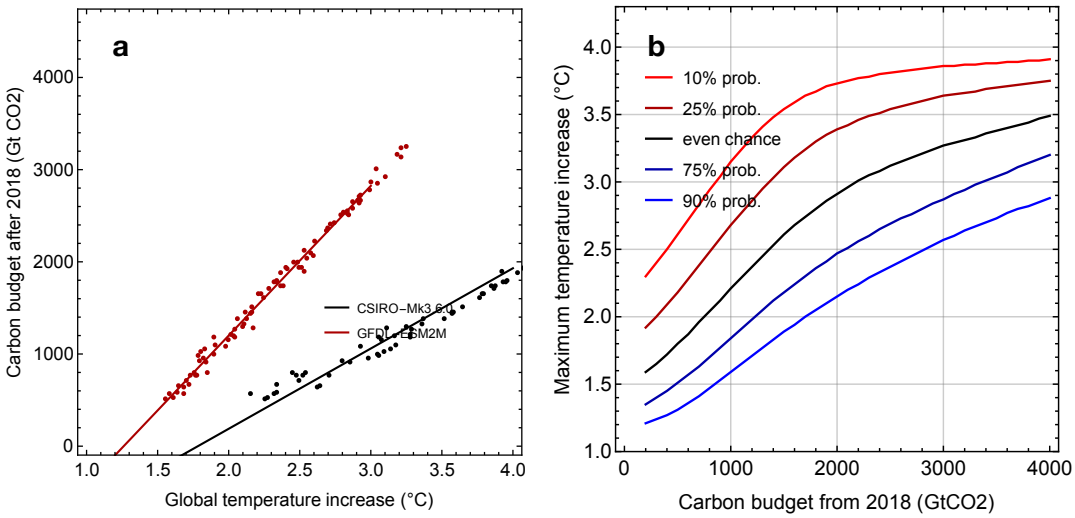

Figure A.28: Plots produced with non-linear forcing from Equation B11 from Table B.1.

As described in Section 2.6 and Section 3.6, the implementation of the non-linear forcing framework uses fixed-point iteration. In addition to the proof in Section 2.6, we tested the implication the number of iterations had on the RCB estimates, based on the full RCB estimate in Figure 3.7(d). Thus including carbon-, climate model combinations and internal variability. The estimates were done for Equation B1 and B5 from Table B.1, for 5, 10 and 50 iterations, as illustrated in Figure A.29.

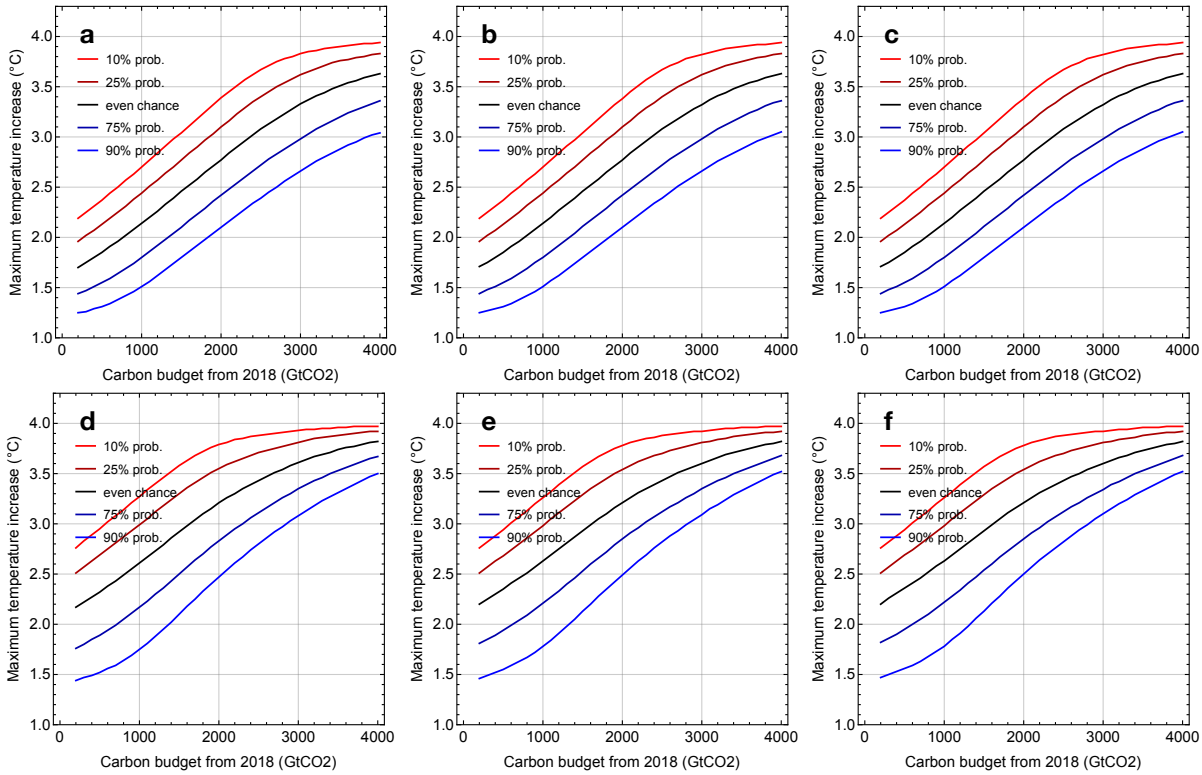

Figure A.29: Illustration of the small impact the number of iterations had on the RCB estimates, based on Figure 3.7(d). **(a,b,c)** denotes the estimate for Equation B1 in Table B.1, for 5, 10 and 50 iterations, respectively. **(d,e,f)** follow in the same manner of 5, 10 and 50 iterations for Equation B5.

Our research partner Andreas Johansen produced additional plots for the study on the Arctic amplification factor (Johansen, 2020) (See Figure A.30-A.32). Each of the following plots were estimated using non-linear forcing relations from Table B.1. The illustration of the RCB estimates with and without the Arctic amplification factor shows in (a) and (b), respectively.

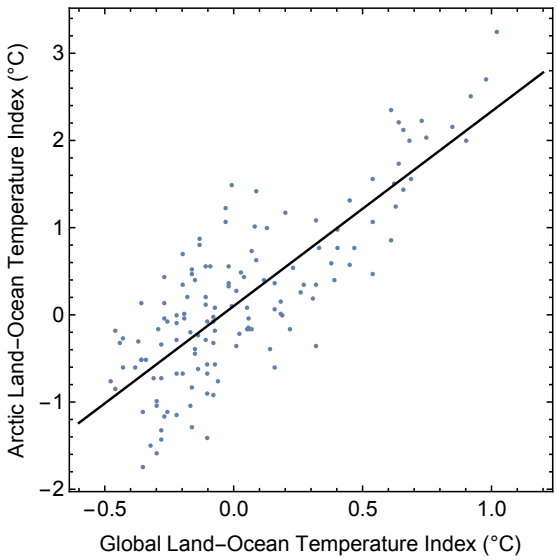

Figure A.30: Relationship between Global- and Arctic Land-Ocean Temperature Index. Estimate of the Arctic amplification factor illustrated with black line.

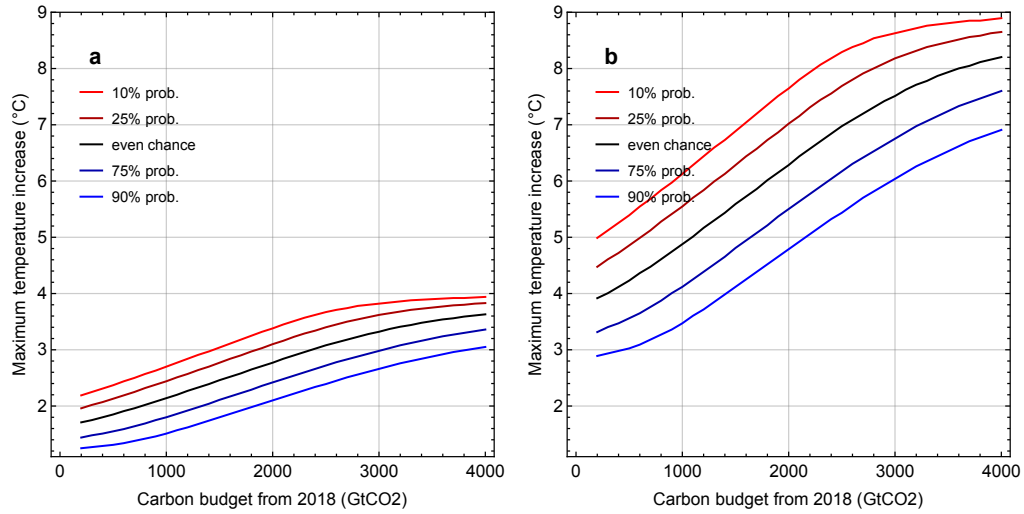

Figure A.31: Estimated when including non-linear forcing from Equation B1 from Table B.1. **(a)** and **(b)** shows the estimated RCB before and after the inclusion of the Arctic amplification factor, respectively.

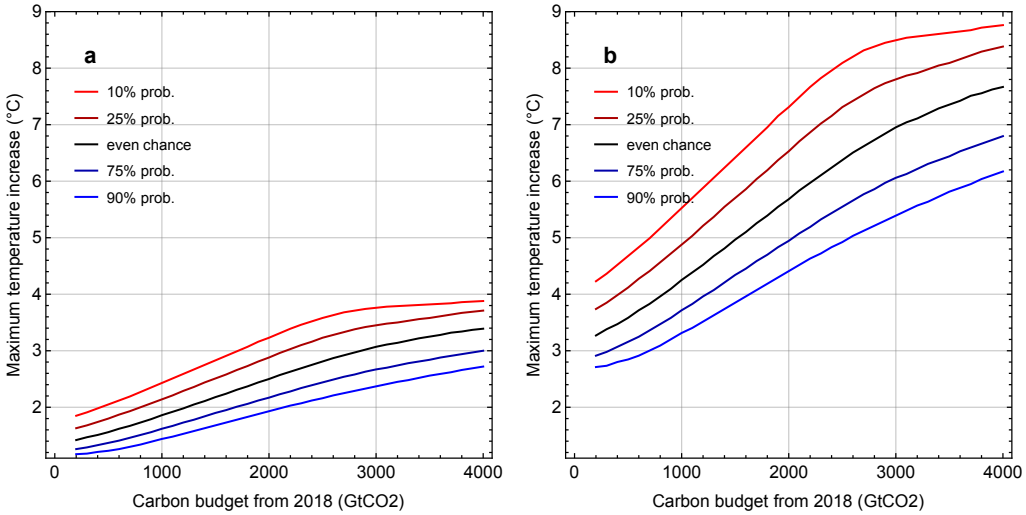

Figure A.32: Estimated when including non-linear forcing from Equation B10 from Table B.1. **(a)** and **(b)** shows the estimated RCB before and after the inclusion of the Arctic amplification factor, respectively.

Martinsen (2020) produced additional plots for the study on the comparison between the RCB estimates of the Simple Response Model and MAGICC.

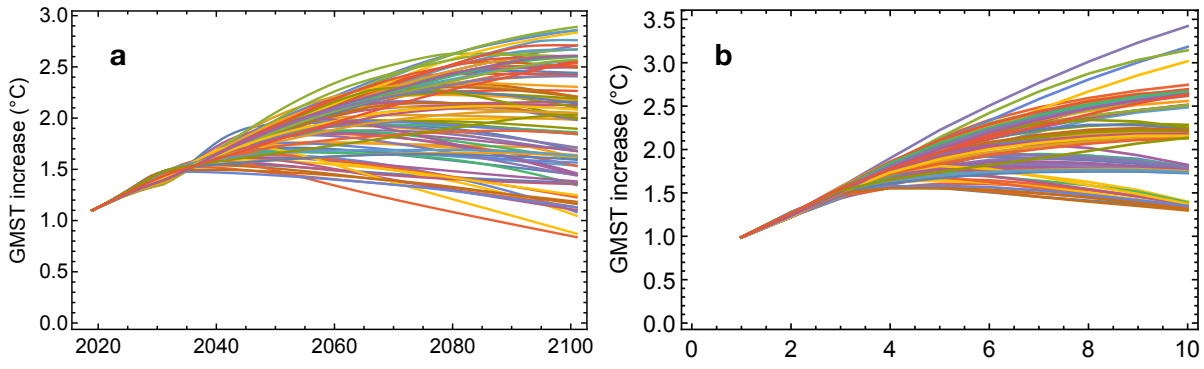

Figure A.33: Estimated temperature response for the linear SRM and MAGICC using the same 86 emission scenarios. Visualised scatterplot in Figure A.18(a) and Figure A.18(d). **(a)** SRM estimate. **(b)** MAGICC estimate.

The following scatterplots compare the impact the non-linear forcing relations from Table B.1 has on the RCB estimates (Martinsen, 2020). More detailed explanation found in figure text of Figure 3.13.

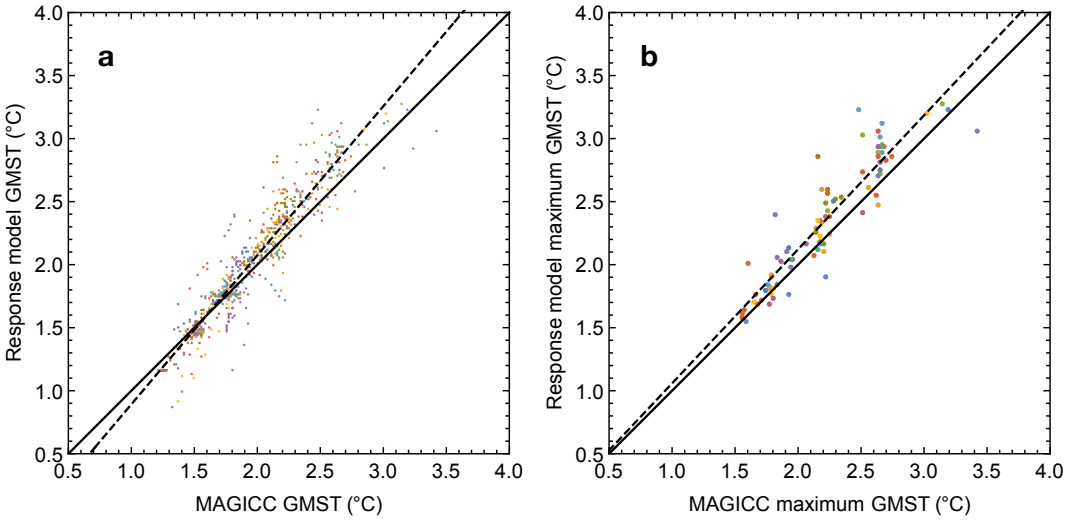

Figure A.34: Estimated SRM impact from Equation B10 in Table B.1 when comparing to MAGICC. **(a)** illustrates the temperature response over each decade for 86 scenarios from 2020-2100, resulting in 774 datapoints. **(b)** illustrates the estimate maximum GMST regardless of time for each scenario.

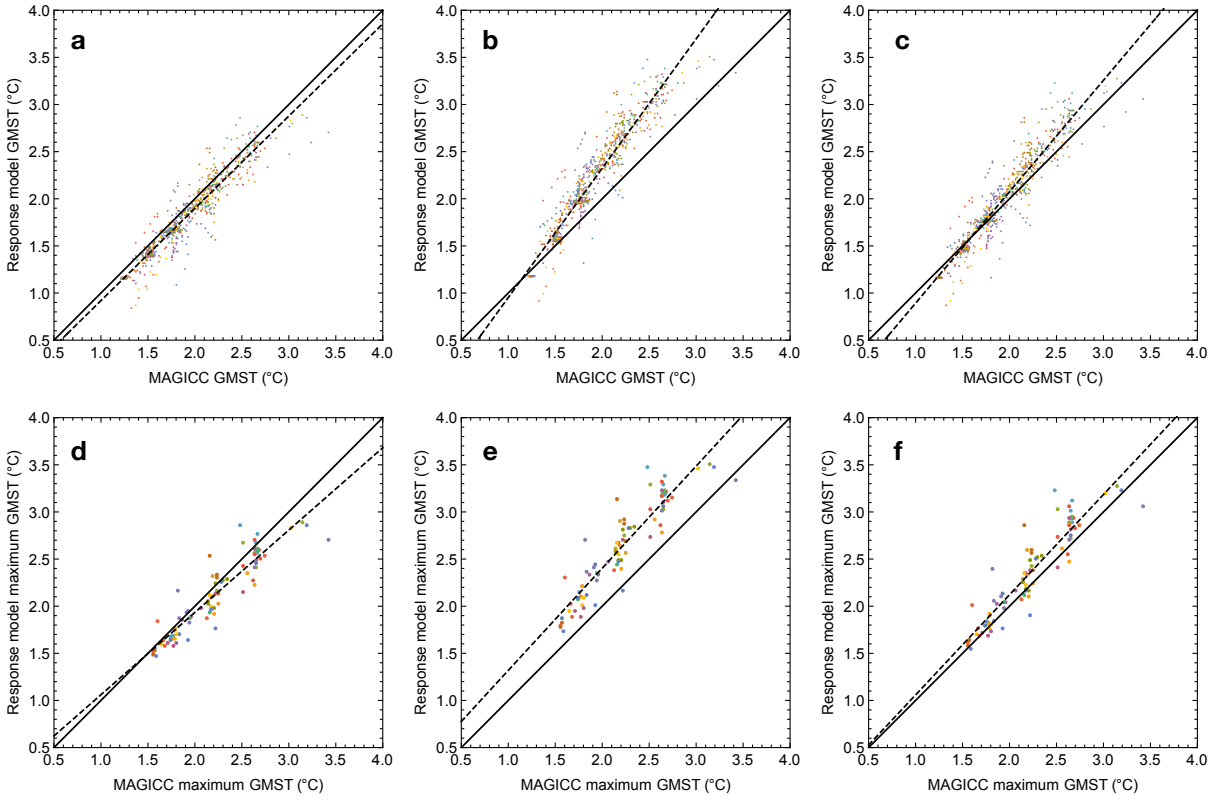

Figure A.35: Comparison between the linear SRM and when including Equation B1 and B10 as non-linear forcing. In **(a,b,c)** we see the temperature response of the linear SRM, Equation B1 and B10, respectively, while **(d,e,f)** shows the estimated maximum temperature response from the linear SRM, Equation B1 and B10, respectively.

Appendix B

Non-linear forcing equations

For the inclusion of non-linear forcing we examined a number of equations. These equations are summarized in Table B.1 with their designated parameters, using one of the two equations below. The hyperbolic tangent relation consists of the variable T, illustrating the global mean surface temperature, the magnitude of the radiative forcing represented by M, the temperature threshold denoted by $T_{\mathrm{THRESHOLD}}$ and the steepness of the forcing through variable, S.

$$\Delta f_{non-lin} = 0.5 \times M \times \left(1 + \mathrm{Tanh}\left(\frac{T - T_{\mathrm{THRESHOLD}}}{S}\right)\right). \qquad (\mathrm{B1} - \mathrm{B8})$$

The linear relation consists of the GMST denoted by variable T and the linear multiplication factor L. Tested equations are summarised in

$$\Delta f_{\mathrm{non-lin}} = L \times T \qquad (\mathrm{B9} - \mathrm{B11})$$

Table B.1: Summary of parameters for the two analysed equations for the non-linear forcing framework discussed in Section 3.6. The variable T, illustrates the GMST, the magnitude of the radiative forcing (W/m^2) represented by M, the temperature threshold denoted by $T_{\mathrm{THRESHOLD}}$ and the steepness of the forcing through variable, S. The column Discarded denotes if the estimated TCRE's broke the approximate linearity, i.e. if they could yield an valid RCB

Equation #	M(Wm^{-2})	$T_{\mathrm{THRESHOLD}}$(°C)	S(°C)	L(Wm^{-2}°C^{-1})	Discarded
B1	1	2	0.5		No
B2	1	2	1		No
B3	1	3	0.5		No
B4	1	3	1		No
B5	2	2	0.5		No
B6	2	2	1		Yes
B7	2	3	0.5		Yes
B8	2	3	1		No
B9				0.1	No
B10				0.2	No
B11				0.45	No

Mean TCRE calculation

This approximation for a SRM mean TCRE bases on Figure A.5, with the best estimate carbon model, 14 of the ESM's from the CMIP5 ensemble. Neither the internal variability or the non-linear forcing framework was included.

By looking at temperature targets for 2°C and 3°C the related RCBs are visually approximated to 1600 $GtCO_2$ and 2600 $GtCO_2$, respectively. Thus we have a TCRE of 1°C/2000$GtCO_2$ (0.5°C/1000$GtCO_2$) which translates to 1°C/545 GtC and 1.8°C/1000 GtC through factor 44/12, due to the molecular weight of the CO_2 molecule in comparison to the carbon atom (Collins et al., 2013).

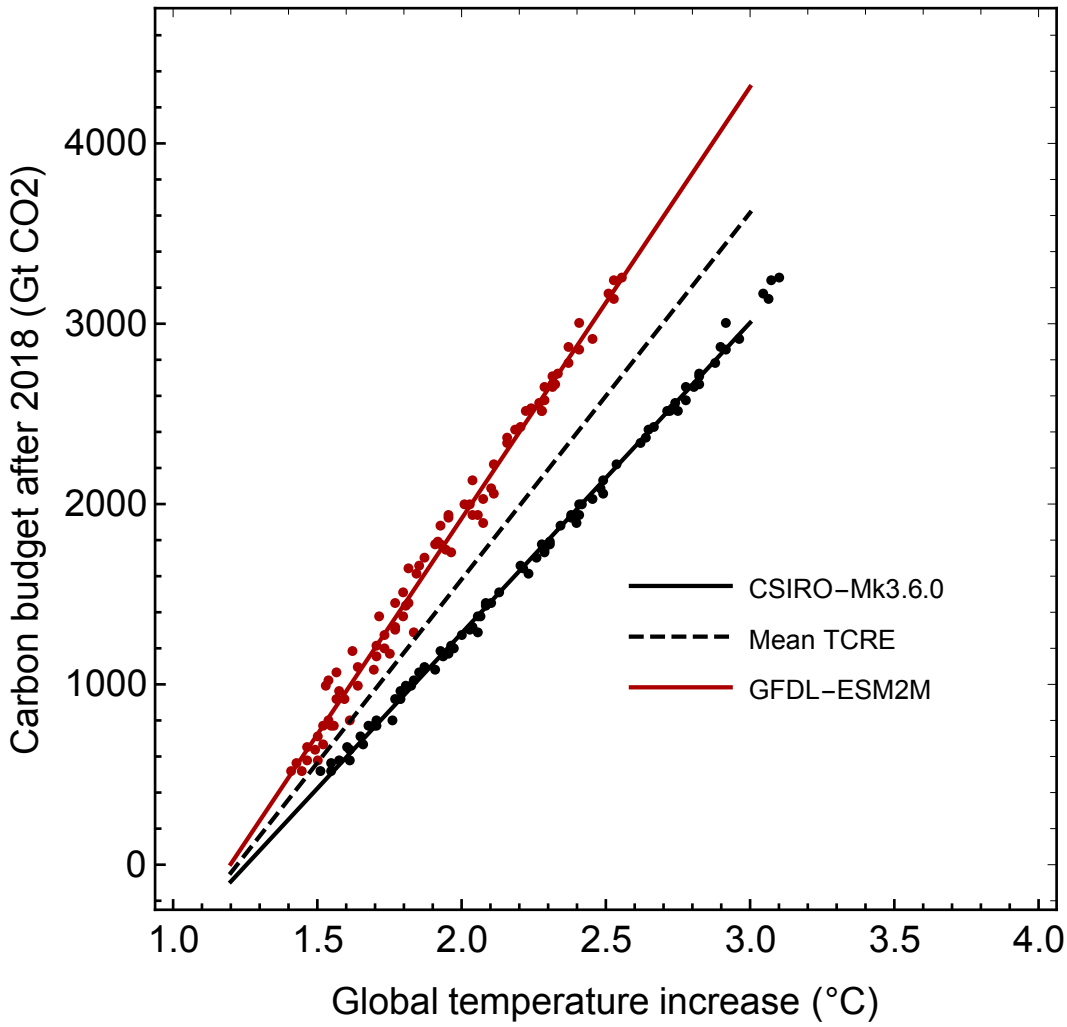

Figure B.1: Illustration of the TCRE for two climate models (black and red line) from the CMIP5 model ensemble, and our best estimate carbon model. Each dot is one of the 86 emission scenarios. The black dashed line denotes the mean TCRE of each of the 14 CMIP5 models.

Appendix C

Code for linear SRM

The following code is used for plotting the linear SRM as described in Section 3.1-3.5. Produced in Mathematica 12.0.0.0 in collaboration with research partners Andreas Johansen, Andreas Martinsen and supervision from Martin Rypdal.

Platform: Mac OS X x86 (64-bit). macOS Catalina: Version 10.15.3.

```
In[283]:= SetDirectory["OneDrive - UiT Office 365"];
Z = Import["SSP_IAM_V2_201811.csv"];
Z = Map[StringSplit[#, ","] &, Z];

In[5]:= hh=157.65890684920566`+1.8942819330281027`zz+0.08520850267749702`zz^2;

In[6]:= Z[[1]]
Out[6]= {{MODEL, "SCENARIO", "REGION", "VARIABLE", "UNIT",
2005, 2010, 2020, 2030, 2040, 2050, 2060, 2070, 2080, 2090, 2100}}

In[7]:= RR=Table[Z[[k]][[1]][[4]],{k,1,Length[Z]}];
Union[RR]

Out[8]= {"Agricultural Demand|Crops", "Agricultural Demand|Crops|Energy",
"Agricultural Demand|Livestock", "Agricultural Production|Crops|Energy",
"Agricultural Production|Crops|Non-Energy","Agricultural Production|Livestock", "Capacity|Electricity",
"Capacity|Electricity|Biomass", "Capacity|Electricity|Coal", "Capacity|Electricity|Gas",
"Capacity|Electricity|Geothermal", "Capacity|Electricity|Hydro", "Capacity|Electricity|Nuclear",
"Capacity|Electricity|Oil", "Capacity|Electricity|Other", "Capacity|Electricity|Solar", "Capacity|Electricity|Solar|CSP",
"Capacity|Electricity|Solar|PV", "Capacity|Electricity|Wind", "Capacity|Electricity|Wind|Offshore",
"Capacity|Electricity|Wind|Onshore", "Consumption", "Diagnostics|MAGICC6|Concentration|CH4",
"Diagnostics|MAGICC6|Concentration|CO2", "Diagnostics|MAGICC6|Concentration|N2O",
"Diagnostics|MAGICC6|Forcing", "Diagnostics|MAGICC6|Forcing|Aerosol", "Diagnostics|MAGICC6|Forcing|CH4",
"Diagnostics|MAGICC6|Forcing|CO2", "Diagnostics|MAGICC6|Forcing|F-Gases",
"Diagnostics|MAGICC6|Forcing|Kyoto Gases", "Diagnostics|MAGICC6|Forcing|N2O",
"Diagnostics|MAGICC6|Temperature|Global Mean", "Emissions|BC", "Emissions|CH4",
"Emissions|CH4|Fossil Fuels and Industry", "Emissions|CH4|Land Use", "Emissions|CO",
"Emissions|CO2", "Emissions|CO2|Carbon Capture and Storage",
"Emissions|CO2|Carbon Capture and Storage|Biomass","Emissions|CO2|Fossil Fuels and Industry",
"Emissions|CO2|Land Use", "Emissions|F-Gases", "Emissions|Kyoto Gases", "Emissions|N2O",
"Emissions|N2O|Land Use", "Emissions|NH3", "Emissions|NOx", "Emissions|OC", "Emissions|Sulfur",
"Emissions|VOC", "Energy Service|Transportation|Freight", "Energy Service|Transportation|Passenger",
"Final Energy","Final Energy|Electricity", "Final Energy|Gases", "Final Energy|Heat",
"Final Energy|Hydrogen", "Final Energy|Industry", "Final Energy|Liquids",
"Final Energy|Residential and Commercial", "Final Energy|Solar","Final Energy|Solids",
"Final Energy|Solids|Biomass","Final Energy|Solids|Biomass|Traditional", "Final Energy|Solids|Coal",
"Final Energy|Transportation", "GDP|PPP", "Harmonized Emissions|BC",
"Harmonized Emissions|CH4|Fossil Fuels and Industry","Harmonized Emissions|CH4|Land Use",
"Harmonized Emissions|CO","Harmonized Emissions|CO2|Fossil Fuels and Industry",
"Harmonized Emissions|CO2|Land Use", "Harmonized Emissions|F-Gases", "Harmonized Emissions|Kyoto Gases",
"Harmonized Emissions|NH3", "Harmonized Emissions|NOx", "Harmonized Emissions|OC",
"Harmonized Emissions|Sulfur", "Harmonized Emissions|VOC","Land Cover|Built-up Area",
"Land Cover|Cropland", "Land Cover|Forest", "Land Cover|Pasture", "Population", "Price|Carbon", "Primary Energy",
"Primary Energy|Biomass", "Primary Energy|Biomass|Traditional", "Primary Energy|Biomass|w/ CCS",
"Primary Energy|Biomass|w/o CCS", "Primary Energy|Coal", "Primary Energy|Coal|w/ CCS",
"Primary Energy|Coal|w/o CCS", "Primary Energy|Fossil", "Primary Energy|Fossil|w/ CCS",
"Primary Energy|Fossil|w/o CCS","Primary Energy|Gas", "Primary Energy|Gas|w/ CCS",
"Primary Energy|Gas|w/o CCS", "Primary Energy|Geothermal","Primary Energy|Hydro",
"Primary Energy|Non-Biomass Renewables","Primary Energy|Nuclear", "Primary Energy|Oil",
```

"Primary Energy|Oil|w/ CCS", "Primary Energy|Oil|w/o CCS","Primary Energy|Other",
"Primary Energy|Secondary Energy Trade","Primary Energy|Solar", "Primary Energy|Wind",
"Secondary Energy|Electricity", "Secondary Energy|Electricity|Biomass",
"Secondary Energy|Electricity|Biomass|w/ CCS","Secondary Energy|Electricity|Biomass|w/o CCS",
"Secondary Energy|Electricity|Coal","Secondary Energy|Electricity|Coal|w/ CCS",
"Secondary Energy|Electricity|Coal|w/o CCS","Secondary Energy|Electricity|Gas",
"Secondary Energy|Electricity|Gas|w/ CCS", "Secondary Energy|Electricity|Gas|w/o CCS",
"Secondary Energy|Electricity|Geothermal","Secondary Energy|Electricity|Hydro",
"Secondary Energy|Electricity|Non-Biomass Renewables","Secondary Energy|Electricity|Nuclear",
"Secondary Energy|Electricity|Oil", "Secondary Energy|Electricity|Solar", "Secondary Energy|Electricity|Wind",
"Secondary Energy|Gases", "Secondary Energy|Gases|Biomass","Secondary Energy|Gases|Coal",
"Secondary Energy|Gases|Natural Gas", "Secondary Energy|Heat", "Secondary Energy|Heat|Geothermal",
"Secondary Energy|Hydrogen", "Secondary Energy|Hydrogen|Biomass",
"Secondary Energy|Hydrogen|Biomass|w/ CCS", "Secondary Energy|Hydrogen|Biomass|w/o CCS",
"Secondary Energy|Hydrogen|Electricity", "Secondary Energy|Liquids", "Secondary Energy|Liquids|Biomass",
"Secondary Energy|Liquids|Biomass|w/ CCS", "Secondary Energy|Liquids|Biomass|w/o CCS",
"Secondary Energy|Liquids|Coal", "Secondary Energy|Liquids|Coal|w/ CCS",
"Secondary Energy|Liquids|Coal|w/o CCS", "Secondary Energy|Liquids|Gas",
"Secondary Energy|Liquids|Gas|w/ CCS", "Secondary Energy|Liquids|Gas|w/o CCS",
"Secondary Energy|Liquids|Oil", "Secondary Energy|Solids", "VARIABLE"}

In[9]:= **RRR=Table[Z[[k]][[1]][[3]],{k,1,Length[Z]}];**
Union[RRR]

Out[10]= {"R5.2ASIA", "R5.2LAM", "R5.2MAF", "R5.2OECD", "R5.2REF", "REGION", "World"}

In[11]:= **co2pos1=Position[RR,_?(#=="\"Emissions|CO2|FossilFuelsandIndustry\""&)];**
co2pos2 = Position[RR, _ ? (# == "\"Emissions|CO2|Land Use\"" &)];
co2pos3 = Position[RRR, _ ? (# == "\"World\"" &)];

In[14]:= **ppos1=Intersection[co2pos3,co2pos1];**
ppos2 = Intersection[co2pos3, co2pos2];

In[16]:= **Extract[Z,co2pos1][[1]]**

Out[16]= {{AIM/CGE, "SSP1-19", "R5.2ASIA", "Emissions|CO2|Fossil Fuels and Industry", "Mt CO2/yr", 8985.6725,
10008.8152, 11790.747500000001,
6131.6627, 3271.4353000000006, 1678.8029, 638.87, 259.4755, 82.29590000000003, -7.9353000000000105, -
103.9171}}

In[17]:= **em1=ToExpression[Map[Drop[Flatten[#],7]&,Extract[Z,ppos1]]];**
em2 = ToExpression[Map[Drop[Flatten[#], 7] &, Extract[Z, ppos2]]];

In[19]:= **ListPlot[em1,PlotRange→All,Joined→True]**

In[20]:= **Length[em1]**
Out[20]= 127

In[21]:= **emissions=Map[#[[1;;2]]&,ToExpression[Map[StringSplit[#] &, Drop[ReadList["emissionsCO2.txt",
String], 31]]]];**
emissions = Table[{emissions[[i, 1]], (44 / 12) * emissions[[i, 2]] / 1000.}, {i, 1, Length[emissions]}];
ListPlot[emissions, Joined → True, PlotStyle → {Black, Thick}, PlotRange → All, Axes → False, Frame → True,
FrameStyle → Directive[14, Black],
FrameLabel → {"year", "CO_2 emissions (Gt CO/yr)"}]
(*historical emissions*)

EM = Join[emissions, {{2018, 37.1}}];
data2 = Table[Prepend[Table[{t, Interpolation[Join[EM, Transpose[{{2030, 2040, 2050, 2060, 2070, 2080,
2090, 2100}, 0.001 * Drop[em1[[k]], 1]}]][t]}, {t, 1751, 2100}], {1750, 0}], {k, 1, Length[em1]}]; totliste = Ta-
ble[data2[[k]][[All, 2]], {k, 1, Length[data2]}];
PLAll = ListPlot[data2, Joined → True, Frame → True, FrameStyle → Directive[Black, 14], PlotRange → All,
FrameLabel → {None, "CO2 emissions (Gt CO2)"}]

```
positivepaths = Table[DeleteCases[Map[# * UnitStep[#] &, totliste[[k]][[269 ;; 351]]], _ ? (# == 0 &)], {k, 1,
Length[totliste]}]; ListPlot[positivepaths, Joined → True, PlotRange → All]
(*Before removal of exceedance scenarios*)

In[29]:= RCBliste2=Map[Plus@@#&,positivepaths];

In[175]:= p1=Position[RCBliste2,_?(#<3300&)];

In[31]:= maxtemp=Map[Max[#]&,templiste];
maxtemp2 = Map[Max[#] &, uptempliste];
maxtemp3 = Map[Max[#] &, lowtempliste];

PL1 = ListPlot[Extract[data2, p1], Joined → True,Frame → True, FrameStyle → Directive[Black, 14], PlotRange
→ All];
PL2 = ListPlot[EM, PlotStyle → Black, Joined → True];
FFC = Show[{PL1, PL2}, FrameLabel → {None, "CO2 emissions (Gt CO2)"}, Epilog → Inset[Style["", 18],
Scaled[{0.1, 0.9}]]]
(*After removal of exceedance scenarios*)

In[37]:= PL1=ListPlot[data2[[1]],Joined→True,Frame→True, FrameStyle → Directive[Black, 14], PlotStyle →
Darker[Blue]];
PL2 = ListPlot[EM, PlotStyle → Black, Joined → True];
FFA = Show[{PL1, PL2}, FrameLabel → {None, "CO2 emissions (Gt CO2)"}, Epilog → Inset[Style["a", 18],
Scaled[{0.1, 0.9}]]]

In[40]:= n=Length[data2[[1]]];
futuretime = 2100 - 2020;
τmetan = 12.4;

In[43]:= (* Carbon model *)
τ1=1;
τ2=10;
τ3 = 100;
τ4 = 1000;
c1mean = 0.152;
c2mean = 0.246;
c4mean = 0.134;
c5mean = 0.194;

Gmean = (12/44) *0.47* (c1mean * Table[Exp[- (i - j) / τ1] * UnitStep[i - j], {i, 1, n}, {j, 1, n}]
+ c2mean * Table[Exp[- (i - j) / τ2] * UnitStep[i - j], {i, 1, n}, {j, 1, n}] + (1 - c1mean - c2mean - c4mean -
c5mean)* Table[Exp[- (i - j) / τ3] * UnitStep[i - j], {i, 1, n}, {j, 1, n}]
+ c4mean * Table[Exp[- (i - j) / τ4] * UnitStep[i - j], {i, 1, n}, {j, 1, n}] + Table[c5mean * UnitStep[i - j], {i, 1, n}, {j,
1, n}]);

In[52]:= (* Carbon models *)
c1upper = 0.11;
c2upper = 0.212;
c4upper = 0.106;
c5upper = 0.262;
c1lower = 0.18;
c2lower = 0.296;
c4lower = 0.122;
c5lower = 0.148;

Glower = (12 / 44) * 0.47 * (c1lower * Table[Exp[- (i - j) / τ1] * UnitStep[i - j], {i, 1, n}, {j, 1, n}] + c2lower * Ta-
ble[Exp[- (i - j) / τ2] * UnitStep[i - j], {i, 1, n}, {j, 1, n}] + (1 - c1lower - c2lower - c4lower - c5lower) * Ta-
ble[Exp[- (i - j) / τ3] * UnitStep[i - j], {i, 1, n}, {j, 1, n}] + c4lower * Table[Exp[- (i - j) / τ4] * UnitStep[i - j], {i, 1,
n}, {j, 1, n}] + Table[c5lower * UnitStep[i - j], {i, 1, n}, {j, 1, n}]);

Gupper = (12/44) *0.47* (c1upper * Table[Exp[- (i - j) / τ1] * UnitStep[i - j], {i, 1, n}, {j, 1, n}] + c2upper * Ta-
ble[Exp[- (i - j) / τ2] * UnitStep[i - j], {i, 1, n}, {j, 1, n}] + (1 - c1upper - c2upper - c4upper - c5upper) *
```

```
Table[Exp[- (i - j) / τ3] * UnitStep[i - j], {i, 1, n}, {j, 1, n}] + c4upper * Table[Exp[- (i - j) / τ4] * UnitStep[i - j], {i,
1, n}, {j, 1, n}] + Table[c5upper * UnitStep[i - j], {i, 1, n}, {j, 1, n}]);

In[62]:=
(*Optimal Estimation of Stochastic Energy Balance Model Parameters *)



In[63]:= (* Climate models *)
models = ReadList["CMIP5parameters.txt", String];
models = Delete[models, {{5}, {12}}];
boxes = StringSplit[models][[All, 2]];
Klimaliste = {};
Γliste = {};
σ2liste = {};
Monitor[
Do[

Clear[A];
modelnr = p; If[boxes[[p]] == "2",

{C1, C2, κ1, κ2, σ1, Γ, σ2} = ToExpression[Drop[StringSplit[models[[modelnr]]], 2]];

A = {{-(κ1+ κ2) /C1, κ2/C1}, {κ2/C2, -κ2/C2}};
g = (MatrixExp[t A].{1 / C1, 0})[[1]];
Gklima = Table[Chop[(g /. t → (i - j)) * UnitStep[i - j]], {i, 1, n}, {j, 1, n}];
Klimaliste = Append[Klimaliste, Gklima];
];

If[ boxes[[p]] == "3",

{C1, C2, C3, κ1, κ2, κ3, σ1, Γ, σ2} = ToExpression[Drop[StringSplit[models[[modelnr]]], 2]];

A = {{-(κ1+ κ2) /C1, κ2/C1, 0}, {κ2/C2, -(κ2+κ3)/C2, κ3/C2},{0, κ3/C3, - κ3/C3}};

g = (MatrixExp[t A].{1 / C1, 0, 0})[[1]];
Gklima = Table[Chop[(g /. t → (i - j)) * UnitStep[i - j]], {i, 1, n}, {j, 1, n}];
Klimaliste = Append[Klimaliste, Gklima];
];

If [ boxes[[p]] == "4",

{C1, C2, C3, C4, κ1, κ2, κ3, κ4, σ1, Γ, σ2} = ToExpression[Drop[StringSplit[models[[modelnr]]], 2]];

A = {{-(κ1+κ2)/C1, κ2/C1, 0, 0} , {κ2/C2, -(κ2+κ3)/C2, κ3/C2, 0},{ 0, κ3/C3, -(κ3+κ4)/C3, κ4/C3},
{0, 0, κ4/C4, -κ4/C4}};

g = (MatrixExp[t A].{1 / C1, 0, 0, 0})[[1]];
Gklima = Table[Chop[(g /. t → (i - j)) * UnitStep[i - j]], {i, 1, n}, {j, 1, n}];
Klimaliste = Append[Klimaliste, Gklima];
];

Γliste = Append[Γliste, Γ];
σ2liste = Append[σ2liste, σ2];
, {p, 1, Length[models]}
];
, {p, boxes[[p]]}
];

In[70]:= RCBliste={};
totliste = {};
```

```
templiste = {};
uptempliste = {};
lowtempliste = {};
alltliste = {};
Δfaeroliste = {};
Δfghgliste = {};
Δfliste = {};
noiseliste = {};

Monitor[
Do[
tot = data2[[u]][[All, 2]]; meanco2 = Gmean.tot + 280;

(* metan *)
del1 = 11.9 * tot[[1 ;; Length[EM]]];
(* The factor 11.9 tunes 2019 methane emmisions in 2019 to 440 Tg Methane *) ;
del2 = hh /. zz → tot[[Length[EM] + 1 ;; Length[tot]]];
del2 = Last[del1] + (del2 - First[del2]) * (Last[del1] - Last[del2]) / (First[del2] - Last[del2]);
metemis = Join[del1, del2];

Gmetan = 0.34 * Table[Exp[- (i - j) / τmetan] * UnitStep[i - j], {i, 1, n}, {j, 1, n}];
(* The factor 0.34 tunes 2019 methane concentration to around 1880 ppb *)
metan = Map[Max[#, 0] &, 700 + Gmetan.metemis];

Δfmetan = 0.036 * (Sqrt[metan] - Sqrt[700]);
Δfco2 = 5.35 Log[1 + (meanco2 - 280) / 280]; (* CO2 til forcing*)
Δfaer= -0.02tot;
Δfaer1 = Δfaer[[1 ;; Length[EM]]] ;
Δfaer2 = Drop[Δfaer, Length[EM]] ;
Δfaer2 = Map[Min[-0.4, #] &, Δfaer2];
Δfaer = Join[Δfaer1, Δfaer2];
Δf = Δfco2 + Δfaer + Δfmetan;

Δfliste = Append[Δfliste, Δf];
Δfaeroliste = Append[Δfaeroliste, Δfaer];
Δfghgliste = Append[Δfghgliste, Δfco2 + Δfmetan];

Tliste = {};
Do[
T2 = Klimaliste[[p]].Δf;
noise = σ2liste[[p]] * (Klimaliste[[p]].RandomReal[NormalDistribution[0, 1], Length[Δf]]);
noise = Drop[noise, 268 - 20];
T2 = T2 * (Γliste[[p]] / Log[4.]) / 5.35;
T2 = Drop[T2, 268];
T2=1.1+T2-T2[[1]];
noiseliste = Append[noiseliste, noise]; Tliste = Append[Tliste, T2];
, {p, 1, Length[models]}];

middel =Table[Mean[Transpose[Tliste][[i]]], {i, 1, Length[Transpose[Tliste]]}];
upper = Table[Mean[Transpose[Tliste][[i]]] + StandardDeviation[ Transpose[Tliste][[i]]], {i, 1, Length[Trans-
pose[Tliste]]}];
lower = Table[Mean[Transpose[Tliste][[i]]] - StandardDeviation[ Transpose[Tliste][[i]]], {i, 1, Length[Trans-
pose[Tliste]]}];
RCB = Plus @@ Drop[tot, 270];
RCBliste = Append[RCBliste, RCB];
totliste = Append[totliste, tot];
alltliste = Join[alltliste, Tliste];
templiste = Append[templiste, middel];
uptempliste = Append[uptempliste, upper];
lowtempliste = Append[lowtempliste, lower];
, {u, 1, Length[data2]}]
, u];
```

In[183]:= **Length[noise]**
Out[183]= 103

In[82]:= **Length[T2]**
Out[82]= 83

In[83]:= **window=10;**
noiseliste2 = Table[MovingAverage[noiseliste[[i]], window][[1 ;; Length[T2]]], {i, 1, Length[noiseliste]}];
noiseliste2 = Transpose[Partition[noiseliste2, 14]];

In[86]:= **Length[noiseliste2]**
Out[86]= 14

In[87]:= **Dimensions[noiseliste2]**
Out[87]= {14, 127, 83}

In[88]:= **Length[noiseliste2[[1]]]**
Out[88]= 127

PLNoise = ListPlot[Map[Transpose[{2018 + Range[Length[templiste[[1]]]], #}] &, noiseliste2[[3]]], Joined → True];
FFNoise = Show[PLNoise, PlotRange → All, Joined → True, Axes → False, Frame → True, FrameStyle → Directive[Black, 14], Joined → True, FrameLabel → {None, "Internal temperature variability(°C)"}, Epilog → Inset[Style["", 18], Scaled[{0.1, 0.9}]]]
(*Plot of internal variability*)

In[90]:= **FFE=ListPlot[Map[Transpose[{2018+Range[Length[templiste[[1]]]],#}]&, Extract[templiste, p1]], PlotRange → All, Joined → True, Axes → False, Frame → True, FrameStyle → Directive[Black, 14], FrameLabel → {None, "GMST increase (°C)"},Epilog → Inset[Style["e", 18], Scaled[{0.1, 0.9}]]]**
(*Temperature response*)

In[121]:= **PL3=ListPlot[Map[Transpose[{1749+Range[Length[Δfaeroliste[[1]]]],#}]&, Extract[Δfliste, p1]], Joined → True];**
FF3 = Show[PL3, PlotRange → All, Joined → True, Axes → False, Frame → True, FrameStyle → Directive[Black, 14], FrameLabel → {None, "Forcing (W/m^2)"}, Epilog → Inset[Style["", 18], Scaled[{0.1, 0.9}]]]
(*Combined forcing for both ghg's and aerosols*)

In[150]:= **PL1=ListPlot[Map[Transpose[{1749+Range[Length[Δfaeroliste[[1]]]],#}]&, Extract[Δfaeroliste, p1]], Joined → True];**
PL2 = ListPlot[Map[Transpose[{1749 + Range[Length[Δfaeroliste[[1]]]], #}] &, Extract[Δfghgliste, p1]], Joined → True];
FFD = Show[{PL1, PL2}, PlotRange → All, Joined → True, Axes → False, Frame → True, FrameStyle → Directive[Black, 14], FrameLabel → {None, "Forcing (W/m^2)"}, Epilog → Inset[Style["", 18], Scaled[{0.1, 0.9}]]]
(*Split forcing for ghg's and aerosols*)

In[94]:=**modellfarger={,,,,,,,,,,,,,,,,,, };**
In[95]:= **pan=LineLegend[modellfarger,Map[StringSplit[#]&,models][[All,1]]]**
Out[95]= BCC-CSM1-1 BNU-ESM CanESM2 CCSM4 CSIRO-Mk3.6.0 FGOALS-s2 GFDL-ESM2M GISS-E2-R HadGEM2-ES INM-CM4 MIROC5 MPI-ESM-LR MRI-CGCM3 NorESM1-M

FFB = ListPlot[Map[Transpose[{2018 + Range[Length[alltliste[[1]]]], #}] &, alltliste[[1 ;; 14]]], PlotRange → All, Joined → True, Axes → False, Frame → True, FrameStyle → Directive[Black, 14], FrameLabel → {None, "GMST increase (°C)"},Epilog → Inset[Style["", 18], Scaled[{0.1, 0.9}]],PlotStyle → Map[{#} &, modellfarger]]
(*Plot for temperature response, 1 scenario and 14 ESMs*)

In[*]:= **Grid[{{Show[FFA,ImageSize→400],Show[FFB,ImageSize→400],pan}}]**
(*Grid plot for one scenario, 14 ESMs*)

Grid[{{Show[FFC, ImageSize → 400,Epilog → Inset[Style["a", 18], Scaled[{0.1, 0.9}]]], Show[FFD, ImageSize → 400, Epilog → Inset[Style["b", 18], Scaled[{0.1, 0.9}]]] , Show[FFE, ImageSize → 400, Epilog → Inset[Style["c",

```
18], Scaled[{0.1, 0.9}]]]}}]
(*Grid plot for emissions, forcing and GMST for 86 scenarios and 1 esm*)

maxtemp = Map[Max[#] &, templiste]; (*mean*)
maxtemp2 = Map[Max[#] &, uptempliste]; (*+1sd*)
maxtemp3 = Map[Max[#] &, lowtempliste] (*-1sd*)


In[*]:= PL1=ListPlot[Extract[Transpose[{maxtemp,RCBliste2}],p1], AspectRatio → 1, PlotRange → All];
PL3 = ListPlot[Extract[Transpose[{maxtemp2, RCBliste2}], p1], AspectRatio → 1, PlotRange → All, PlotStyle →
Red];
PL4 = ListPlot[Extract[Transpose[{maxtemp2, RCBliste2}], p1], AspectRatio → 1, PlotRange → All, PlotStyle →
Red];
gg = Fit[Extract[Transpose[{maxtemp, RCBliste2}], p1], {zz, 1}, zz]; PL2 = Plot[gg, {zz, 1.2, 3}];
gg2 = Fit[Extract[Transpose[{maxtemp2, RCBliste2}], p1], {zz, 1}, zz]; PL4 = Plot[gg2, {zz, 1.2, 3}];
Show[{PL1, PL2}, PlotRange → All]
(*TCRE plot w/o pdf*)

In[*]:= pairs=Extract[Transpose[{maxtemp,RCBliste2}],p1];
error = pairs[[All, 2]] - (gg /. zz → pairs[[All, 1]]);
S = Sqrt[(Plus @@ (error^2)) / (Length[pairs] - 2)];
σx = StandardDeviation[pairs[[All, 1]]];

σf[x_] := S * Sqrt[1 + 1 / Length[pairs] + (x - Mean[pairs[[All, 1]]])^2 / (Length[pairs] * σx^2)];

In[*]:= pdf=(PDF[NormalDistribution[gg,σf[zz]]][p])/.zz→1.5;
pdf2 = (PDF[NormalDistribution[gg, σf[zz]]][p]) /. zz → 2.5;
Plot[{pdf, pdf2}, {p, 0, 5200}, PlotRange → All]

In[*]:= PL1=ListPlot[Extract[Transpose[{maxtemp,RCBliste2}],p1],AspectRatio→1, PlotRange → {{1, 4}, {0,
4000}}, PlotStyle → Darker[Blue]];
PL2 = Plot[gg, {zz, 1, 3}, PlotStyle → Darker[Blue]];
l1 = Graphics[{Black, Line[{{1.5, 0}, {1.5, gg /. zz → 1.5}}]}];
l2 = Graphics[{Black, Line[{{1.5, gg /. zz → 1.5}, {1, gg /. zz → 1.5}}]}]; inset = ParametricPlot[{1 + 60 * pdf, p},
{p, 0, 1200}, Axes → False, PlotStyle → {Black, Thickness[0.01]}];

l11 = Graphics[{Black, Line[{{2.5, 0}, {2.5, gg /. zz → 2.5}}]}];
l22 = Graphics[{Black, Line[{{2.5, gg /. zz → 2.5}, {1, gg /. zz → 2.5}}]}]; inset2 = ParametricPlot[{1 + 60 * pdf2,
p}, {p, 1900, 3000}, Axes → False, PlotStyle → {Black, Thickness[0.01]}];

FA = Show[{PL1, PL2, l1, l2, l11, l22, inset, inset2}, Axes → False, Frame → True, FrameStyle → Directive[Black,
14], FrameLabel → {"global temperature increase (°C)", "carbon budget after 2018 (Gt CO2)"}, Epilog → In-
set[Style["a", 18], Scaled[{0.1, 0.9}]], ImageSize → 400, PlotRange → {{1, 4}, {0, 4500}}]
(*TCRE with pdf, 1 ESM*)
```

ALL CLIMATE MODELS

```
In[*]:= maxtemp=Partition[Map[Max[#]&,alltliste],14][[All,5]];
PL1 = ListPlot[Extract[Transpose[{maxtemp, RCBliste2}], p1], AspectRatio → 1, PlotRange → All, PlotStyle →
Black];
gg = Fit[Extract[Transpose[{maxtemp, RCBliste2}], p1], {zz, 1}, zz];
PL2 = Plot[gg, {zz, 1.2, 3.5}, PlotStyle → Black];
QL1 = Show[{PL1, PL2}, PlotRange → All];
maxtemp = Partition[Map[Max[#] &, alltliste], 14][[All, 7]];
PL1 = ListPlot[Extract[Transpose[{maxtemp, RCBliste2}], p1], AspectRatio → 1, PlotRange → All, PlotStyle →
Darker[Red]];
gg = Fit[Extract[Transpose[{maxtemp, RCBliste2}], p1], {zz, 1}, zz]; PL2 = Plot[gg, {zz, 1.2, 3}, PlotStyle →
Darker[Red]];
QL2 = Show[{PL1, PL2}, PlotRange → All];
```

```
FB = Show[{QL1, QL2}, Axes → False, Frame → True, FrameStyle → Directive[Black, 14], FrameLabel →
{"global temperature increase (°C)", "carbon budget after 2018 (Gt CO2)"}, Epilog → {Inset[Style["b", 18],
Scaled[{0.1, 0.9}]], Inset[LineLegend[{Black, Darker[Red]}, {"CSIRO-Mk3.6.0", "GFDL-ESM2M"}], Scaled[{0.7,
0.3}]]}, ImageSize → 400, PlotRange → {{1, 4}, {0, 4500}}]

In[*]:= Grid[{{FA,FB}}]
(*TCREs for two ESM's*)

(*MEAN TCRE CALCULATION*)

In[*]:= maxtemp1=Partition[Map[Max[#]&,alltliste],14][[All,1]];
maxtemp2 = Partition[Map[Max[#] &, alltliste], 14][[All, 2]];
maxtemp3 = Partition[Map[Max[#] &, alltliste], 14][[All, 3]];
maxtemp4 = Partition[Map[Max[#] &, alltliste], 14][[All, 4]];
maxtemp5 = Partition[Map[Max[#] &, alltliste], 14][[All, 5]];
maxtemp6 = Partition[Map[Max[#] &, alltliste], 14][[All, 6]];
maxtemp7 = Partition[Map[Max[#] &, alltliste], 14][[All, 7]];
maxtemp8 = Partition[Map[Max[#] &, alltliste], 14][[All, 8]];
maxtemp9 = Partition[Map[Max[#] &, alltliste], 14][[All, 9]];
maxtemp10 = Partition[Map[Max[#] &, alltliste], 14][[All, 10]];
maxtemp11 = Partition[Map[Max[#] &, alltliste], 14][[All, 11]];
maxtemp12 = Partition[Map[Max[#] &, alltliste], 14][[All, 12]];
maxtemp13 = Partition[Map[Max[#] &, alltliste], 14][[All, 13]];
maxtemp14 = Partition[Map[Max[#] &, alltliste], 14][[All, 14]];

ggm1 = Fit[Extract[Transpose[{maxtemp1, RCBliste2}], p1], {zz, 1}, zz];
ggm2 = Fit[Extract[Transpose[{maxtemp2, RCBliste2}], p1], {zz, 1}, zz];
ggm3 = Fit[Extract[Transpose[{maxtemp3, RCBliste2}], p1], {zz, 1}, zz];
ggm4 = Fit[Extract[Transpose[{maxtemp4, RCBliste2}], p1], {zz, 1}, zz];
ggm5 = Fit[Extract[Transpose[{maxtemp5, RCBliste2}], p1], {zz, 1}, zz];
ggm6 = Fit[Extract[Transpose[{maxtemp6, RCBliste2}], p1], {zz, 1}, zz];
ggm7 = Fit[Extract[Transpose[{maxtemp7, RCBliste2}], p1], {zz, 1}, zz];
ggm8 = Fit[Extract[Transpose[{maxtemp8, RCBliste2}], p1], {zz, 1}, zz];
ggm9 = Fit[Extract[Transpose[{maxtemp9, RCBliste2}], p1], {zz, 1}, zz];
ggm10 = Fit[Extract[Transpose[{maxtemp10, RCBliste2}], p1], {zz, 1}, zz];
ggm11 = Fit[Extract[Transpose[{maxtemp11, RCBliste2}], p1], {zz, 1}, zz];
ggm12 = Fit[Extract[Transpose[{maxtemp12, RCBliste2}], p1], {zz, 1}, zz];
ggm13 = Fit[Extract[Transpose[{maxtemp13, RCBliste2}], p1], {zz, 1}, zz];
ggm14 = Fit[Extract[Transpose[{maxtemp14, RCBliste2}], p1], {zz, 1}, zz];

PLm5 = ListPlot[Extract[Transpose[{maxtemp5, RCBliste2}], p1], AspectRatio → 1, PlotRange → All, PlotStyle
→ Black];
PLm7 = ListPlot[Extract[Transpose[{maxtemp7, RCBliste2}], p1], AspectRatio → 1, PlotRange → All, PlotStyle
→ Darker[Red]];
PLm7dot = Plot[ggm7, {zz, 1.2, 3}, PlotStyle → Darker[Red]]; PLm5dot = Plot[ggm5, {zz, 1.2, 3}, PlotStyle →
Black];

meanTCRE=
(ggm1+ggm2+ggm3+ggm4+ggm5+ggm6+ggm7+ggm8+ggm9+ggm10+ggm11+ggm12+ggm13+ggm14)/14;

PLmeanTCRE = Plot[meanTCRE, {zz, 1.2, 3}, PlotStyle → {Black, Dashed}];
QLmeanTCRE = Show[{PLm5dot, PLm5, PLm7dot, PLm7, PLmeanTCRE}, Axes → False, Frame → True, Frame-
Style → Directive[Black, 14], AspectRatio → 1, FrameLabel → {"global temperature increase (°C)", "carbon
budget after 2018 (Gt CO2)"}, ImageSize → 400, PlotRange → {{1, 4}, {0, 4500}},Epilog → Inset[LineL-
egend[{Black, {Black, Dashed}, Darker[Red]}, {"CSIRO-Mk3.6.0", "Mean TCRE", "GFDL-ESM2M"}], Scaled[{0.7,
0.3}]]]
(*mean TCRE plot*)
```

PDF estimation

```
In[*]:= smliste={};
tliste = {};
Monitor[ Do[
```

```
pdfliste = {}; Do[
maxtemp = Partition[Map[Max[#] &, alltliste], 14][[All, kk]];
gg = Fit[Extract[Transpose[{maxtemp, RCBliste2}], p1], {zz, 1}, zz];
pairs = Extract[Transpose[{maxtemp, RCBliste2}], p1];
error = pairs[[All, 2]] - (gg /. zz → pairs[[All, 1]]);
S = Sqrt[(Plus @@ (error^2)) / (Length[pairs] - 2)];
σx = StandardDeviation[pairs[[All, 1]]];
σf[x_] := S * Sqrt[1 + 1 / Length[pairs] + (x - Mean[pairs[[All, 1]]])^2 / (Length[pairs] * σx^2)];
pdf = Chop[(PDF[NormalDistribution[gg, σf[zz]]][p]) /. zz → target];
pdfliste = Append[pdfliste, pdf];
, {kk, 1, 14}];

g = Mean[pdfliste];
smooth = Convolve[PDF[NormalDistribution[0, 400]][p], g, p, x]; sm = smooth /. x → Range[7000];
smliste = Append[smliste, sm];
tliste = Append[tliste, target];
, {target, 1.1, 4.0, 0.01}];
, target];

In[*]:= budget=500;
Δt = tliste[[2]] - tliste[[1]];
y = Transpose[smliste][[budget]];
y = y/ ((Plus@@y) * Δt); ListPlot[Transpose[{tliste, y}], Joined → True]
In[*]:= budget=1500;
Δt = tliste[[2]] - tliste[[1]];
y = Transpose[smliste][[budget]];
y = y/ ((Plus@@y) * Δt); ListPlot[Transpose[{tliste, y}], Joined → True]

In[*]:= bliste={};
Do[
Δt = tliste[[2]] - tliste[[1]];
y = Transpose[smliste][[budget]]; y = y/ ((Plus@@y) * Δt);
t1= tliste[[First[Position[FoldList[Plus, 0, y * Δt], _ ? (# > 0.90 &)]][[1]] - 1]];
t2 = tliste[[First[Position[FoldList[Plus, 0, y * Δt], _ ? (# > 0.75 &)]][[1]] - 1]];
t3 = tliste[[First[Position[FoldList[Plus, 0, y * Δt], _ ? (# > 0.5 &)]][[1]] - 1]];
t4= tliste[[First[Position[FoldList[Plus, 0, y * Δt], _ ? (# > 0.25 &)]][[1]] - 1]];
t5 = tliste[[First[Position[FoldList[Plus, 0, y * Δt], _ ? (# > 0.10 &)]][[1]] - 1]];
bliste = Append[bliste, {budget, t1, t2, t3, t4, t5}];
, {budget, 200, 4000, 100}]

In[*]:= farger={Red,Darker[Red],Black,Darker[Blue],Blue};

In[*]:= GGA=ListPlot[{Transpose[{bliste[[All,1]],bliste[[All,2]]}], Transpose[{bliste[[All, 1]], bliste[[All, 3]]}],
Transpose[{bliste[[All, 1]], bliste[[All, 4]]}], Transpose[{bliste[[All, 1]], bliste[[All, 5]]}], Trans-
pose[{bliste[[All, 1]], bliste[[All, 6]]}]}, Joined → True, AspectRatio → 1, PlotRange → {1, 4}, Axes → False,
Frame → True, FrameStyle → Directive[Black, 14], PlotStyle → Table[farger[[i]], {i, 1, 5}], GridLines → Auto-
matic, FrameLabel → {"Carbon budget from 2018 (GtCO2)", "Maximum temperature increase (°C)"}, PlotLeg-
ends → Placed[{"10% prob.", "25% prob.", "even chance", "75% prob.", "90% prob."}, {Scaled[{0.05, 0.7}], {0,
0.5}}]]

(*RCB plot one carbon, 14 ESMs*)
```

TWO CARBON MODELS, MEAN CLIMATE MODEL

```
In[*]:= RCBliste={};
totliste = {};
templiste = {};
uptempliste = {};
lowtempliste = {};
```

```
alltliste = {};
Monitor[
Do[
tot = data2[[u]][[All, 2]];
meanco2 = Gmean.tot + 280;
meanco2upper = Gupper.tot + 280;
meanco2lower = Glower.tot + 280; (* forcing *)

(* metan *)
del1 = 11.9 * tot[[1 ;; Length[EM]]];
(* The factor 3.0 tunes 2019 methane emmisions in 2019 to 440 Tg Methane *)
del2 = hh /. zz → tot[[Length[EM] + 1 ;; Length[tot]]];
del2 = Last[del1] + (del2 - First[del2]) * (Last[del1] - Last[del2]) / (First[del2] - Last[del2]);
metemis = Join[del1, del2];

Gmetan = 0.34 * Table[Exp[- (i - j) / τmetan] * UnitStep[i - j], {i, 1, n}, {j, 1, n}];
(* The factor 0.35 tunes 2019 methane concentration to around 1880 ppb *)
metan = Map[Max[#, 0] &, 700 + Gmetan.metemis];
Δfmetan = 0.036 * (Sqrt[metan] - Sqrt[700]);
Δfco2 = 5.35 Log[1 + (meanco2 - 280) / 280]; (* CO2 til forcing*)
Δfco2upper = 5.35 Log[1 + (meanco2upper - 280) / 280]; (* CO2 til forcing*)
Δfco2lower = 5.35 Log[1 + (meanco2lower - 280) / 280]; (* CO2 til forcing*)
Δfaer= -0.02tot; (* aerosols *)
Δfaer1 = Δfaer[[1 ;; Length[EM]]] ;
Δfaer2 = Drop[Δfaer, Length[EM]] ;
Δfaer2 = Map[Min[-0.4, #] &, Δfaer2];  (*-0.4 asymptote*)
Δfaer = Join[Δfaer1, Δfaer2];
Δf = Δfco2 + Δfaer + Δfmetan;
Δfupper = Δfco2upper + Δfaer + Δfmetan;
Δflower = Δfco2lower + Δfaer + Δfmetan;

Tliste = {};
Do[
(*T2=Klimaliste[[p]].Δf;
T2=T2*(Γliste[[p]]/Log[4.])/5.35;
T2=Drop[T2,268]; T2=1.0+T2-T2[[1]];
Tliste=Append[Tliste,T2];*)

T2 = Klimaliste[[p]].Δfupper;
T2 = T2 * (Γliste[[p]] / Log[4.]) / 5.35;
T2 = Drop[T2, 268]; T2=1.1+T2-T2[[1]];
Tliste = Append[Tliste, T2];

T2 = Klimaliste[[p]].Δflower;
T2 = T2 * (Γliste[[p]] / Log[4.]) / 5.35;
T2 = Drop[T2, 268]; T2=1.0+T2-T2[[1]];
Tliste = Append[Tliste, T2];
, {p, 1, Length[models]}];

Tlisteupper = Partition[Tliste, 2][[All, 1]];
Tlistelower = Partition[Tliste, 2][[All, 2]];
meanupper = Map[Mean[#] &, Transpose[Tlisteupper]];
meanlower = Map[Mean[#] &, Transpose[Tlistelower]];
Tliste = {meanupper, meanlower};

middel =Table[Mean[Transpose[Tliste][[i]]], {i, 1, Length[Transpose[Tliste]]}];
upper = Table[Mean[Transpose[Tliste][[i]]] + StandardDeviation[ Transpose[Tliste][[i]]], {i, 1, Length[Trans-
pose[Tliste]]}];
lower = Table[Mean[Transpose[Tliste][[i]]] - StandardDeviation[ Transpose[Tliste][[i]]], {i, 1, Length[Trans-
pose[Tliste]]}];

RCB = Plus @@ Drop[tot, 270];
RCBliste = Append[RCBliste, RCB];
totliste = Append[totliste, tot];
```

```
alltliste = Join[alltliste, Tliste];
templiste = Append[templiste, middel];
uptempliste = Append[uptempliste, upper];
lowtempliste = Append[lowtempliste, lower];
, {u, 1, Length[data2]}]
,u]
```

In[*]:=
```
Dimensions[alltliste]
```
Out[*]= {254, 83}

In[*]:=
```
3556/14
```
Out[*]= 254

In[*]:=
```
CM = {};
cm1 =
Table[Partition[Extract[Partition[Map[Max[#] &, alltliste], 2], p1][[kk]], 2][[ All, 1]], {kk, 1, Length[p1]}];
cm2 = Table[Partition[Extract[Partition[Map[Max[#] &, alltliste], 2], p1][[kk]], 2][[All, 2]], {kk, 1,
Length[p1]}];

Do[
CM = Append[CM, Transpose[{Extract[RCBliste2, p1], Transpose[cm1][[j]]}]];
CM = Append[CM, Transpose[{Extract[RCBliste2, p1], Transpose[cm2][[j]]}]];
, {j, 1, Length[Transpose[cm2]]}];
```

In[*]:=
```
ListPlot[{CM[[1]],CM[[2]]}]
```

In[*]:=
```
smliste={};
tliste = {};

Monitor[ Do[
pdfliste = {}; Do[
gg = Fit[Map[Reverse[#] &, CM[[kk]]], {zz, 1}, zz];
pairs = Map[Reverse[#] &, CM[[kk]]];
error = pairs[[All, 2]] - (gg /. zz → pairs[[All, 1]]);
S = Sqrt[(Plus @@ (error^2)) / (Length[pairs] - 2)];
σx = StandardDeviation[pairs[[All, 1]]];
σf[x_] := S * Sqrt[1 + 1 / Length[pairs] + (x - Mean[pairs[[All, 1]]])^2 / (Length[pairs] * σx^2)];
pdf = Chop[(PDF[NormalDistribution[gg, σf[zz]]][p]) /. zz → target];
pdfliste = Append[pdfliste, pdf];
, {kk, 1, 2}];

g = Mean[pdfliste];
smooth = Convolve[PDF[NormalDistribution[0, 400]][p], g, p, x];
sm = smooth /. x → Range[7000];
smliste = Append[smliste, sm];
tliste = Append[tliste, target];
, {target, 1.1, 4.0, 0.01}];
, target];
```

In[*]:=
```
budget=500;
Δt = tliste[[2]] - tliste[[1]];
y = Transpose[smliste][[budget]];
y = y/ ((Plus@@y) * Δt); ListPlot[Transpose[{tliste, y}], Joined → True]
```

In[*]:=
```
budget=1500;
Δt = tliste[[2]] - tliste[[1]];
y = Transpose[smliste][[budget]];
y = y/ ((Plus@@y) * Δt); ListPlot[Transpose[{tliste, y}], Joined → True]
```

In[*]:=
```
bliste={};
Do[
Δt = tliste[[2]] - tliste[[1]];
y = Transpose[smliste][[budget]]; y = y/ ((Plus@@y) * Δt);
t1= tliste[[First[Position[FoldList[Plus, 0, y * Δt], _ ? (# > 0.90 &)]][[1]] - 1]];
```

```
t2 = tliste[[First[Position[FoldList[Plus, 0, y * Δt], _ ? (# > 0.75 &)]][[1]] - 1]];
t3 = tliste[[First[Position[FoldList[Plus, 0, y * Δt], _ ? (# > 0.5 &)]][[1]] - 1]];
t4= tliste[[First[Position[FoldList[Plus, 0, y * Δt], _ ? (# > 0.25 &)]][[1]] - 1]];
t5 = tliste[[First[Position[FoldList[Plus, 0, y * Δt], _ ? (# > 0.10 &)]][[1]] - 1]];
bliste = Append[bliste, {budget, t1, t2, t3, t4, t5}]; , {budget, 200, 4000, 100}]
```

In[*]:= farger={Red,Darker[Red],Black,Darker[Blue],Blue};

In[*]:= a=ListPlot[{Transpose[{bliste[[All,1]],bliste[[All,2]]}], Transpose[{bliste[[All, 1]], bliste[[All, 3]]}], Transpose[{bliste[[All, 1]], bliste[[All, 4]]}], Transpose[{bliste[[All, 1]], bliste[[All, 5]]}], Transpose[{bliste[[All, 1]], bliste[[All, 6]]}]}, Joined → True, AspectRatio → 1, PlotRange → {1, 4}, Axes → False, Frame → True, FrameStyle → Directive[Black, 14],PlotStyle → Table[farger[[i]], {i, 1, 5}], GridLines → Automatic, FrameLabel → {"Carbon budget from 2018 (GtCO2)", "Maximum temperature increase (°C)"}, PlotLegends → Placed[{"10% prob.", "25% prob.", "even chance", "75% prob.", "90% prob."}, {Scaled[{0.05, 0.7}], {0, 0.5}}]]; l = Graphics[{Black, Line[{{1294, 1}, {1294, 2.5}}]}];
GGB = Show[{a}]

(*RCB estimate two carbons, mean ESM*)

INTERNAL VARIABILITY

```
RCBliste = {};
totliste = {};
templiste = {};
uptempliste = {};
lowtempliste = {};
alltliste = {};

Monitor[ Do[
tot = data2[[u]][[All, 2]];
meanco2 = Gmean.tot + 280;
meanco2upper = Gupper.tot + 280;
meanco2lower = Glower.tot + 280; (* forcing *)

(* metan *)
del1 = 11.9 * tot[[1 ;; Length[EM]]];
(* The factor 3.0 tunes 2019 methane emmisions in 2019 to 440 Tg Methane *)
del2 = hh /. zz → tot[[Length[EM] + 1 ;; Length[tot]]];
del2 = Last[del1] + (del2 - First[del2]) * (Last[del1] - Last[del2]) / (First[del2] - Last[del2]);
metemis = Join[del1, del2];

Gmetan = 0.34 * Table[Exp[- (i - j) / τmetan] * UnitStep[i - j], {i, 1, n}, {j, 1, n}];
(* The factor 0.35 tunes 2019 methane concentration to around 1880 ppb *)
metan = Map[Max[#, 0] &, 700 + Gmetan.metemis];
Δfmetan = 0.036 * (Sqrt[metan] - Sqrt[700]);
Δfco2 = 5.35 Log[1 + (meanco2 - 280) / 280]; (* CO2 til forcing*)
Δfco2upper = 5.35 Log[1 + (meanco2upper - 280) / 280]; (* CO2 til forcing*)
Δfco2lower = 5.35 Log[1 + (meanco2lower - 280) / 280]; (* CO2 til forcing*)
(* aerosols *)
Δfaer= -0.02tot;
Δfaer1 = Δfaer[[1 ;; Length[EM]]] ; Δfaer2 = Drop[Δfaer, Length[EM]] ; Δfaer2 = Map[Min[-0.4, #] &, Δfaer2];
Δfaer = Join[Δfaer1, Δfaer2];
Δf = Δfco2 + Δfaer + Δfmetan;
Δfupper = Δfco2upper + Δfaer + Δfmetan;
Δflower = Δfco2lower + Δfaer + Δfmetan;

Tliste = {};
Do[
T2 = Klimaliste[[p]].Δf;
T2 = T2 * (Γliste[[p]] / Log[4.]) / 5.35;
```

```
T2 = Drop[T2, 268];
T2=1.1+T2-T2[[1]];
Tliste = Append[Tliste, T2 + StandardDeviation[Flatten[noiseliste2[[p]]]]];
, {p, 1, Length[models]}];

Tlisteupper = Partition[Tliste, 2][[All, 1]];
Tlistelower = Partition[Tliste, 2][[All, 2]];
mupper = {};
mlower = {};

Do[
meanupper = Map[Mean[#] &, Transpose[Tlisteupper]] + StandardDeviation[Flatten[noiseliste2[[p]]]];
meanlower = Map[Mean[#] &, Transpose[Tlistelower]] - StandardDeviation[Flatten[noiseliste2[[p]]]];
mupper = Append[mupper, meanupper]; mlower = Append[mlower, meanlower]; , {p, 1, 14}];
Tliste = Join[mupper, mlower];

middel =Table[Mean[Transpose[Tliste][[i]]], {i, 1, Length[Transpose[Tliste]]}];
upper = Table[Mean[Transpose[Tliste][[i]]] + StandardDeviation[ Transpose[Tliste][[i]]], {i, 1, Length[Trans-
pose[Tliste]]}];
lower = Table[Mean[Transpose[Tliste][[i]]] - StandardDeviation[ Transpose[Tliste][[i]]], {i, 1, Length[Trans-
pose[Tliste]]}];
RCB = Plus @@ Drop[tot, 270];
RCBliste = Append[RCBliste, RCB];
totliste = Append[totliste, tot];
alltliste = Join[alltliste, Tliste];
templiste = Append[templiste, middel];
uptempliste = Append[uptempliste, upper];
lowtempliste = Append[lowtempliste, lower];
, {u, 1, Length[data2]}]
,u]

In[*]:= Dimensions[alltliste]
Out[*]= {3556, 83}

In[*]:= CM = {};
cm1 = Table[Partition[Extract[Partition[Map[Max[#] &, alltliste], 2 * 14], p1][[kk]], 2][[ All, 1]], {kk, 1,
Length[p1]}];
cm2 = Table[Partition[Extract[Partition[Map[Max[#] &, alltliste], 2 * 14], p1][[ kk]], 2][[All, 2]], {kk, 1,
Length[p1]}];

Do[ CM = Append[CM, Transpose[{Extract[RCBliste2, p1], Transpose[cm1][[j]]}]];
CM = Append[CM, Transpose[{Extract[RCBliste2, p1], Transpose[cm2][[j]]}]]; , {j, 1, Length[Trans-
pose[cm2]]}];

In[*]:= ListPlot[{CM[[1]],CM[[2]]}]

In[*]:= smliste={};
tliste = {};
Monitor[ Do[

pdfliste = {}; Do[
gg = Fit[Map[Reverse[#] &, CM[[kk]]], {zz, 1}, zz];
pairs = Map[Reverse[#] &, CM[[kk]]];
error = pairs[[All, 2]] - (gg /. zz → pairs[[All, 1]]);
S = Sqrt[(Plus @@ (error^2)) / (Length[pairs] - 2)];
σx = StandardDeviation[pairs[[All, 1]]];
σf[x_] := S * Sqrt[1 + 1 / Length[pairs] + (x - Mean[pairs[[All, 1]]])^2 / (Length[pairs] * σx^2)];
pdf = Chop[(PDF[NormalDistribution[gg, σf[zz]]][p]) /. zz → target];
pdfliste = Append[pdfliste, pdf];
,{kk,1,2*14}];

g = Mean[pdfliste];
smooth = Convolve[PDF[NormalDistribution[0, 400]][p], g, p, x];
```

```
sm = smooth /. x → Range[7000];
smliste = Append[smliste, sm];
tliste = Append[tliste, target];
, {target, 1.1, 4.0, 0.01}];
, target];

In[*]:= budget=500;
Δt = tliste[[2]] - tliste[[1]];
y = Transpose[smliste][[budget]];
y = y/ ((Plus@@y) * Δt); ListPlot[Transpose[{tliste, y}], Joined → True]

In[*]:= budget=1500;
Δt = tliste[[2]] - tliste[[1]];
y = Transpose[smliste][[budget]];
y = y/ ((Plus@@y) * Δt); ListPlot[Transpose[{tliste, y}], Joined → True]

In[*]:= bliste={};
Do[ Δt = tliste[[2]] - tliste[[1]];
y = Transpose[smliste][[budget]];
y = y/ ((Plus@@y) * Δt);
t1= tliste[[First[Position[FoldList[Plus, 0, y * Δt], _ ? (# > 0.90 &)]][[1]] - 1]];
t2 = tliste[[First[Position[FoldList[Plus, 0, y * Δt], _ ? (# > 0.75 &)]][[1]] - 1]];
t3 = tliste[[First[Position[FoldList[Plus, 0, y * Δt], _ ? (# > 0.5 &)]][[1]] - 1]];
t4= tliste[[First[Position[FoldList[Plus, 0, y * Δt], _ ? (# > 0.25 &)]][[1]] - 1]];
t5 = tliste[[First[Position[FoldList[Plus, 0, y * Δt], _ ? (# > 0.10 &)]][[1]] - 1]];
bliste = Append[bliste, {budget, t1, t2, t3, t4, t5}];
, {budget, 200, 4000, 100}]

In[*]:= farger={Red,Darker[Red],Black,Darker[Blue],Blue};

In[*]:= a=ListPlot[{Transpose[{bliste[[All,1]],bliste[[All,2]]}], Transpose[{bliste[[All, 1]], bliste[[All, 3]]}], Transpose[{bliste[[All, 1]], bliste[[All, 4]]}], Transpose[{bliste[[All, 1]], bliste[[All, 5]]}], Transpose[{bliste[[All, 1]], bliste[[All, 6]]}]}, Joined → True, AspectRatio → 1, PlotRange → {1, 4.0}, Axes → False, Frame → True, FrameStyle → Directive[Black, 14], PlotStyle → Table[farger[[i]], {i, 1, 5}], GridLines → Automatic, FrameLabel → {"Carbon budget from 2018 (GtCO2)", "Maximum temperature increase (°C)"}, PlotLegends → Placed[{"10% prob.", "25% prob.", "even chance", "75% prob.", "90% prob."}, {Scaled[{0.05, 0.7}], {0, 0.5}}]];
l = Graphics[{Black, Line[{{1294, 1}, {1294, 2.5}}]}];
GGC = Show[{a}]
(*RCB estimate internal variability*)
```

COMBINATION BETWEEN TWO CARBON MODELS, 14 ESMs AND INTERNAL VARIABILITY

```
RCBliste = {};
totliste = {};
templiste = {};
uptempliste = {};
lowtempliste = {};
alltliste = {};

Monitor[ Do[
tot = data2[[u]][[All, 2]];
meanco2 = Gmean.tot + 280;
meanco2upper = Gupper.tot + 280;
meanco2lower = Glower.tot + 280; (* forcing *)

(* metan *)
del1 = 11.9 * tot[[1 ;; Length[EM]]];
(* The factor 3.0 tunes 2019 methane emmisions in 2019 to 440 Tg Methane *)
del2 = hh /. zz → tot[[Length[EM] + 1 ;; Length[tot]]];
del2 = Last[del1] + (del2 - First[del2]) * (Last[del1] - Last[del2]) / (First[del2] - Last[del2]);
```

```
metemis = Join[del1, del2];

Gmetan = 0.34 * Table[Exp[- (i - j) / τmetan] * UnitStep[i - j], {i, 1, n}, {j, 1, n}];
(* The factor 0.35 tunes 2019 methane concentration to around 1880 ppb *)
metan = Map[Max[#, 0] &, 700 + Gmetan.metemis];

Δfmetan = 0.036 * (Sqrt[metan] - Sqrt[700]);
Δfco2 = 5.35 Log[1 + (meanco2 - 280) / 280]; (* CO2 til forcing*)
Δfco2upper = 5.35 Log[1 + (meanco2upper - 280) / 280]; (* CO2 til forcing*)
Δfco2lower = 5.35 Log[1 + (meanco2lower - 280) / 280]; (* CO2 til forcing*)
(* aerosols *)
Δfaer= -0.02tot;
Δfaer1 = Δfaer[[1 ;; Length[EM]]] ; Δfaer2 = Drop[Δfaer, Length[EM]] ; Δfaer2 = Map[Min[-0.4, #] &, Δfaer2];
Δfaer = Join[Δfaer1, Δfaer2];
Δf = Δfco2 + Δfaer + Δfmetan;
Δfupper = Δfco2upper + Δfaer + Δfmetan;
Δflower = Δfco2lower + Δfaer + Δfmetan;

Tliste = {};
Do[

T2 = Klimaliste[[p]].Δfupper;
T2 = T2 * (Γliste[[p]] / Log[4.]) / 5.35;
T2 = Drop[T2, 268];
T2=1.1+T2-T2[[1]];
Tliste = Append[Tliste, T2 + StandardDeviation[Flatten[noiseliste2[[p]]]]];

(*T2=Klimaliste[[p]].Δfupper;
T2=T2*(Γliste[[p]]/Log[4.])/5.35;
T2=Drop[T2,268];
T2=1.1+T2-T2[[1]]; Tliste=Append[Tliste,T2-StandardDeviation[Flatten[noiseliste2[[p]]]];*)

(*T2=Klimaliste[[p]].Δflower;
T2=T2*(Γliste[[p]]/Log[4.])/5.35;
T2=Drop[T2,268];
T2=1.0+T2-T2[[1]]; Tliste=Append[Tliste,T2+StandardDeviation[Flatten[noiseliste2[[p]]]];*)

T2 = Klimaliste[[p]].Δflower;
T2 = T2 * (Γliste[[p]] / Log[4.]) / 5.35;
T2 = Drop[T2, 268];
T2=1.0+T2-T2[[1]];
Tliste = Append[Tliste, T2 - StandardDeviation[Flatten[noiseliste2[[p]]]];

, {p, 1, Length[models]}];

middel = Table[Mean[Transpose[Tliste][[i]]], {i, 1, Length[Transpose[Tliste]]}];
upper = Table[Mean[Transpose[Tliste][[i]]] + StandardDeviation[Transpose[Tliste][[i]]], {i, 1, Length[Trans-
pose[Tliste]]}];
lower = Table[Mean[Transpose[Tliste][[i]]] - StandardDeviation[Transpose[Tliste][[i]]], {i, 1, Length[Trans-
pose[Tliste]]}];
RCB = Plus @@ Drop[tot, 270];
RCBliste = Append[RCBliste, RCB];
totliste = Append[totliste, tot];

alltliste = Join[alltliste, Tliste];
templiste = Append[templiste, middel];
uptempliste = Append[uptempliste, upper];
lowtempliste = Append[lowtempliste, lower];
, {u, 1, Length[data2]}]
,u]

In[*]:= Dimensions[alltliste]
Out[*]= {3556, 83}
```

```
In[*]:= CM = {};
cm1 = Table[ Partition[Extract[Partition[Map[Max[#] &, alltliste], 2 * 14], p1][[kk]], 2][[ All, 1]], {kk, 1,
Length[p1]}];
cm2 = Table[Partition[Extract[Partition[Map[Max[#] &, alltliste], 2 * 14], p1][[ kk]], 2][[All, 2]], {kk, 1,
Length[p1]}];

Do[
CM = Append[CM, Transpose[{Extract[RCBliste2, p1], Transpose[cm1][[j]]}]];
CM = Append[CM, Transpose[{Extract[RCBliste2, p1], Transpose[cm2][[j]]}]];
, {j, 1, Length[Transpose[cm2]]}];

In[*]:= ListPlot[{CM[[1]],CM[[2]]}]

In[*]:= smliste={};
tliste = {};
Monitor[ Do[
pdfliste = {}; Do[

gg = Fit[Map[Reverse[#] &, CM[[kk]]], {zz, 1}, zz];
pairs = Map[Reverse[#] &, CM[[kk]]];
error = pairs[[All, 2]] - (gg /. zz → pairs[[All, 1]]);
S = Sqrt[(Plus @@ (error^2)) / (Length[pairs] - 2)];
σx = StandardDeviation[pairs[[All, 1]]];
σf[x_] := S * Sqrt[1 + 1 / Length[pairs] + (x - Mean[pairs[[All, 1]]])^2 / (Length[pairs] * σx^2)];
pdf = Chop[(PDF[NormalDistribution[gg, σf[zz]]][p]) /. zz → target];
pdfliste = Append[pdfliste, pdf];
,{kk,1,2*14}];

g = Mean[pdfliste];
smooth = Convolve[PDF[NormalDistribution[0, 400]][p], g, p, x];
sm = smooth /. x → Range[7000];
smliste = Append[smliste, sm];
tliste = Append[tliste, target];
, {target, 1.1, 4.0, 0.01}];
, target];

In[*]:= budget=500;
Δt = tliste[[2]] - tliste[[1]];
y = Transpose[smliste][[budget]];
y = y/ ((Plus@@y) * Δt); ListPlot[Transpose[{tliste, y}], Joined → True]

In[*]:= budget=1500;
Δt = tliste[[2]] - tliste[[1]];
y = Transpose[smliste][[budget]];
y = y/ ((Plus@@y) * Δt); ListPlot[Transpose[{tliste, y}], Joined → True]

In[*]:= bliste={};
Do[
Δt = tliste[[2]] - tliste[[1]];
y = Transpose[smliste][[budget]];
y = y/ ((Plus@@y) * Δt);
t1= tliste[[First[Position[FoldList[Plus, 0, y * Δt], _ ? (# > 0.90 &)]][[1]] - 1]];
t2 = tliste[[First[Position[FoldList[Plus, 0, y * Δt], _ ? (# > 0.75 &)]][[1]] - 1]];
t3 = tliste[[First[Position[FoldList[Plus, 0, y * Δt], _ ? (# > 0.5 &)]][[1]] - 1]];
t4= tliste[[First[Position[FoldList[Plus, 0, y * Δt], _ ? (# > 0.25 &)]][[1]] - 1]];
t5 = tliste[[First[Position[FoldList[Plus, 0, y * Δt], _ ? (# > 0.10 &)]][[1]] - 1]];
bliste = Append[bliste, {budget, t1, t2, t3, t4, t5}];
, {budget, 200, 4000, 100}]

In[*]:= farger={Red,Darker[Red],Black,Darker[Blue],Blue};

In[*]:= a=ListPlot[{Transpose[{bliste[[All,1]],bliste[[All,2]]}], Transpose[{bliste[[All, 1]], bliste[[All, 3]]}], Trans-
pose[{bliste[[All, 1]], bliste[[All, 4]]}], Transpose[{bliste[[All, 1]], bliste[[All, 5]]}], Transpose[{bliste[[All, 1]],
```

```
bliste[[All, 6]]}]}, Joined → True, AspectRatio → 1, PlotRange → {1, 4.0}, Axes → False, Frame → True, Frame-
Style → Directive[Black, 14], PlotStyle → Table[farger[[i]], {i, 1, 5}], GridLines → Automatic, FrameLabel →
{"Carbon budget from 2018 (GtCO2)", "Maximum temperature increase (°C)"}, PlotLegends → Placed[{"10%
prob.", "25% prob.", "even chance", "75% prob.", "90% prob."}, {Scaled[{0.05, 0.7}], {0, 0.5}}]];
l = Graphics[{Black, Line[{{1294, 1}, {1294, 2.5}}]}];
GGD = Show[{a}]
(*RCB estimate for 2 carbon models, 14 ESMs and internal variability*)

(*Comparison plot*)

(*GGA = all climate - GGB = mean climate + 2 carbon - GGC = mean climate + mean carbon + internal - GGD = All climate + 2 carbon + internal*)

Grid[{{
Show[GGA, PlotRange → {{0, 4000}, {1.1, 4.3}}, ImageSize → 380, Epilog → Inset[Style["a", 18], Scaled[{0.1,
0.9}]]],
Show[GGB, PlotRange → {{0, 4000}, {1.1, 4.3}}, ImageSize → 380, Epilog → Inset[Style["b", 18], Scaled[{0.1,
0.9}]]]},

{Show[GGC, PlotRange → {{0, 4000}, {1.1, 4.3}}, ImageSize → 380, Epilog → Inset[Style["c", 18], Scaled[{0.1,
0.9}]]],
Show[GGD, PlotRange → {{0, 4000}, {1.1, 4.3}}, ImageSize → 380, Epilog → Inset[Style["d", 18], Scaled[{0.1,
0.9}]]]}}]

(*Grid plot *)
```

CODE FOR IMPLEMENTATION OF NON-LINEAR FRAMEWORK.

The following code is used the non-linear framework in the SRM as described in Section 3.6. Produced in Mathematica: Version: 12.0.0.0 in collaboration with research partners Andreas Johansen, Andreas Martinsen and supervision from Martin Rypdal.
Platform: Mac OS X x86 (64-bit). macOS Catalina: Version 10.15.3.

```
In[283]:= SetDirectory["OneDrive - UiT Office 365"];
Z = Import["SSP_IAM_V2_201811.csv"];
Z = Map[StringSplit[#, ","] &, Z];

In[5]:= hh=157.65890684920566`+1.8942819330281027`zz+0.08520850267749702`zz^2;

In[6]:= Z[[1]]
Out[6]= {{MODEL, "SCENARIO", "REGION", "VARIABLE", "UNIT",
2005, 2010, 2020, 2030, 2040, 2050, 2060, 2070, 2080, 2090, 2100}}

In[7]:= RR=Table[Z[[k]][[1]][[4]],{k,1,Length[Z]}];
Union[RR]

Out[8]= {"Agricultural Demand|Crops", "Agricultural Demand|Crops|Energy",
"Agricultural Demand|Livestock", "Agricultural Production|Crops|Energy",
"Agricultural Production|Crops|Non-Energy","Agricultural Production|Livestock", "Capacity|Electricity",
"Capacity|Electricity|Biomass", "Capacity|Electricity|Coal", "Capacity|Electricity|Gas",
"Capacity|Electricity|Geothermal", "Capacity|Electricity|Hydro", "Capacity|Electricity|Nuclear",
"Capacity|Electricity|Oil", "Capacity|Electricity|Other", "Capacity|Electricity|Solar", "Capacity|Electricity|Solar|CSP",
"Capacity|Electricity|Solar|PV", "Capacity|Electricity|Wind", "Capacity|Electricity|Wind|Offshore",
"Capacity|Electricity|Wind|Onshore", "Consumption", "Diagnostics|MAGICC6|Concentration|CH4",
"Diagnostics|MAGICC6|Concentration|CO2", "Diagnostics|MAGICC6|Concentration|N2O",
"Diagnostics|MAGICC6|Forcing", "Diagnostics|MAGICC6|Forcing|Aerosol", "Diagnostics|MAGICC6|Forcing|CH4",
"Diagnostics|MAGICC6|Forcing|CO2", "Diagnostics|MAGICC6|Forcing|F-Gases",
"Diagnostics|MAGICC6|Forcing|Kyoto Gases", "Diagnostics|MAGICC6|Forcing|N2O",
"Diagnostics|MAGICC6|Temperature|Global Mean", "Emissions|BC", "Emissions|CH4",
"Emissions|CH4|Fossil Fuels and Industry", "Emissions|CH4|Land Use", "Emissions|CO",
"Emissions|CO2", "Emissions|CO2|Carbon Capture and Storage",
"Emissions|CO2|Carbon Capture and Storage|Biomass","Emissions|CO2|Fossil Fuels and Industry",
"Emissions|CO2|Land Use", "Emissions|F-Gases", "Emissions|Kyoto Gases", "Emissions|N2O",
"Emissions|N2O|Land Use", "Emissions|NH3", "Emissions|NOx", "Emissions|OC", "Emissions|Sulfur",
"Emissions|VOC", "Energy Service|Transportation|Freight", "Energy Service|Transportation|Passenger",
"Final Energy","Final Energy|Electricity", "Final Energy|Gases", "Final Energy|Heat",
"Final Energy|Hydrogen", "Final Energy|Industry", "Final Energy|Liquids",
"Final Energy|Residential and Commercial", "Final Energy|Solar","Final Energy|Solids",
"Final Energy|Solids|Biomass","Final Energy|Solids|Biomass|Traditional", "Final Energy|Solids|Coal",
"Final Energy|Transportation", "GDP|PPP", "Harmonized Emissions|BC",
"Harmonized Emissions|CH4|Fossil Fuels and Industry","Harmonized Emissions|CH4|Land Use",
"Harmonized Emissions|CO","Harmonized Emissions|CO2|Fossil Fuels and Industry",
"Harmonized Emissions|CO2|Land Use", "Harmonized Emissions|F-Gases", "Harmonized Emissions|Kyoto Gases",
"Harmonized Emissions|NH3", "Harmonized Emissions|NOx", "Harmonized Emissions|OC",
"Harmonized Emissions|Sulfur", "Harmonized Emissions|VOC","Land Cover|Built-up Area",
"Land Cover|Cropland", "Land Cover|Forest", "Land Cover|Pasture", "Population", "Price|Carbon", "Primary Energy",
"Primary Energy|Biomass", "Primary Energy|Biomass|Traditional", "Primary Energy|Biomass|w/ CCS",
"Primary Energy|Biomass|w/o CCS", "Primary Energy|Coal", "Primary Energy|Coal|w/ CCS",
"Primary Energy|Coal|w/o CCS", "Primary Energy|Fossil", "Primary Energy|Fossil|w/ CCS",
"Primary Energy|Fossil|w/o CCS","Primary Energy|Gas", "Primary Energy|Gas|w/ CCS",
"Primary Energy|Gas|w/o CCS", "Primary Energy|Geothermal","Primary Energy|Hydro",
"Primary Energy|Non-Biomass Renewables","Primary Energy|Nuclear", "Primary Energy|Oil",
"Primary Energy|Oil|w/ CCS", "Primary Energy|Oil|w/o CCS","Primary Energy|Other",
"Primary Energy|Secondary Energy Trade","Primary Energy|Solar", "Primary Energy|Wind",
```

"Secondary Energy|Electricity", "Secondary Energy|Electricity|Biomass",
"Secondary Energy|Electricity|Biomass|w/ CCS","Secondary Energy|Electricity|Biomass|w/o CCS",
"Secondary Energy|Electricity|Coal","Secondary Energy|Electricity|Coal|w/ CCS",
"Secondary Energy|Electricity|Coal|w/o CCS","Secondary Energy|Electricity|Gas",
"Secondary Energy|Electricity|Gas|w/ CCS", "Secondary Energy|Electricity|Gas|w/o CCS",
"Secondary Energy|Electricity|Geothermal","Secondary Energy|Electricity|Hydro",
"Secondary Energy|Electricity|Non-Biomass Renewables","Secondary Energy|Electricity|Nuclear",
"Secondary Energy|Electricity|Oil", "Secondary Energy|Electricity|Solar", "Secondary Energy|Electricity|Wind",
"Secondary Energy|Gases", "Secondary Energy|Gases|Biomass","Secondary Energy|Gases|Coal",
"Secondary Energy|Gases|Natural Gas", "Secondary Energy|Heat", "Secondary Energy|Heat|Geothermal",
"Secondary Energy|Hydrogen", "Secondary Energy|Hydrogen|Biomass",
"Secondary Energy|Hydrogen|Biomass|w/ CCS", "Secondary Energy|Hydrogen|Biomass|w/o CCS",
"Secondary Energy|Hydrogen|Electricity", "Secondary Energy|Liquids", "Secondary Energy|Liquids|Biomass",
"Secondary Energy|Liquids|Biomass|w/ CCS", "Secondary Energy|Liquids|Biomass|w/o CCS",
"Secondary Energy|Liquids|Coal", "Secondary Energy|Liquids|Coal|w/ CCS",
"Secondary Energy|Liquids|Coal|w/o CCS", "Secondary Energy|Liquids|Gas",
"Secondary Energy|Liquids|Gas|w/ CCS", "Secondary Energy|Liquids|Gas|w/o CCS",
"Secondary Energy|Liquids|Oil", "Secondary Energy|Solids", "VARIABLE"}

In[9]:= **RRR=Table[Z[[k]][[1]][[3]],{k,1,Length[Z]}];**
Union[RRR]

Out[10]= {"R5.2ASIA", "R5.2LAM", "R5.2MAF", "R5.2OECD", "R5.2REF", "REGION", "World"}

In[11]:= **co2pos1=Position[RR,_?(#=="\"Emissions|CO2|FossilFuelsandIndustry\""&)];**
co2pos2 = Position[RR, _ ? (# == "\"Emissions|CO2|Land Use\"" &)];
co2pos3 = Position[RRR, _ ? (# == "\"World\"" &)];

In[14]:= **ppos1=Intersection[co2pos3,co2pos1];**
ppos2 = Intersection[co2pos3, co2pos2];

In[16]:= **Extract[Z,co2pos1][[1]]**

Out[16]= {{AIM/CGE, "SSP1-19", "R5.2ASIA", "Emissions|CO2|Fossil Fuels and Industry", "Mt CO2/yr", 8985.6725, 10008.8152, 11790.747500000001,
6131.6627, 3271.4353000000006, 1678.8029, 638.87, 259.4755, 82.29590000000003, -7.9353000000000105, -103.9171}}

In[17]:= **em1=ToExpression[Map[Drop[Flatten[#],7]&,Extract[Z,ppos1]]];**
em2 = ToExpression[Map[Drop[Flatten[#], 7] &, Extract[Z, ppos2]]];

In[19]:= **ListPlot[em1,PlotRange→All,Joined→True]**

In[20]:= **Length[em1]**
Out[20]= 127

In[21]:= **emissions=Map[#[[1;;2]]&,ToExpression[Map[StringSplit[#] &, Drop[ReadList["emissionsCO2.txt", String], 31]]]];**
emissions = Table[{emissions[[i, 1]], (44 / 12) * emissions[[i, 2]] / 1000.}, {i, 1, Length[emissions]}];
ListPlot[emissions, Joined → True, PlotStyle → {Black, Thick}, PlotRange → All, Axes → False, Frame → True, FrameStyle → Directive[14, Black],
FrameLabel → {"year", "CO_2 emissions (Gt CO/yr)"}]
(*historical emissions*)

EM = Join[emissions, {{2018, 37.1}}];
data2 = Table[Prepend[Table[{t, Interpolation[Join[EM, Transpose[{{2030, 2040, 2050, 2060, 2070, 2080, 2090, 2100}, 0.001 * Drop[em1[[k]], 1]}]][t]}, {t, 1751, 2100}], {1750, 0}], {k, 1, Length[em1]}]; totliste = Table[data2[[k]][[All, 2]], {k, 1, Length[data2]}];
PLAll = ListPlot[data2, Joined → True, Frame → True, FrameStyle → Directive[Black, 14], PlotRange → All, FrameLabel → {None, "CO2 emissions (Gt CO2)"}]
positivepaths = Table[DeleteCases[Map[# * UnitStep[#] &, totliste[[k]][[269 ;; 351]]], _ ? (# == 0 &)], {k, 1,

```
Length[totliste]}]; ListPlot[positivepaths, Joined → True, PlotRange → All]
(*Before removal of exceedance scenarios*)

In[29]:= RCBliste2=Map[Plus@@#&,positivepaths];

In[175]:= p1=Position[RCBliste2,_?(#<3300&)];

In[31]:= maxtemp=Map[Max[#]&,templiste];
maxtemp2 = Map[Max[#] &, uptempliste];
maxtemp3 = Map[Max[#] &, lowtempliste];

PL1 = ListPlot[Extract[data2, p1], Joined → True,Frame → True, FrameStyle → Directive[Black, 14], PlotRange
→ All];
PL2 = ListPlot[EM, PlotStyle → Black, Joined → True];
FFC = Show[{PL1, PL2}, FrameLabel → {None, "CO2 emissions (Gt CO2)"}, Epilog → Inset[Style["", 18],
Scaled[{0.1, 0.9}]]]
(*After removal of exceedance scenarios*)

In[37]:= PL1=ListPlot[data2[[1]],Joined→True,Frame→True, FrameStyle → Directive[Black, 14], PlotStyle →
Darker[Blue]];
PL2 = ListPlot[EM, PlotStyle → Black, Joined → True];
FFA = Show[{PL1, PL2}, FrameLabel → {None, "CO2 emissions (Gt CO2)"}, Epilog → Inset[Style["a", 18],
Scaled[{0.1, 0.9}]]]

In[40]:= n=Length[data2[[1]]];
futuretime = 2100 - 2020;
τmetan = 12.4;

In[43]:= (* Carbon model *)
τ1=1;
τ2=10;
τ3 = 100;
τ4 = 1000;
c1mean = 0.152;
c2mean = 0.246;
c4mean = 0.134;
c5mean = 0.194;

Gmean = (12/44) *0.47* (c1mean * Table[Exp[- (i - j) / τ1] * UnitStep[i - j], {i, 1, n}, {j, 1, n}]
+ c2mean * Table[Exp[- (i - j) / τ2] * UnitStep[i - j], {i, 1, n}, {j, 1, n}] + (1 - c1mean - c2mean - c4mean -
c5mean)* Table[Exp[- (i - j) / τ3] * UnitStep[i - j], {i, 1, n}, {j, 1, n}]
+ c4mean * Table[Exp[- (i - j) / τ4] * UnitStep[i - j], {i, 1, n}, {j, 1, n}] + Table[c5mean * UnitStep[i - j], {i, 1, n}, {j,
1, n}]);

In[52]:= (* Carbon models *)
c1upper = 0.11;
c2upper = 0.212;
c4upper = 0.106;
c5upper = 0.262;
c1lower = 0.18;
c2lower = 0.296;
c4lower = 0.122;
c5lower = 0.148;

Glower = (12 / 44) * 0.47 * (c1lower * Table[Exp[- (i - j) / τ1] * UnitStep[i - j], {i, 1, n}, {j, 1, n}] +
c2lower * Table[Exp[- (i - j) / τ2] * UnitStep[i - j], {i, 1, n}, {j, 1, n}] +
(1 - c1lower - c2lower - c4lower - c5lower) * Table[Exp[- (i - j) / τ3] * UnitStep[i - j], {i, 1, n}, {j, 1, n}] +
c4lower * Table[Exp[- (i - j) / τ4] * UnitStep[i - j], {i, 1, n}, {j, 1, n}] +
Table[c5lower * UnitStep[i - j], {i, 1, n}, {j, 1, n}]);

Gupper = (12/44) *0.47* (c1upper * Table[Exp[- (i - j) / τ1] * UnitStep[i - j], {i, 1, n}, {j, 1, n}] +
c2upper * Table[Exp[- (i - j) / τ2] * UnitStep[i - j], {i, 1, n}, {j, 1, n}] +
(1 - c1upper - c2upper - c4upper - c5upper) * Table[Exp[- (i - j) / τ3] * UnitStep[i - j], {i, 1, n}, {j, 1, n}] +
```

```
c4upper * Table[Exp[- (i - j) / τ4] * UnitStep[i - j], {i, 1, n}, {j, 1, n}] +
Table[c5upper * UnitStep[i - j], {i, 1, n}, {j, 1, n}]);

In[62]:=
(*Optimal Estimation of Stochastic Energy Balance Model Parameters *)

In[63]:= (* Climate models *)
models = ReadList["CMIP5parameters.txt", String];
models = Delete[models, {{5}, {12}}];
boxes = StringSplit[models][[All, 2]];
Klimaliste = {};
Γliste = {};
σ2liste = {};
Monitor[
Do[

Clear[A];
modelnr = p; If[boxes[[p]] == "2",

{C1, C2, κ1, κ2, σ1, Γ, σ2} = ToExpression[Drop[StringSplit[models[[modelnr]]], 2]];

A = {{-(κ1+ κ2) /C1, κ2/C1}, {κ2/C2, -κ2/C2}};
g = (MatrixExp[t A].{1 / C1, 0})[[1]];
Gklima = Table[Chop[(g /. t → (i - j)) * UnitStep[i - j]], {i, 1, n}, {j, 1, n}];
Klimaliste = Append[Klimaliste, Gklima];
];

If[ boxes[[p]] == "3",

{C1, C2, C3, κ1, κ2, κ3, σ1, Γ, σ2} = ToExpression[Drop[StringSplit[models[[modelnr]]], 2]];

A = {{-(κ1+ κ2) /C1, κ2/C1, 0}, {κ2/C2, -(κ2+κ3)/C2, κ3/C2},{0, κ3/C3, - κ3/C3}};

g = (MatrixExp[t A].{1 / C1, 0, 0})[[1]];
Gklima = Table[Chop[(g /. t → (i - j)) * UnitStep[i - j]], {i, 1, n}, {j, 1, n}];
Klimaliste = Append[Klimaliste, Gklima];
];

If [ boxes[[p]] == "4",

{C1, C2, C3, C4, κ1, κ2, κ3, κ4, σ1, Γ, σ2} = ToExpression[Drop[StringSplit[models[[modelnr]]], 2]];

A = {{-(κ1+κ2)/C1, κ2/C1, 0, 0} , {κ2/C2, -(κ2+κ3)/C2, κ3/C2, 0},{ 0, κ3/C3, -(κ3+κ4)/C3, κ4/C3},
{0, 0, κ4/C4, -κ4/C4}};

g = (MatrixExp[t A].{1 / C1, 0, 0, 0})[[1]];
Gklima = Table[Chop[(g /. t → (i - j)) * UnitStep[i - j]], {i, 1, n}, {j, 1, n}];
Klimaliste = Append[Klimaliste, Gklima];
];

Γliste = Append[Γliste, Γ];
σ2liste = Append[σ2liste, σ2];
, {p, 1, Length[models]}
];
, {p, boxes[[p]]}
];
```

```
(*Nonlin parameter changes*)

styrke = 1; (*w/m^2*)
terskel = 2; (*grader*)
bratthet = 0.5;
Plot[styrke * 0.5 * (1 + Tanh[(T - terskel) / bratthet]), {T, 0, 4}]
(*Test plot to visualise the non-linear forcing*)

RCBliste={};
totliste = {};
templiste = {};
uptempliste = {};
lowtempliste = {};
alltliste = {};
Δfaeroliste = {};
Δfghgliste = {};
Δfliste = {};
noiseliste = {};

Monitor[ Do[
tot = data2[[u]][[All, 2]];
meanco2 = Gmean.tot + 280;
(* metan *)
del1 = 11.9 * tot[[1 ;; Length[EM]]];
(* The factor 11.9 tunes 2019 methane emmisions in 2019 to 440 Tg Methane *)
del2 = hh /. zz → tot[[Length[EM] + 1 ;; Length[tot]]];
del2 = Last[del1] + (del2 - First[del2]) * (Last[del1] - Last[del2]) / (First[del2] - Last[del2]);
metemis = Join[del1, del2];

Gmetan = 0.34 * Table[Exp[- (i - j) / τmetan] * UnitStep[i - j], {i, 1, n}, {j, 1, n}];
(* The factor 0.34 tunes 2019 methane concentration to around 1880 ppb *)
metan = Map[Max[#, 0] &, 700 + Gmetan.metemis];
Δfmetan = 0.036 * (Sqrt[metan] - Sqrt[700]);

Δfco2 = 5.35 Log[1 + (meanco2 - 280) / 280]; (* CO2 til forcing*)
Δfaer= -0.02tot;
Δfaer1 = Δfaer[[1 ;; Length[EM]]] ;
Δfaer2 = Drop[Δfaer, Length[EM]] ;
Δfaer2 = Map[Min[-0.4, #] &, Δfaer2];
Δfaer = Join[Δfaer1, Δfaer2];
Δf = Δfco2 + Δfaer + Δfmetan;
Δfliste = Append[Δfliste, Δf];
Δfaeroliste = Append[Δfaeroliste, Δfaer];
Δfghgliste = Append[Δfghgliste, Δfco2 + Δfmetan];

Tliste = {}; Do[
T2 = Klimaliste[[p]].Δf;

(*nonlin loop*)
Do[
T2 = Klimaliste[[p]].(Δf + styrke * 0.5 * (1 + Tanh[(T2 - terskel) / bratthet])); , {10}]; (*number of iterations*)
noise = σ2liste[[p]] * (Klimaliste[[p]].RandomReal[NormalDistribution[0, 1], Length[Δf]]);
noise = Drop[noise, 268 - 20];
T2 = T2 * (Γliste[[p]] / Log[4.]) / 5.35;
T2 = Drop[T2, 268]; T2=1.1+T2-T2[[1]];
noiseliste = Append[noiseliste, noise];
Tliste = Append[Tliste, T2];
, {p, 1, Length[models]}];

middel =Table[Mean[Transpose[Tliste][[i]]], {i, 1, Length[Transpose[Tliste]]}];
upper = Table[Mean[Transpose[Tliste][[i]]] + StandardDeviation[ Transpose[Tliste][[i]]], {i, 1, Length[Trans-
pose[Tliste]]}];
```

```
lower = Table[Mean[Transpose[Tliste][[i]]] - StandardDeviation[ Transpose[Tliste][[i]]], {i, 1, Length[Trans-
pose[Tliste]]}];

RCB = Plus @@ Drop[tot, 270];
RCBliste = Append[RCBliste, RCB];
totliste = Append[totliste, tot]; alltliste = Join[alltliste, Tliste];
templiste = Append[templiste, middel];
uptempliste = Append[uptempliste, upper];
lowtempliste = Append[lowtempliste, lower]; , {u, 1, Length[data2]}]
, u];
```

In[258]:= **Length[noise]**
Out[!]= 103

In[259]:= **Length[T2]**
Out[!]= 83

```
In[260]:= window=10;
noiseliste2 = Table[MovingAverage[noiseliste[[i]], window][[1 ;; Length[T2]]], {i, 1, Length[noiseliste]}];
noiseliste2 = Transpose[Partition[noiseliste2, 14]];
```

In[263]:= **Length[noiseliste2]**
Out[!]= 14

In[264]:= **Dimensions[noiseliste2]**
Out[!]= {14, 127, 83}

In[265]:= **Length[noiseliste2[[1]]]**
Out[!]= 127

```
PLNoise = ListPlot[Map[Transpose[{2018 + Range[Length[templiste[[1]]]], #}] &, noiseliste2[[3]]], Joined →
True];
FFNoise = Show[PLNoise, PlotRange → All, Joined → True, Axes → False, Frame → True, FrameStyle → Di-
rective[Black, 14], Joined → True, FrameLabel → {None, "Internal temperature variability(°C)"}, Epilog → In-
set[Style["", 18], Scaled[{0.1, 0.9}]]]

FFE=ListPlot[Map[Transpose[{2018+Range[Length[templiste[[1]]]],#}]&, Extract[templiste, p1]], PlotRange
→ All, Joined → True, Axes → False, Frame → True, FrameStyle → Directive[Black, 14], FrameLabel → {None,
"GMST increase (°C)"}, Epilog → Inset[Style["e", 18], Scaled[{0.1, 0.9}]]]
PL1 = ListPlot[Map[Transpose[{1749 + Range[Length[Δfaeroliste[[1]]]], #}] &, Extract[Δfaeroliste, p1]],
Joined → True];
PL2 = ListPlot[Map[Transpose[{1749 + Range[Length[Δfaeroliste[[1]]]], #}] &, Extract[Δfghgliste, p1]], Joined
→ True];
FFD = Show□{PL1, PL2}, PlotRange → All, Joined → True, Axes → False, Frame → True, FrameStyle → Di-
rective[Black, 14], FrameLabel → □None, "Forcing (W/m^2)"э, Epilog → Inset[Style["d", 18], Scaled[{0.1, 0.9}]]]
```

In[267]:=

```
In[271]:=modellfarger={,,,,,,,,,,,,,,,, };
In[272]:= pan=LineLegend[modellfarger,Map[StringSplit[#]&,models][[All,1]]]

In[273]:= FFB=ListPlot[Map[Transpose[{2018+Range[Length[alltliste[[1]]]],#}]&, alltliste[[1 ;; 14]]], PlotRange →
All, Joined → True, Axes → False, Frame → True, FrameStyle → Directive[Black, 14], FrameLabel → {None,
"GMST increase (°C)"}, Epilog → Inset[Style["b", 18], Scaled[{0.1, 0.9}]], PlotStyle → Map[{#} &, modellfarger]]

In[!]:= Grid[{{Show[FFA,ImageSize→400],Show[FFB,ImageSize→400],pan}}]

In[!]:= Grid[{{Show[FFC,ImageSize→400, Epilog → Inset[Style["a", 18], Scaled[{0.1, 0.9}]]], Show[FFD, ImageSize
→ 400, Epilog → Inset[Style["b", 18], Scaled[{0.1, 0.9}]]] , Show[FFE, ImageSize → 400, Epilog → Inset[Style["c",
18], Scaled[{0.1, 0.9}]]]}}]
```

```
In[]:= maxtemp=Map[Max[#]&,templiste];
maxtemp2 = Map[Max[#] &, uptempliste];
maxtemp3 = Map[Max[#] &, lowtempliste];

In[]:= PL1=ListPlot[Extract[Transpose[{maxtemp,RCBliste2}],p1], AspectRatio → 1, PlotRange → All];
PL3 = ListPlot[Extract[Transpose[{maxtemp2, RCBliste2}], p1], AspectRatio → 1, PlotRange → All, PlotStyle →
Red];
PL4 = ListPlot[Extract[Transpose[{maxtemp2, RCBliste2}], p1], AspectRatio → 1, PlotRange → All, PlotStyle →
Red];
gg = Fit[Extract[Transpose[{maxtemp, RCBliste2}], p1], {zz, 1}, zz]; PL2 = Plot[gg, {zz, 1.2, 3.5}];
gg2 = Fit[Extract[Transpose[{maxtemp2, RCBliste2}], p1], {zz, 1}, zz]; PL4 = Plot[gg2, {zz, 1.2, 3}];
Show[{PL1, PL2}, PlotRange → All]

In[]:= pairs=Extract[Transpose[{maxtemp,RCBliste2}],p1];
error = pairs[[All, 2]] - (gg /. zz → pairs[[All, 1]]);
S = Sqrt[(Plus @@ (error^2)) / (Length[pairs] - 2)];
σx = StandardDeviation[pairs[[All, 1]]];
σf[x_] := S * Sqrt[1 + 1 / Length[pairs] + (x - Mean[pairs[[All, 1]]])^2 / (Length[pairs] * σx^2)];

In[]:= pdf=(PDF[NormalDistribution[gg,σf[zz]]][p])/.zz→2.0;
pdf2 = (PDF[NormalDistribution[gg, σf[zz]]][p]) /. zz → 3.0;
Plot[{pdf, pdf2}, {p, 0, 5200}, PlotRange → All]

PL1 = ListPlot[Extract[Transpose[{maxtemp, RCBliste2}], p1], AspectRatio → 1, PlotRange → {{1, 4}, {0,
4000}}, PlotStyle → Darker[Blue]];

PL2 = Plot[gg, {zz, 1, 3.5}, PlotStyle → Darker[Blue]];
l1 = Graphics[{Black, Line[{{2.0, 0}, {2.0, gg /. zz → 2.0}}]}];
l2 = Graphics[{Black, Line[{{2.0, gg /. zz → 2.0}, {1, gg /. zz → 2.0}}]}]; inset = ParametricPlot[{1 + 60 * pdf, p},
{p, 400, 1200}, Axes → False, PlotStyle → {Black, Thickness[0.01]}]; (*{p, budget low, budget high}*)
l11 = Graphics[{Black, Line[{{3.0, 0}, {3.0, gg /. zz → 3.0}}]}];
l22 = Graphics[{Black, Line[{{3.0, gg /. zz → 3.0}, {1, gg /. zz → 3.0}}]}]; inset2 = ParametricPlot[{1 + 60 * pdf2,
p}, {p, 1900, 2700}, Axes → False, PlotStyle → {Black, Thickness[0.01]}];(*{p, budget low, budget high}*)

FA = Show[{PL1, PL2, l1, l2, l11, l22, inset, inset2}, Axes → False, Frame → True, FrameStyle → Directive[Black,
14], FrameLabel → {"Global temperature increase (°C)", "Carbon budget after 2018 (Gt CO2)"}, Epilog → In-
set[Style["a", 18], Scaled[{0.1, 0.9}]], ImageSize → 400, PlotRange → {{1, 4}, {0, 4500}}]
(*TCRE for 1 ESM, 86 scenarios*)
```

ALL CLIMATE MODELS

(*Just to get the TCRE plots*)

```
maxtemp = Partition[Map[Max[#] &, alltliste], 14][[All, 5]]; PL1 = ListPlot[Extract[Transpose[{maxtemp,
RCBliste2}], p1], AspectRatio → 1, PlotRange → All, PlotStyle → Black];
gg = Fit[Extract[Transpose[{maxtemp, RCBliste2}], p1], {zz, 1}, zz];
PL2 = Plot[gg, {zz, 1.2, 3.5}, PlotStyle → Black];
QL1 = Show[{PL1, PL2}, PlotRange → All];

maxtemp = Partition[Map[Max[#] &, alltliste], 14][[All, 7]];
PL1 = ListPlot[Extract[Transpose[{maxtemp, RCBliste2}], p1], AspectRatio → 1, PlotRange → All, PlotStyle →
Darker[Red]];
gg = Fit[Extract[Transpose[{maxtemp, RCBliste2}], p1], {zz, 1}, zz];
PL2 = Plot[gg, {zz, 1.2, 3.5}, PlotStyle → Darker[Red]];
QL2 = Show[{PL1, PL2}, PlotRange → All];
FB = Show[{QL1, QL2}, Axes → False, Frame → True, FrameStyle → Directive[Black, 14], FrameLabel →
{"Global temperature increase (°C)", "Carbon budget after 2018 (Gt CO2)"}, Epilog → {Inset[Style["b", 18],
Scaled[{0.1, 0.9}]], Inset[LineLegend[{Black, Darker[Red]}, {"CSIRO-Mk3.6.0", "GFDL-ESM2M"}], Scaled[{0.7,
0.3}]]}, ImageSize → 400, PlotRange → {{1, 4}, {0, 4500}}]
```

```
In[]:= Grid[{{FA,FB}}]
(*Grid plot of TCRE's *)
```

ALL CLIMATE MODELS, 2 CARBON MODELS AND INTERNAL VARIABILITY

```
RCBliste = {};
totliste = {};
templiste = {};
uptempliste = {};
lowtempliste = {};
alltliste = {};

Monitor[ Do[
tot = data2[[u]][[All, 2]];
meanco2 = Gmean.tot + 280;
meanco2upper = Gupper.tot + 280;
meanco2lower = Glower.tot + 280; (* forcing *)

(* metan *)
del1 = 11.9 * tot[[1 ;; Length[EM]]];
(* The factor 3.0 tunes 2019 methane emmisions in 2019 to 440 Tg Methane *)
del2 = hh /. zz → tot[[Length[EM] + 1 ;; Length[tot]]];
del2 = Last[del1] + (del2 - First[del2]) * (Last[del1] - Last[del2]) / (First[del2] - Last[del2]);
metemis = Join[del1, del2];

Gmetan = 0.34 * Table[Exp[- (i - j) / τmetan] * UnitStep[i - j], {i, 1, n}, {j, 1, n}];
(* The factor 0.35 tunes 2019 methane concentration to around 1880 ppb *)
metan = Map[Max[#, 0] &, 700 + Gmetan.metemis];

Δfmetan = 0.036 * (Sqrt[metan] - Sqrt[700]);
Δfco2 = 5.35 Log[1 + (meanco2 - 280) / 280]; (* CO2 til forcing*)
Δfco2upper = 5.35 Log[1 + (meanco2upper - 280) / 280];(* CO2 til forcing*)
Δfco2lower = 5.35 Log[1 + (meanco2lower - 280) / 280]; (* CO2 til forcing*)
(* aerosols *)
Δfaer= -0.02tot;
Δfaer1 = Δfaer[[1 ;; Length[EM]]] ;
Δfaer2 = Drop[Δfaer, Length[EM]] ;
Δfaer2 = Map[Min[-0.4, #] &, Δfaer2];
Δfaer = Join[Δfaer1, Δfaer2];
Δf = Δfco2 + Δfaer + Δfmetan;
Δfupper = Δfco2upper + Δfaer + Δfmetan;
Δflower = Δfco2lower + Δfaer + Δfmetan;

Tliste = {};
Do[
T2 = Klimaliste[[p]].Δfupper;

(*nonlin loop*)
Do[
T2 = Klimaliste[[p]].
(Δfupper + styrke * 0.5 * (1 + Tanh[(T2 - terskel) / bratthet]));
, {10}]; (*number of iterations*)

T2 = T2 * (Γliste[[p]] / Log[4.]) / 5.35;
T2 = Drop[T2, 268];
T2=1.1+T2-T2[[1]];
Tliste = Append[Tliste, T2 + StandardDeviation[Flatten[noiseliste2[[p]]]]];
```

```
(*T2=Klimaliste[[p]].Δfupper;
T2=T2*(Γliste[[p]]/Log[4.])/5.35;
T2=Drop[T2,268];
T2=1.1+T2-T2[[1]]; Tliste=Append[Tliste,T2-StandardDeviation[Flatten[noiseliste2[[p]]]]];*)

(*T2=Klimaliste[[p]].Δflower;
T2=T2*(Γliste[[p]]/Log[4.])/5.35;
T2=Drop[T2,268];
T2=1.0+T2-T2[[1]]; Tliste=Append[Tliste,T2+StandardDeviation[Flatten[noiseliste2[[p]]]]];*)

T2 = Klimaliste[[p]].Δflower;
(*nonlin loop*)
Do[
T2 = Klimaliste[[p]].
(Δflower + styrke * 0.5 * (1 + Tanh[(T2 - terskel) / bratthet]));
, {10}]; (*number of iterations*)

T2 = T2 * (Γliste[[p]] / Log[4.]) / 5.35;
T2 = Drop[T2, 268]; T2=1.0+T2-T2[[1]];

Tliste = Append[Tliste, T2 - StandardDeviation[Flatten[noiseliste2[[p]]]]];
, {p, 1, Length[models]}];

middel = Table[Mean[Transpose[Tliste][[i]]], {i, 1, Length[Transpose[Tliste]]}];
upper = Table[Mean[Transpose[Tliste][[i]]] + StandardDeviation[ Transpose[Tliste][[i]]], {i, 1, Length[Trans-
pose[Tliste]]}];
lower = Table[Mean[Transpose[Tliste][[i]]] - StandardDeviation[ Transpose[Tliste][[i]]], {i, 1, Length[Trans-
pose[Tliste]]}]; RCB = Plus @@ Drop[tot, 270];

RCBliste = Append[RCBliste, RCB];
totliste = Append[totliste, tot];
alltliste = Join[alltliste, Tliste];
templiste = Append[templiste, middel];
uptempliste = Append[uptempliste, upper];
lowtempliste = Append[lowtempliste, lower];
, {u, 1, Length[data2]}]
,u]

In[]:= Dimensions[alltliste]
Out[]= {3556, 83}

In[]:= CM = {};
cm1 = Table[ Partition[Extract[Partition[Map[Max[#] &, alltliste], 2 * 14], p1][[kk]], 2][[ All, 1]], {kk, 1,
Length[p1]}];
cm2 = Table[Partition[Extract[Partition[Map[Max[#] &, alltliste], 2 * 14], p1][[ kk]], 2][[All, 2]], {kk, 1,
Length[p1]}];

Do[
CM = Append[CM, Transpose[{Extract[RCBliste2, p1], Transpose[cm1][[j]]}]];
CM = Append[CM, Transpose[{Extract[RCBliste2, p1], Transpose[cm2][[j]]}]];
, {j, 1, Length[Transpose[cm2]]}];

In[]:= ListPlot[{CM[[1]],CM[[2]]}]

In[]:= smliste={};
tliste = {};

Monitor[ Do[
pdfliste = {}; Do[

gg = Fit[Map[Reverse[#] &, CM[[kk]]], {zz, 1}, zz];
pairs = Map[Reverse[#] &, CM[[kk]]];
error = pairs[[All, 2]] - (gg /. zz → pairs[[All, 1]]);
```

```
S = Sqrt[(Plus @@ (error^2)) / (Length[pairs] - 2)];
σx = StandardDeviation[pairs[[All, 1]]];
σf[x_] := S * Sqrt[1 + 1 / Length[pairs] + (x - Mean[pairs[[All, 1]]])^2 / (Length[pairs] * σx^2)];
pdf = Chop[(PDF[NormalDistribution[gg, σf[zz]]][p]) /. zz → target];
pdfliste = Append[pdfliste, pdf];
,{kk,1,2*14}];

g = Mean[pdfliste];
smooth = Convolve[PDF[NormalDistribution[0, 400]][p], g, p, x];
sm = smooth /. x → Range[7000];
smliste = Append[smliste, sm];
tliste = Append[tliste, target];
, {target, 1.1, 4.0, 0.01}];
, target];

In[]:= budget=500;
Δt = tliste[[2]] - tliste[[1]];
y = Transpose[smliste][[budget]];
y = y/ ((Plus@@y) * Δt); ListPlot[Transpose[{tliste, y}], Joined → True]

In[]:= budget=1500;
Δt = tliste[[2]] - tliste[[1]];
y = Transpose[smliste][[budget]];
y = y/ ((Plus@@y) * Δt); ListPlot[Transpose[{tliste, y}], Joined → True]

In[]:= bliste={};

Do[
Δt = tliste[[2]] - tliste[[1]];
y = Transpose[smliste][[budget]];
y = y/ ((Plus@@y) * Δt);

t1= tliste[[First[Position[FoldList[Plus, 0, y * Δt], _ ? (# > 0.90 &)]][[1]] - 1]];
t2 = tliste[[First[Position[FoldList[Plus, 0, y * Δt], _ ? (# > 0.75 &)]][[1]] - 1]];
t3 = tliste[[First[Position[FoldList[Plus, 0, y * Δt], _ ? (# > 0.5 &)]][[1]] - 1]];
t4= tliste[[First[Position[FoldList[Plus, 0, y * Δt], _ ? (# > 0.25 &)]][[1]] - 1]];
t5 = tliste[[First[Position[FoldList[Plus, 0, y * Δt], _ ? (# > 0.10 &)]][[1]] - 1]];
bliste = Append[bliste, {budget, t1, t2, t3, t4, t5}];
, {budget, 200, 4000, 100}]

In[]:= farger={Red,Darker[Red],Black,Darker[Blue],Blue};
a = ListPlot[{Transpose[{bliste[[All, 1]], bliste[[All, 2]]}],

Transpose[{bliste[[All, 1]], bliste[[All, 3]]}], Transpose[{bliste[[All, 1]], bliste[[All, 4]]}], Trans-
pose[{bliste[[All, 1]], bliste[[All, 5]]}], Transpose[{bliste[[All, 1]], bliste[[All, 6]]}]}, Joined → True, AspectRatio
→ 1, PlotRange → {1, 4.0}, Axes → False, Frame → True, FrameStyle → Directive[Black, 14], PlotStyle → Ta-
ble[farger[[i]], {i, 1, 5}], GridLines → Automatic, FrameLabel → {"Carbon budget from 2018 (GtCO2)", "Maxi-
mum temperature increase (°C)"}, PlotLegends → Placed[{"10% prob.", "25% prob.", "even chance", "75%
prob.", "90% prob."}, {Scaled[{0.05, 0.7}], {0, 0.5}}]]; l = Graphics[{Black, Line[{{1294, 1}, {1294, 2.5}}]}];
GGD = Show[{a}, PlotRange → {{0, 4000}, {1, 4.3}}]

(*RCB estimates for non-linear framework *)
```

CODE FOR IMPLEMENTATION OF THE ARCTIC AMPLIFICATION FACTOR

The following code is used the non-linear framework in the SRM as described in Section 3.7. Produced in Mathematica: Version: 12.0.0.0 in collaboration with research partners Andreas Johansen, Andreas Martinsen and supervision from Martin Rypdal.
Platform: Mac OS X x86 (64-bit). macOS Catalina: Version 10.15.3.

```
In[283]:= SetDirectory["OneDrive - UiT Office 365"];
Z = Import["SSP_IAM_V2_201811.csv"];
Z = Map[StringSplit[#, ","] &, Z];

In[5]:= hh=157.65890684920566`+1.8942819330281027`zz+0.08520850267749702`zz^2;

In[6]:= Z[[1]]
Out[6]= {{MODEL, "SCENARIO", "REGION", "VARIABLE", "UNIT",
2005, 2010, 2020, 2030, 2040, 2050, 2060, 2070, 2080, 2090, 2100}}

In[7]:= RR=Table[Z[[k]][[1]][[4]],{k,1,Length[Z]}];
Union[RR]

Out[8]= {"Agricultural Demand|Crops", "Agricultural Demand|Crops|Energy",
"Agricultural Demand|Livestock", "Agricultural Production|Crops|Energy",
"Agricultural Production|Crops|Non-Energy","Agricultural Production|Livestock", "Capacity|Electricity",
"Capacity|Electricity|Biomass", "Capacity|Electricity|Coal", "Capacity|Electricity|Gas",
"Capacity|Electricity|Geothermal", "Capacity|Electricity|Hydro", "Capacity|Electricity|Nuclear",
"Capacity|Electricity|Oil", "Capacity|Electricity|Other", "Capacity|Electricity|Solar", "Capacity|Electricity|Solar|CSP",
"Capacity|Electricity|Solar|PV", "Capacity|Electricity|Wind", "Capacity|Electricity|Wind|Offshore",
"Capacity|Electricity|Wind|Onshore", "Consumption", "Diagnostics|MAGICC6|Concentration|CH4",
"Diagnostics|MAGICC6|Concentration|CO2", "Diagnostics|MAGICC6|Concentration|N2O",
"Diagnostics|MAGICC6|Forcing", "Diagnostics|MAGICC6|Forcing|Aerosol", "Diagnostics|MAGICC6|Forcing|CH4",
"Diagnostics|MAGICC6|Forcing|CO2", "Diagnostics|MAGICC6|Forcing|F-Gases",
"Diagnostics|MAGICC6|Forcing|Kyoto Gases", "Diagnostics|MAGICC6|Forcing|N2O",
"Diagnostics|MAGICC6|Temperature|Global Mean", "Emissions|BC", "Emissions|CH4",
"Emissions|CH4|Fossil Fuels and Industry", "Emissions|CH4|Land Use", "Emissions|CO",
"Emissions|CO2", "Emissions|CO2|Carbon Capture and Storage",
"Emissions|CO2|Carbon Capture and Storage|Biomass","Emissions|CO2|Fossil Fuels and Industry",
"Emissions|CO2|Land Use", "Emissions|F-Gases", "Emissions|Kyoto Gases", "Emissions|N2O",
"Emissions|N2O|Land Use", "Emissions|NH3", "Emissions|NOx", "Emissions|OC", "Emissions|Sulfur",
"Emissions|VOC", "Energy Service|Transportation|Freight", "Energy Service|Transportation|Passenger",
"Final Energy","Final Energy|Electricity", "Final Energy|Gases", "Final Energy|Heat",
"Final Energy|Hydrogen", "Final Energy|Industry", "Final Energy|Liquids",
"Final Energy|Residential and Commercial", "Final Energy|Solar","Final Energy|Solids",
"Final Energy|Solids|Biomass","Final Energy|Solids|Biomass|Traditional", "Final Energy|Solids|Coal",
"Final Energy|Transportation", "GDP|PPP", "Harmonized Emissions|BC",
"Harmonized Emissions|CH4|Fossil Fuels and Industry","Harmonized Emissions|CH4|Land Use",
"Harmonized Emissions|CO","Harmonized Emissions|CO2|Fossil Fuels and Industry",
"Harmonized Emissions|CO2|Land Use", "Harmonized Emissions|F-Gases", "Harmonized Emissions|Kyoto Gases",
"Harmonized Emissions|NH3", "Harmonized Emissions|NOx", "Harmonized Emissions|OC",
"Harmonized Emissions|Sulfur", "Harmonized Emissions|VOC","Land Cover|Built-up Area",
"Land Cover|Cropland", "Land Cover|Forest", "Land Cover|Pasture", "Population", "Price|Carbon", "Primary Energy",
"Primary Energy|Biomass", "Primary Energy|Biomass|Traditional", "Primary Energy|Biomass|w/ CCS",
"Primary Energy|Biomass|w/o CCS", "Primary Energy|Coal", "Primary Energy|Coal|w/ CCS",
"Primary Energy|Coal|w/o CCS", "Primary Energy|Fossil", "Primary Energy|Fossil|w/ CCS",
"Primary Energy|Fossil|w/o CCS","Primary Energy|Gas", "Primary Energy|Gas|w/ CCS",
"Primary Energy|Gas|w/o CCS", "Primary Energy|Geothermal","Primary Energy|Hydro",
"Primary Energy|Non-Biomass Renewables","Primary Energy|Nuclear", "Primary Energy|Oil",
"Primary Energy|Oil|w/ CCS", "Primary Energy|Oil|w/o CCS","Primary Energy|Other",
"Primary Energy|Secondary Energy Trade","Primary Energy|Solar", "Primary Energy|Wind",
```

"Secondary Energy|Electricity", "Secondary Energy|Electricity|Biomass",
"Secondary Energy|Electricity|Biomass|w/ CCS","Secondary Energy|Electricity|Biomass|w/o CCS",
"Secondary Energy|Electricity|Coal","Secondary Energy|Electricity|Coal|w/ CCS",
"Secondary Energy|Electricity|Coal|w/o CCS","Secondary Energy|Electricity|Gas",
"Secondary Energy|Electricity|Gas|w/ CCS", "Secondary Energy|Electricity|Gas|w/o CCS",
"Secondary Energy|Electricity|Geothermal","Secondary Energy|Electricity|Hydro",
"Secondary Energy|Electricity|Non-Biomass Renewables","Secondary Energy|Electricity|Nuclear",
"Secondary Energy|Electricity|Oil", "Secondary Energy|Electricity|Solar", "Secondary Energy|Electricity|Wind",
"Secondary Energy|Gases", "Secondary Energy|Gases|Biomass","Secondary Energy|Gases|Coal",
"Secondary Energy|Gases|Natural Gas", "Secondary Energy|Heat", "Secondary Energy|Heat|Geothermal",
"Secondary Energy|Hydrogen", "Secondary Energy|Hydrogen|Biomass",
"Secondary Energy|Hydrogen|Biomass|w/ CCS", "Secondary Energy|Hydrogen|Biomass|w/o CCS",
"Secondary Energy|Hydrogen|Electricity", "Secondary Energy|Liquids", "Secondary Energy|Liquids|Biomass",
"Secondary Energy|Liquids|Biomass|w/ CCS", "Secondary Energy|Liquids|Biomass|w/o CCS",
"Secondary Energy|Liquids|Coal", "Secondary Energy|Liquids|Coal|w/ CCS",
"Secondary Energy|Liquids|Coal|w/o CCS", "Secondary Energy|Liquids|Gas",
"Secondary Energy|Liquids|Gas|w/ CCS", "Secondary Energy|Liquids|Gas|w/o CCS",
"Secondary Energy|Liquids|Oil", "Secondary Energy|Solids", "VARIABLE"}

In[9]:=
```
RRR=Table[Z[[k]][[1]][[3]],{k,1,Length[Z]}];
Union[RRR]
```

Out[10]= {"R5.2ASIA", "R5.2LAM", "R5.2MAF", "R5.2OECD", "R5.2REF", "REGION", "World"}

In[11]:=
```
co2pos1=Position[RR,_?(#=="\"Emissions|CO2|FossilFuelsandIndustry\""&)];
co2pos2 = Position[RR, _ ? (# == "\"Emissions|CO2|Land Use\"" &)];
co2pos3 = Position[RRR, _ ? (# == "\"World\"" &)];
```

In[14]:=
```
ppos1=Intersection[co2pos3,co2pos1];
ppos2 = Intersection[co2pos3, co2pos2];
```

In[16]:=
```
Extract[Z,co2pos1][[1]]
```

Out[16]= {{AIM/CGE, "SSP1-19", "R5.2ASIA", "Emissions|CO2|Fossil Fuels and Industry", "Mt CO2/yr", 8985.6725, 10008.8152, 11790.747500000001,
6131.6627, 3271.4353000000006, 1678.8029, 638.87, 259.4755, 82.29590000000003, -7.9353000000000105, -103.9171}}

In[17]:=
```
em1=ToExpression[Map[Drop[Flatten[#],7]&,Extract[Z,ppos1]]];
em2 = ToExpression[Map[Drop[Flatten[#], 7] &, Extract[Z, ppos2]]];
```

In[19]:=
```
ListPlot[em1,PlotRange→All,Joined→True]
```

In[20]:=
```
Length[em1]
```
Out[20]= 127

In[21]:=
```
emissions=Map[#[[1;;2]]&,ToExpression[Map[StringSplit[#] &, Drop[ReadList["emissionsCO2.txt", String], 31]]]];
emissions = Table[{emissions[[i, 1]], (44 / 12) * emissions[[i, 2]] / 1000.}, {i, 1, Length[emissions]}];
ListPlot[emissions, Joined → True, PlotStyle → {Black, Thick}, PlotRange → All, Axes → False, Frame → True,
FrameStyle → Directive[14, Black],
FrameLabel → {"year", "CO2 emissions (Gt CO/yr)"}]
(*historical emissions*)

EM = Join[emissions, {{2018, 37.1}}];
data2 = Table[Prepend[Table[{t, Interpolation[Join[EM, Transpose[{{2030, 2040, 2050, 2060, 2070, 2080, 2090, 2100}, 0.001 * Drop[em1[[k]], 1]}]][t]}, {t, 1751, 2100}], {1750, 0}], {k, 1, Length[em1]}]; totliste = Table[data2[[k]][[All, 2]], {k, 1, Length[data2]}];
PLAll = ListPlot[data2, Joined → True, Frame → True, FrameStyle → Directive[Black, 14], PlotRange → All,
FrameLabel → {None, "CO2 emissions (Gt CO2)"}]

positivepaths = Table[DeleteCases[Map[# * UnitStep[#] &, totliste[[k]][[269 ;; 351]]], _ ? (# == 0 &)], {k, 1,
```

```
Length[totliste]}]; ListPlot[positivepaths, Joined → True, PlotRange → All]
(*Before removal of exceedance scenarios*)

In[29]:= RCBliste2=Map[Plus@@#&,positivepaths];

In[175]:= p1=Position[RCBliste2,_?(#<3300&)];

In[31]:= maxtemp=Map[Max[#]&,templiste];
maxtemp2 = Map[Max[#] &, uptempliste];
maxtemp3 = Map[Max[#] &, lowtempliste];

PL1 = ListPlot[Extract[data2, p1], Joined → True,Frame → True, FrameStyle → Directive[Black, 14], PlotRange
→ All];
PL2 = ListPlot[EM, PlotStyle → Black, Joined → True];
FFC = Show[{PL1, PL2}, FrameLabel → {None, "CO2 emissions (Gt CO2)"}, Epilog → Inset[Style["", 18],
Scaled[{0.1, 0.9}]]]
(*After removal of exceedance scenarios*)

In[37]:= PL1=ListPlot[data2[[1]],Joined→True,Frame→True, FrameStyle → Directive[Black, 14], PlotStyle →
Darker[Blue]];
PL2 = ListPlot[EM, PlotStyle → Black, Joined → True];
FFA = Show[{PL1, PL2}, FrameLabel → {None, "CO2 emissions (Gt CO2)"}, Epilog → Inset[Style["a", 18],
Scaled[{0.1, 0.9}]]]

In[40]:= n=Length[data2[[1]]];
futuretime = 2100 - 2020;
τmetan = 12.4;

In[43]:= (* Carbon model *)
τ1=1;
τ2=10;
τ3 = 100;
τ4 = 1000;
c1mean = 0.152;
c2mean = 0.246;
c4mean = 0.134;
c5mean = 0.194;

Gmean = (12/44) *0.47* (c1mean * Table[Exp[- (i - j) / τ1] * UnitStep[i - j], {i, 1, n}, {j, 1, n}]
+ c2mean * Table[Exp[- (i - j) / τ2] * UnitStep[i - j], {i, 1, n}, {j, 1, n}] + (1 - c1mean - c2mean - c4mean -
c5mean)* Table[Exp[- (i - j) / τ3] * UnitStep[i - j], {i, 1, n}, {j, 1, n}]
+ c4mean * Table[Exp[- (i - j) / τ4] * UnitStep[i - j], {i, 1, n}, {j, 1, n}] + Table[c5mean * UnitStep[i - j], {i, 1, n}, {j,
1, n}]);

In[52]:= (* Carbon models *)
c1upper = 0.11;
c2upper = 0.212;
c4upper = 0.106;
c5upper = 0.262;
c1lower = 0.18;
c2lower = 0.296;
c4lower = 0.122;
c5lower = 0.148;

Glower = (12 / 44) * 0.47 * (c1lower * Table[Exp[- (i - j) / τ1] * UnitStep[i - j], {i, 1, n}, {j, 1, n}] +
c2lower * Table[Exp[- (i - j) / τ2] * UnitStep[i - j], {i, 1, n}, {j, 1, n}] +
(1 - c1lower - c2lower - c4lower - c5lower) * Table[Exp[- (i - j) / τ3] * UnitStep[i - j], {i, 1, n}, {j, 1, n}] +
c4lower * Table[Exp[- (i - j) / τ4] * UnitStep[i - j], {i, 1, n}, {j, 1, n}] +
Table[c5lower * UnitStep[i - j], {i, 1, n}, {j, 1, n}]);

Gupper = (12/44) *0.47* (c1upper * Table[Exp[- (i - j) / τ1] * UnitStep[i - j], {i, 1, n}, {j, 1, n}] +
c2upper * Table[Exp[- (i - j) / τ2] * UnitStep[i - j], {i, 1, n}, {j, 1, n}] +
(1 - c1upper - c2upper - c4upper - c5upper) * Table[Exp[- (i - j) / τ3] * UnitStep[i - j], {i, 1, n}, {j, 1, n}] +
```

```
c4upper * Table[Exp[- (i - j) / τ4] * UnitStep[i - j], {i, 1, n}, {j, 1, n}] +
Table[c5upper * UnitStep[i - j], {i, 1, n}, {j, 1, n}]);

In[62]:=
(*Optimal Estimation of Stochastic Energy Balance Model Parameters *)

In[63]:= (* Climate models *)
models = ReadList["CMIP5parameters.txt", String];
models = Delete[models, {{5}, {12}}];
boxes = StringSplit[models][[All, 2]];
Klimaliste = {};
Γliste = {};
σ2liste = {};
Monitor[
Do[

Clear[A];
modelnr = p; If[boxes[[p]] == "2",

{C1, C2, κ1, κ2, σ1, Γ, σ2} = ToExpression[Drop[StringSplit[models[[modelnr]]], 2]];

A = {{-(κ1+ κ2) /C1, κ2/C1}, {κ2/C2, -κ2/C2}};
g = (MatrixExp[t A].{1 / C1, 0})[[1]];
Gklima = Table[Chop[(g /. t → (i - j)) * UnitStep[i - j]], {i, 1, n}, {j, 1, n}];
Klimaliste = Append[Klimaliste, Gklima];
];

If[ boxes[[p]] == "3",

{C1, C2, C3, κ1, κ2, κ3, σ1, Γ, σ2} = ToExpression[Drop[StringSplit[models[[modelnr]]], 2]];

A = {{-(κ1+ κ2) /C1, κ2/C1, 0}, {κ2/C2, -(κ2+κ3)/C2, κ3/C2},{0, κ3/C3, - κ3/C3}};

g = (MatrixExp[t A].{1 / C1, 0, 0})[[1]];
Gklima = Table[Chop[(g /. t → (i - j)) * UnitStep[i - j]], {i, 1, n}, {j, 1, n}];
Klimaliste = Append[Klimaliste, Gklima];
];

If [ boxes[[p]] == "4",

{C1, C2, C3, C4, κ1, κ2, κ3, κ4, σ1, Γ, σ2} = ToExpression[Drop[StringSplit[models[[modelnr]]], 2]];

A = {{-(κ1+κ2)/C1, κ2/C1, 0, 0} , {κ2/C2, -(κ2+κ3)/C2, κ3/C2, 0},{ 0, κ3/C3, -(κ3+κ4)/C3, κ4/C3},
{0, 0, κ4/C4, -κ4/C4}};

g = (MatrixExp[t A].{1 / C1, 0, 0, 0})[[1]];
Gklima = Table[Chop[(g /. t → (i - j)) * UnitStep[i - j]], {i, 1, n}, {j, 1, n}];
Klimaliste = Append[Klimaliste, Gklima];
];

Γliste = Append[Γliste, Γ];
σ2liste = Append[σ2liste, σ2];
, {p, 1, Length[models]}
];
, {p, boxes[[p]]}
];
```

```
(*Nonlin parameter changes*)

styrke = 1; (*w/m^2*)
terskel = 2; (*grader*)
bratthet = 0.5;
Plot[styrke * 0.5 * (1 + Tanh[(T - terskel) / bratthet]), {T, 0, 4}]
(*Test plot to visualise the non-linear forcing*)

In[]:= RCBliste={};
totliste = {};
templiste = {};
uptempliste = {};
lowtempliste = {};
alltliste = {};
Δfaeroliste = {};
Δfghgliste = {};
Δfliste = {};
noiseliste = {};

Monitor[
Do[
tot = data2[[u]][[All, 2]]; meanco2 = Gmean.tot + 280;
(* metan *)
del1 = 11.9 * tot[[1 ;; Length[EM]]];
(* The factor 11.9 tunes 2019 methane emmisions in 2019 to 440 Tg Methane *)
del2 = hh /. zz → tot[[Length[EM] + 1 ;; Length[tot]]];
del2 = Last[del1] + (del2 - First[del2]) * (Last[del1] - Last[del2]) / (First[del2] - Last[del2]);
metemis = Join[del1, del2];

Gmetan = 0.34 * Table[Exp[- (i - j) / τmetan] * UnitStep[i - j], {i, 1, n}, {j, 1, n}];
(* The factor 0.34 tunes 2019 methane concentration to around 1880 ppb *)
metan = Map[Max[#, 0] &, 700 + Gmetan.metemis];
Δfmetan = 0.036 * (Sqrt[metan] - Sqrt[700]);

Δfco2 = 5.35 Log[1 + (meanco2 - 280) / 280]; (* CO2 til forcing*)
Δfaer= -0.02tot;
Δfaer1 = Δfaer[[1 ;; Length[EM]]] ;
Δfaer2 = Drop[Δfaer, Length[EM]] ;
Δfaer2 = Map[Min[-0.4, #] &, Δfaer2];
Δfaer = Join[Δfaer1, Δfaer2];
Δf = Δfco2 + Δfaer + Δfmetan;
Δfliste = Append[Δfliste, Δf];
Δfaeroliste = Append[Δfaeroliste, Δfaer];
Δfghgliste = Append[Δfghgliste, Δfco2 + Δfmetan];

Tliste = {};
Do[
T2 = Klimaliste[[p]].Δf;

(*nonlin nonlin loop*) (*Do[
T2=Klimaliste[[p]].(Δf+styrke*0.5*(1+Tanh[(T2-terskel)/bratthet])); ,{10}];*)
(*nonlin lin loop*)
Do[
T2 = Klimaliste[[p]].(Δf + 0.2 T2); , {10}];
noise = σ2liste[[p]] * (Klimaliste[[p]].RandomReal[NormalDistribution[0, 1], Length[Δf]]);
noise = Drop[noise, 268 - 20];
T2 = T2 * (Γliste[[p]] / Log[4.]) / 5.35; T2 = Drop[T2, 268]; T2=1.1+T2-T2[[1]];
noiseliste = Append[noiseliste, noise]; Tliste = Append[Tliste, T2];
, {p, 1, Length[models]}];

middel =Table[Mean[Transpose[Tliste][[i]]], {i, 1, Length[Transpose[Tliste]]}];
upper = Table[Mean[Transpose[Tliste][[i]]] + StandardDeviation[ Transpose[Tliste][[i]]], {i, 1, Length[Trans-
pose[Tliste]]}];
```

```
lower = Table[Mean[Transpose[Tliste][[i]]] - StandardDeviation[ Transpose[Tliste][[i]]], {i, 1, Length[Trans-
pose[Tliste]]}];

RCB = Plus @@ Drop[tot, 270];
RCBliste = Append[RCBliste, RCB];
totliste = Append[totliste, tot];
alltliste = Join[alltliste, Tliste];
templiste = Append[templiste, middel];
uptempliste = Append[uptempliste, upper];
lowtempliste = Append[lowtempliste, lower];
, {u, 1, Length[data2]}]
, u];

In[]:= Length[noise]
Out[]= 103
In[]:= Length[T2]
Out[]= 83

In[]:= window=10;
noiseliste2 = Table[MovingAverage[noiseliste[[i]], window][[1 ;; Length[T2]]], {i, 1, Length[noiseliste]}];
noiseliste2 = Transpose[Partition[noiseliste2, 14]];

In[]:= Length[noiseliste2]
Out[]= 14
In[]:= Dimensions[noiseliste2]
Out[]= {14, 127, 83}
In[]:= Length[noiseliste2[[1]]]
Out[]= 127

In[]:= ListPlot[noiseliste2[[3]],Joined→True]
In[]:= FFE=ListPlot[Map[Transpose[{2018+Range[Length[templiste[[1]]]],#}]&, Extract[templiste, p1]],
PlotRange → All, Joined → True, Axes → False, Frame → True, FrameStyle → Directive[Black, 14], FrameLabel
→ {None, "GMST increase (°C)"}, Epilog → Inset[Style["e", 18], Scaled[{0.1, 0.9}]]]

In[]:= PL1=ListPlot[Map[Transpose[{1749+Range[Length[Δfaeroliste[[1]]]],#}]&, Extract[Δfaeroliste, p1]],
Joined → True];
PL2 = ListPlot[Map[Transpose[{1749 + Range[Length[Δfaeroliste[[1]]]], #}] &, Extract[Δfghgliste, p1]], Joined
→ True];

FFD = Show[{PL1, PL2}, PlotRange → All, Joined → True, Axes → False, Frame → True, FrameStyle → Di-
rective[Black, 14], FrameLabel → {None, "forcing"},Epilog → Inset[Style["d", 18], Scaled[{0.1, 0.9}]]]

modellfarger={,,,,,,,,,,,,,,,,, };
In[]:= pan=LineLegend[modellfarger,Map[StringSplit[#]&,models][[All,1]]]
Out[]= BCC-CSM1-1 BNU-ESM CanESM2 CCSM4 CSIRO-Mk3.6.0 FGOALS-s2 GFDL-ESM2M GISS-E2-R
HadGEM2-ES INM-CM4 MIROC5 MPI-ESM-LR MRI-CGCM3 NorESM1-M

In[]:= FFB=ListPlot[Map[Transpose[{2018+Range[Length[alltliste[[1]]]],#}]&, alltliste[[1 ;; 14]]], PlotRange →
All, Joined → True, Axes → False, Frame → True, FrameStyle → Directive[Black, 14], FrameLabel → {None,
"GMST increase (°C)"},Epilog → Inset[Style["b", 18], Scaled[{0.1, 0.9}]], PlotStyle → Map[{#} &, modellfarger]]

In[]:= Grid[{{Show[FFA,ImageSize→400],Show[FFB,ImageSize→400],pan}}]

In[]:= Grid[{{Show[FFC,ImageSize→400, Epilog → Inset[Style["a", 18], Scaled[{0.1, 0.9}]]], Show[FFD, ImageSize
→ 400, Epilog → Inset[Style["b", 18], Scaled[{0.1, 0.9}]]] , Show[FFE, ImageSize → 400, Epilog → Inset[Style["c",
18], Scaled[{0.1, 0.9}]]]}}]

In[]:= maxtemp=Map[Max[#]&,templiste];
maxtemp2 = Map[Max[#] &, uptempliste];
maxtemp3 = Map[Max[#] &, lowtempliste];

In[]:= PL1=ListPlot[Extract[Transpose[{maxtemp,RCBliste2}],p1], AspectRatio → 1, PlotRange → All];
```

```
PL3 = ListPlot[Extract[Transpose[{maxtemp2, RCBliste2}], p1], AspectRatio → 1, PlotRange → All, PlotStyle → Red];
PL4 = ListPlot[Extract[Transpose[{maxtemp2, RCBliste2}], p1], AspectRatio → 1, PlotRange → All, PlotStyle → Red];
gg = Fit[Extract[Transpose[{maxtemp, RCBliste2}], p1], {zz, 1}, zz]; PL2 = Plot[gg, {zz, 1.2, 3}];
gg2 = Fit[Extract[Transpose[{maxtemp2, RCBliste2}], p1], {zz, 1}, zz]; PL4 = Plot[gg2, {zz, 1.2, 3}];
Show[{PL1, PL2}, PlotRange → All]

In[]:= pairs=Extract[Transpose[{maxtemp,RCBliste2}],p1];
error = pairs[[All, 2]] - (gg /. zz → pairs[[All, 1]]);
S = Sqrt[(Plus @@ (error^2)) / (Length[pairs] - 2)];
σx = StandardDeviation[pairs[[All, 1]]];
σf[x_] := S * Sqrt[1 + 1 / Length[pairs] + (x - Mean[pairs[[All, 1]]])^2 / (Length[pairs] * σx^2)];

In[]:= pdf=(PDF[NormalDistribution[gg,σf[zz]]][p])/.zz→1.5;
pdf2 = (PDF[NormalDistribution[gg, σf[zz]]][p]) /. zz → 2.5;
Plot[{pdf, pdf2}, {p, 0, 5200}, PlotRange → All]

In[]:= PL1=ListPlot[Extract[Transpose[{maxtemp,RCBliste2}],p1],AspectRatio→1, PlotRange → {{1, 4}, {0, 4000}}, PlotStyle → Darker[Blue]];
PL2 = Plot[gg, {zz, 1, 3}, PlotStyle → Darker[Blue]];
l1 = Graphics[{Black, Line[{{1.5, 0}, {1.5, gg /. zz → 1.5}}]}];
l2 = Graphics[{Black, Line[{{1.5, gg /. zz → 1.5}, {1, gg /. zz → 1.5}}]}]; inset = ParametricPlot[{1 + 60 * pdf, p}, {p, 0, 1200}, Axes → False, PlotStyle → {Black, Thickness[0.01]}];

l11 = Graphics[{Black, Line[{{2.5, 0}, {2.5, gg /. zz → 2.5}}]}];
l22 = Graphics[{Black, Line[{{2.5, gg /. zz → 2.5}, {1, gg /. zz → 2.5}}]}]; inset2 = ParametricPlot[{1 + 60 * pdf2, p}, {p, 1900, 3000}, Axes → False, PlotStyle → {Black, Thickness[0.01]}];

FA = Show[{PL1, PL2, l1, l2, l11, l22, inset, inset2}, Axes → False, Frame → True, FrameStyle → Directive[Black, 14], FrameLabel → {"global temperature increase (°C)", "carbon budget after 2018 (Gt CO2)"}, Epilog → Inset[Style["a", 18], Scaled[{0.1, 0.9}]],ImageSize → 400, PlotRange → {{1, 4}, {0, 4500}}]

In[]:= maxtemp=Partition[Map[Max[#]&,alltliste],14][[All,5]];
PL1 = ListPlot[Extract[Transpose[{maxtemp, RCBliste2}], p1], AspectRatio → 1, PlotRange → All, PlotStyle → Black];
gg = Fit[Extract[Transpose[{maxtemp, RCBliste2}], p1], {zz, 1}, zz];
PL2 = Plot[gg, {zz, 1.2, 4}, PlotStyle → Black];
QL1 = Show[{PL1, PL2}, PlotRange → All];

maxtemp = Partition[Map[Max[#] &, alltliste], 14][[All, 7]];
PL1 = ListPlot[Extract[Transpose[{maxtemp, RCBliste2}], p1], AspectRatio → 1, PlotRange → All, PlotStyle → Darker[Red]];
gg = Fit[Extract[Transpose[{maxtemp, RCBliste2}], p1], {zz, 1}, zz];
PL2 = Plot[gg, {zz, 1.2, 3.5}, PlotStyle → Darker[Red]];
QL2 = Show[{PL1, PL2}, PlotRange → All];
FB = Show[{QL1, QL2}, Axes → False, Frame → True, FrameStyle → Directive[Black, 14], FrameLabel → {"global temperature increase (°C)", "carbon budget after 2018 (Gt CO2)"}, Epilog → {Inset[Style["b", 18], Scaled[{0.1, 0.9}]], Inset[LineLegend[{Black, Darker[Red]}, {"CSIRO-Mk3.6.0", "GFDL-ESM2M"}],

Scaled[{0.7, 0.3}]]}, ImageSize → 400, PlotRange → {{1, 4}, {0, 4500}}] In[]:= Grid[{{FA,FB}}]
```

14 ESMS FROM CMIP5, 2 CARBONMODELS FROM SRM, INTERNAL VARIABILITY

```
RCBliste = {};
totliste = {};
templiste = {};
uptempliste = {};
lowtempliste = {};
alltliste = {};
```

```
Monitor[
Do[
tot = data2[[u]][[All, 2]];
meanco2 = Gmean.tot + 280;
meanco2upper = Gupper.tot + 280;
meanco2lower = Glower.tot + 280; (* forcing *)

(* metan *)
del1 = 11.9 * tot[[1 ;; Length[EM]]];
(* The factor 3.0 tunes 2019 methane emmisions in 2019 to 440 Tg Methane *)
del2 = hh /. zz → tot[[Length[EM] + 1 ;; Length[tot]]];
del2 = Last[del1] + (del2 - First[del2]) * (Last[del1] - Last[del2]) / (First[del2] - Last[del2]);
metemis = Join[del1, del2];

Gmetan = 0.34 * Table[Exp[- (i - j) / τmetan] * UnitStep[i - j], {i, 1, n}, {j, 1, n}];
(* The factor 0.35 tunes 2019 methane concentration to around 1880 ppb *)
metan = Map[Max[#, 0] &, 700 + Gmetan.metemis];
Δfmetan = 0.036 * (Sqrt[metan] - Sqrt[700]);
Δfco2 = 5.35 Log[1 + (meanco2 - 280) / 280]; (* CO2 til forcing*)
Δfco2upper = 5.35 Log[1 + (meanco2upper - 280) / 280]; (* CO2 til forcing*)
Δfco2lower = 5.35 Log[1 + (meanco2lower - 280) / 280]; (* CO2 til forcing*)
(* aerosols *)
Δfaer= -0.02tot;
Δfaer1 = Δfaer[[1 ;; Length[EM]]] ;
Δfaer2 = Drop[Δfaer, Length[EM]] ;
Δfaer2 = Map[Min[-0.4, #] &, Δfaer2];
Δfaer = Join[Δfaer1, Δfaer2];
Δf = Δfco2 + Δfaer + Δfmetan;
Δfupper = Δfco2upper + Δfaer + Δfmetan;
Δflower = Δfco2lower + Δfaer + Δfmetan;

Tliste = {};
Do[
T2 = Klimaliste[[p]].Δfupper;

(*nonlin loop*) (*Do[
T2=Klimaliste[[p]].(Δfupper+styrke*0.5*(1+Tanh[(T2-terskel)/bratthet]));
,{10}];*)

(*nonlin lin loop*) Do[
T2 = Klimaliste[[p]].(Δfupper + 0.2 T2);
, {10}];

T2 = T2 * (Γliste[[p]] / Log[4.]) / 5.35;
T2 = Drop[T2, 268];
T2=1.1+T2-T2[[1]];
Tliste = Append[Tliste, T2 + StandardDeviation[Flatten[noiseliste2[[p]]]]];

(*T2=Klimaliste[[p]].Δfupper;
T2=T2*(Γliste[[p]]/Log[4.])/5.35;
T2=Drop[T2,268];
T2=1.1+T2-T2[[1]]; Tliste=Append[Tliste,T2-StandardDeviation[Flatten[noiseliste2[[p]]]]];*)

(*T2=Klimaliste[[p]].Δflower;
T2=T2*(Γliste[[p]]/Log[4.])/5.35;
T2=Drop[T2,268];
T2=1.0+T2-T2[[1]]; Tliste=Append[Tliste,T2+StandardDeviation[Flatten[noiseliste2[[p]]]]];*)

T2 = Klimaliste[[p]].Δflower;

(*nonlin loop*) (*Do[
T2=Klimaliste[[p]].(Δflower+styrke*0.5*(1+Tanh[(T2-terskel)/bratthet]));
,{10}];*)
```

```
(*nonlin lin loop*) Do[
T2 = Klimaliste[[p]].(Δflower + 0.2 T2);
, {10}];
(* Comment out everything between: Do[ T2=Klimaliste[[p]].Δfupper; to here to look at linear comparison*)

T2 = T2 * (Γliste[[p]] / Log[4.]) / 5.35;
T2 = Drop[T2, 268];
T2=1.0+T2-T2[[1]];
Tliste = Append[Tliste, T2 - StandardDeviation[Flatten[noiseliste2[[p]]]]];
, {p, 1, Length[models]}];

middel = Table[Mean[Transpose[Tliste][[i]]], {i, 1, Length[Transpose[Tliste]]}];
upper = Table[Mean[Transpose[Tliste][[i]]] + StandardDeviation[ Transpose[Tliste][[i]]], {i, 1, Length[Trans-
pose[Tliste]]}];
lower = Table[Mean[Transpose[Tliste][[i]]] - StandardDeviation[ Transpose[Tliste][[i]]], {i, 1, Length[Trans-
pose[Tliste]]}]; RCB = Plus @@ Drop[tot, 270];
RCBliste = Append[RCBliste, RCB];
totliste = Append[totliste, tot];

alltliste = Join[alltliste, Tliste];
templiste = Append[templiste, middel];
uptempliste = Append[uptempliste, upper];
lowtempliste = Append[lowtempliste, lower];
, {u, 1, Length[data2]}]
,u]

In[]:= Dimensions[alltliste]
Out[]= {3556, 83}

In[]:= CM = {};
cm1 = Table[ Partition[Extract[Partition[Map[Max[#] &, alltliste], 2 * 14], p1][[kk]], 2][[ All, 1]], {kk, 1,
Length[p1]}];
cm2 = Table[Partition[Extract[Partition[Map[Max[#] &, alltliste], 2 * 14], p1][[ kk]], 2][[All, 2]], {kk, 1,
Length[p1]}];

Do[
CM = Append[CM, Transpose[{Extract[RCBliste2, p1], Transpose[cm1][[j]]}]]; CM = Append[CM, Trans-
pose[{Extract[RCBliste2, p1], Transpose[cm2][[j]]}]]; , {j, 1, Length[Transpose[cm2]]}];

In[]:= ListPlot[{CM[[1]],CM[[2]]}]

In[]:= smliste={};
tliste = {};

Monitor[ Do[
pdfliste = {};
Do[
gg = Fit[Map[Reverse[#] &, CM[[kk]]], {zz, 1}, zz];
pairs = Map[Reverse[#] &, CM[[kk]]];
error = pairs[[All, 2]] - (gg /. zz → pairs[[All, 1]]);
S = Sqrt[(Plus @@ (error^2)) / (Length[pairs] - 2)];
σx = StandardDeviation[pairs[[All, 1]]];
σf[x_] := S * Sqrt[1 + 1 / Length[pairs] + (x - Mean[pairs[[All, 1]]])^2 / (Length[pairs] * σx^2)];
pdf = Chop[(PDF[NormalDistribution[gg, σf[zz]]][p]) /. zz → target];
pdfliste = Append[pdfliste, pdf];
,{kk,1,2*14}];

g = Mean[pdfliste];
smooth = Convolve[PDF[NormalDistribution[0, 400]][p], g, p, x];
sm = smooth /. x → Range[7000];
smliste = Append[smliste, sm];
tliste = Append[tliste, target];
, {target, 1.1, 4.0, 0.01}];
, target];
```

```
In[]:= (*forsterkningsfaktor a+bT: 0.10034007260683281`+2.2321837475237376` x*)

In[]:= a=0.10034;
b = 2.23218;
Δtarc = a+b* Δt;

In[]:= budget=500;
Δt = tliste[[2]] - tliste[[1]];
y = Transpose[smliste][[budget]];
y = y/ ((Plus@@y) * Δt); ListPlot[Transpose[{tliste, y}], Joined → True]

In[]:= budget=1500;
Δt = tliste[[2]] - tliste[[1]];
y = Transpose[smliste][[budget]];
y = y/ ((Plus@@y) * Δt); ListPlot[Transpose[{tliste, y}], Joined → True]

In[]:= bliste={};
Do[
Δt = tliste[[2]] - tliste[[1]];
y = Transpose[smliste][[budget]];
y = y/ ((Plus@@y) * Δt);
t1= tliste[[First[Position[FoldList[Plus, 0, y * Δt], _ ? (# > 0.90 &)]][[1]] - 1]];
t2 = tliste[[First[Position[FoldList[Plus, 0, y * Δt], _ ? (# > 0.75 &)]][[1]] - 1]];
t3 = tliste[[First[Position[FoldList[Plus, 0, y * Δt], _ ? (# > 0.5 &)]][[1]] - 1]];
t4= tliste[[First[Position[FoldList[Plus, 0, y * Δt], _ ? (# > 0.25 &)]][[1]] - 1]];
t5 = tliste[[First[Position[FoldList[Plus, 0, y * Δt], _ ? (# > 0.10 &)]][[1]] - 1]];
bliste = Append[bliste, {budget, t1, t2, t3, t4, t5}]; , {budget, 200, 4000, 100}]

In[]:= farger={Red,Darker[Red],Black,Darker[Blue],Blue};
aa = ListPlot[{Transpose[{bliste[[All, 1]], bliste[[All, 2]]}],

Transpose[{bliste[[All, 1]], bliste[[All, 3]]}], Transpose[{bliste[[All, 1]], bliste[[All, 4]]}], Transpose[{bliste[[All, 1]], bliste[[All, 5]]}], Transpose[{bliste[[All, 1]], bliste[[All, 6]]}]}, Joined → True, AspectRatio → 1, PlotRange → {{1, 9}}, Axes → False,Frame → True, FrameStyle → Directive[Black, 14] ,PlotStyle → Table[farger[[i]], {i, 1, 5}], GridLines → Automatic, FrameLabel → {"Carbon budget from 2018 (GtCO2)", "Maximum temperature increase (°C)"}, PlotLegends → Placed[{"10% prob.", "25% prob.", "even chance", "75% prob.", "90% prob."}, {Scaled[{0.05, 0.7}], {0, 0.5}}]]; l = Graphics[{Black, Line[{{1294, 1}, {1294, 2.5}}]}];
GGD = Show[{aa}]

In[]:= Tclow=Graphics[{Black,Line[{{0,8},{4000,8}}]}]; (*Greenland paper critical values*)
Tcupper = Graphics[{Black, Line[{{0, 8.5}, {4000, 8.5}}]}];

In[]:= farger={Red,Darker[Red],Black,Darker[Blue],Blue};
aaa = ListPlot[{Transpose[{bliste[[All, 1]], a + b * bliste[[All, 2]]}], Transpose[{bliste[[All, 1]], a + b * bliste[[All, 3]]}], Transpose[{bliste[[All, 1]], a + b * bliste[[All, 4]]}], Transpose[{bliste[[All, 1]], a + b * bliste[[All, 5]]}], Transpose[{bliste[[All, 1]], a + b * bliste[[All, 6]]}]}, Joined → True, AspectRatio → 1, PlotRange → {{1, 9}} , Axes → False, Frame → True, FrameStyle → Directive[Black, 14], PlotStyle → Table[farger[[i]], {i, 1, 5}], GridLines → Automatic, FrameLabel → {"Carbon budget from 2018 (GtCO2)", "Maximum temperature increase (°C)"}, PlotLegends → Placed[{"10% prob.", "25% prob.", "even chance", "75% prob.", "90% prob."}, {Scaled[{0.05, 0.7}], {0, 0.5}}]]; l = Graphics[{Black, Line[{{1294, 1}, {1294, 2.5}}]}];
GGD = Show[{aaa, Tclow, Tcupper}, PlotRange → {{0, 4000}, {1.1, 10}}]

In[]:= Max[a+b*bliste[[All,2]]]
Out[]= 8.7612

COMPARISON

In[]:= Grid[{{Show[aa,PlotRange→{{0,4000},{1.1,9}}, ImageSize → 400, Epilog → Inset[Style["a", 18], Scaled[{0.1, 0.9}]]], Show[aaa, PlotRange → {{0, 4000}, {1.1, 9}} , ImageSize → 400, Epilog → Inset[Style["b", 18], Scaled[{0.1, 0.9}]]]
}}]
```

ESTIMATION OF THE ARCTIC AMPLIFICATION FACTOR

```
(* GLOBAL LAND-OCEAN TEMPERATURE*)
SetDirectory["OneDrive - UiT Office 365"];
global = Drop[Drop[Import["GLB.Ts+dSST.csv", {"Data", All, 14}], 2], - 1];
In[]:= PL1=ListPlot[global,Joined→True,PlotRange → All, DataRange → {1880, 1880 + Length[global]}]
(*base period 1951-1980*)
In[]:= global;

(* ANNUAL MEAN LAND-OCEAN TEMPERATURE 64N-90N (ARCTIC IS 66.34N)*)
arctic = Drop[Import["ZonAnn.Ts+dSST.csv", {"Data", All, 8}], 1];
In[]:= PL2=ListPlot[arctic,Joined→True,PlotRange→All, PlotStyle → Orange, DataRange → {1880, 1880 +
Length[arctic]}]
(*base period 1951-1980*)
In[]:= Show[{PL1,PL2}, PlotRange->All]
(* COMPARISON*)
comp = Transpose[{global, arctic}];

In[]:= compPlot=ListPlot[comp,PlotRange→All, AxesLabel → {"global", "arctic"}, AspectRatio → 1]
In[]:= lm=LinearModelFit[comp,x,x](*forsterkningsfaktor=2.23218*)
Out[]= FittedModel 0.10034 + 2.23218 x
In[]:= Fit[comp,{zz,1},zz]
Out[]= 0.10034+2.23218zz
In[]:= fit=Plot[lm[x],{x,-3,5}];
In[]:= Show[{compPlot,fit}, PlotRange->All, FrameStyle → Directive[Black, 14], Axes → False, Frame → True,
FrameLabel → {"Global Land-Ocean Temperature Index (°C)", "Arctic Land-Ocean Temperature Index (°C)"}]
```

CODE FOR COMPARISON OF A SIMPLE RESPONSE MODEL TO MAGICC6.

The following code is used the non-linear framework in the SRM as described in Section 3.8. Produced in Mathematica: Version: 12.0.0.0 in collaboration with research partners Andreas Johansen, Andreas Martinsen and supervision from Martin Rypdal.
Platform: Mac OS X x86 (64-bit). macOS Catalina: Version 10.15.3.

```
SetDirectory["OneDrive - UiT Office 365"] M = Import["SSP_IAM_V2_201811.csv"];
M[[1]]
```
Out[]= {MODEL,"SCENARIO","REGION","VARIABLE","UNIT",2005,2010,2020,2030,2040,2050,2060
,2070,2080,2090,2100}

```
In[]:= M=Map[StringSplit[#,","]&,M];
In[]:= TT=Table[M[[k]][[1]][[4]],{k,1,Length[M]}]; Union[TT];
TTT = Table[M[[k]][[1]][[3]], {k, 1, Length[M]}];

In[]:= MAG=Position[TT,_?(#=="\"Diagnostics|MAGICC6|Temperature|GlobalMean\""&)];
In[]:= MAGpos=Position[TTT,_?(#=="\"World\""&)];
In[]:= mpos1=Intersection[MAGpos,MAG]; Extract[M, MAG][[1]];
In[]:= temp1=ToExpression[Map[Drop[Flatten[#],6]&,Extract[M,mpos1]]]; ListPlot[temp1, Joined → True]
```

SRM MODEL

```
In[]:= hh=157.65890684920566`+1.8942819330281027`zz+0.08520850267749702`zz^2;
In[]:= RR=Table[M[[k]][[1]][[4]],{k,1,Length[M]}];
Union[RR];
In[]:= RRR=Table[M[[k]][[1]][[3]],{k,1,Length[M]}];

Union[RRR]
```
Out[]= {"R5.2ASIA", "R5.2LAM", "R5.2MAF", "R5.2OECD", "R5.2REF", "REGION", "World"}

```
In[]:= co2pos1=Position[RR,_?(#=="\"Emissions|CO2|FossilFuelsandIndustry\""&)];
co2pos2 = Position[RR, _ ? (# == "\"Emissions|CO2|Land Use\"" &)];
co2pos3 = Position[RRR, _ ? (# == "\"World\"" &)];

In[]:= ppos1=Intersection[co2pos3,co2pos1];
ppos2 = Intersection[co2pos3, co2pos2];

In[]:= Extract[M,co2pos1][[1]]
```

Out[]= {{AIM/CGE, "SSP1-19", "R5.2ASIA", "Emissions|CO2|Fossil Fuels and Industry",
"Mt CO2/yr", 8985.6725, 10008.8152, 11790.747500000001,
6131.6627, 3271.4353000000006, 1678.8029, 638.87, 259.4755, 82.29590000000003, -7.9353000000000105, -
103.9171}}

```
In[]:= em1=ToExpression[Map[Drop[Flatten[#],7]&,Extract[M,ppos1]]];
em2 = ToExpression[Map[Drop[Flatten[#], 7] &, Extract[M, ppos2]]];

In[]:= ListPlot[em1,PlotRange→All,Joined→True]
emissions = Map[#[[1 ;; 2]] &, ToExpression[ Map[StringSplit[#] &, Drop[ReadList["emissionsCO2.txt", String],
31]]]];

In[]:= emissions=Table[{emissions[[i,1]],(44/12)*emissions[[i,2]]/1000.}
, {i, 1, Length[emissions]}];
```

```
In[]:= EM=Join[emissions,{{2018,37.1}}];
data2 = Table[Prepend[Table[{t, Interpolation[Join[EM, Transpose[{{2030, 2040, 2050, 2060, 2070, 2080,
2090, 2100}, 0.001 * Drop[em1[[k]], 1]}]]][t]}, {t, 1751, 2100}], {1750, 0}], {k, 1, Length[em1]}];
totliste = Table[data2[[k]][[All, 2]], {k, 1, Length[data2]}];

In[]:= positivepaths= Table[DeleteCases[Map[# * UnitStep[#] &, totliste[[k]][[269 ;; 351]]], _?(#
==0&)],{k,1,Length[totliste]}]; ListPlot[positivepaths, Joined → True]

In[]:= RCBliste2=Map[Plus@@#&,positivepaths];
In[]:= p1=Position[RCBliste2,_?(#<3300&)];
In[]:= ListPlot[data2,Joined→True,PlotRange→All]

In[]:= n=Length[data2[[1]]];
futuretime = 2100 - 2020;
τmetan = 12.4;

In[43]:= (* Carbon model *)
τ1=1;
τ2=10;
τ3 = 100;
τ4 = 1000;
c1mean = 0.152;
c2mean = 0.246;
c4mean = 0.134;
c5mean = 0.194;

Gmean = (12/44) *0.47* (c1mean * Table[Exp[- (i - j) / τ1] * UnitStep[i - j], {i, 1, n}, {j, 1, n}]+
c2mean * Table[Exp[- (i - j) / τ2] * UnitStep[i - j], {i, 1, n}, {j, 1, n}] +
(1 - c1mean - c2mean - c4mean - c5mean)* Table[Exp[- (i - j) / τ3] * UnitStep[i - j], {i, 1, n}, {j, 1, n}]+
c4mean * Table[Exp[- (i - j) / τ4] * UnitStep[i - j], {i, 1, n}, {j, 1, n}] +
Table[c5mean * UnitStep[i - j], {i, 1, n}, {j, 1, n}]);

In[52]:= (* Carbon models *)
c1upper = 0.11;
c2upper = 0.212;
c4upper = 0.106;
c5upper = 0.262;
c1lower = 0.18;
c2lower = 0.296;
c4lower = 0.122;
c5lower = 0.148;

Glower = (12 / 44) * 0.47 * (c1lower * Table[Exp[- (i - j) / τ1] * UnitStep[i - j], {i, 1, n}, {j, 1, n}] +
c2lower * Table[Exp[- (i - j) / τ2] * UnitStep[i - j], {i, 1, n}, {j, 1, n}] +
(1 - c1lower - c2lower - c4lower - c5lower) * Table[Exp[- (i - j) / τ3] * UnitStep[i - j], {i, 1, n}, {j, 1, n}] +
c4lower * Table[Exp[- (i - j) / τ4] * UnitStep[i - j], {i, 1, n}, {j, 1, n}] +
Table[c5lower * UnitStep[i - j], {i, 1, n}, {j, 1, n}]);

Gupper = (12/44) *0.47* (c1upper * Table[Exp[- (i - j) / τ1] * UnitStep[i - j], {i, 1, n}, {j, 1, n}] +
c2upper * Table[Exp[- (i - j) / τ2] * UnitStep[i - j], {i, 1, n}, {j, 1, n}] +
(1 - c1upper - c2upper - c4upper - c5upper) * Table[Exp[- (i - j) / τ3] * UnitStep[i - j], {i, 1, n}, {j, 1, n}] + c4up-
per * Table[Exp[- (i - j) / τ4] * UnitStep[i - j], {i, 1, n}, {j, 1, n}] +
Table[c5upper * UnitStep[i - j], {i, 1, n}, {j, 1, n}]);

In[62]:=
(*Optimal Estimation of Stochastic Energy Balance Model Parameters *)

In[63]:= (* Climate models *)
models = ReadList["CMIP5parameters.txt", String];
models = Delete[models, {{5}, {12}}];
boxes = StringSplit[models][[All, 2]];
Klimaliste = {};
Γliste = {};
σ2liste = {};
```

```
Monitor[
Do[

Clear[A];
modelnr = p; If[boxes[[p]] == "2",

{C1, C2, κ1, κ2, σ1, Γ, σ2} = ToExpression[Drop[StringSplit[models[[modelnr]]], 2]];

A = {{-(κ1+ κ2) /C1, κ2/C1}, {κ2/C2, -κ2/C2}};
g = (MatrixExp[t A].{1 / C1, 0})[[1]];
Gklima = Table[Chop[(g /. t → (i - j)) * UnitStep[i - j]], {i, 1, n}, {j, 1, n}];
Klimaliste = Append[Klimaliste, Gklima];
];

If[ boxes[[p]] == "3",

{C1, C2, C3, κ1, κ2, κ3, σ1, Γ, σ2} = ToExpression[Drop[StringSplit[models[[modelnr]]], 2]];

A = {{-(κ1+ κ2) /C1, κ2/C1, 0}, {κ2/C2, -(κ2+κ3)/C2, κ3/C2},{0, κ3/C3, - κ3/C3}};

g = (MatrixExp[t A].{1 / C1, 0, 0})[[1]];
Gklima = Table[Chop[(g /. t → (i - j)) * UnitStep[i - j]], {i, 1, n}, {j, 1, n}];
Klimaliste = Append[Klimaliste, Gklima];
];

If [ boxes[[p]] == "4",

{C1, C2, C3, C4, κ1, κ2, κ3, κ4, σ1, Γ, σ2} = ToExpression[Drop[StringSplit[models[[modelnr]]], 2]];

A = {{-(κ1+κ2)/C1, κ2/C1, 0, 0} , {κ2/C2, -(κ2+κ3)/C2, κ3/C2, 0},{ 0, κ3/C3, -(κ3+κ4)/C3, κ4/C3},
{0, 0, κ4/C4, -κ4/C4}};

g = (MatrixExp[t A].{1 / C1, 0, 0, 0})[[1]];
Gklima = Table[Chop[(g /. t → (i - j)) * UnitStep[i - j]], {i, 1, n}, {j, 1, n}];
Klimaliste = Append[Klimaliste, Gklima];
];

Γliste = Append[Γliste, Γ];
σ2liste = Append[σ2liste, σ2];
, {p, 1, Length[models]}
];
, {p, boxes[[p]]}
];




(*Nonlin parameter changes*)

styrke = 1; (*w/m^2*)
terskel = 2; (*grader*)
bratthet = 0.5;
Plot[styrke * 0.5 * (1 + Tanh[(T - terskel) / bratthet]), {T, 0, 4}]
(*Test plot to visualise the non-linear forcing*)

RCBliste = {}; totliste = {}; templiste = {}; uptempliste = {}; lowtempliste = {}; alltliste = {}; Δfaeroliste = {};
Δfghgliste = {}; Δfliste = {}; noiseliste = {}; Monitor[
```

```
Do[
tot = data2[[u]][[All, 2]]; meanco2 = Gmean.tot + 280;

(* metan *)
del1 = 11.9 * tot[[1 ;; Length[EM]]];
(* The factor 11.9 tunes 2019 methane emmisions in 2019 to 440 Tg Methane *) del2 = hh /. zz →
tot[[Length[EM] + 1 ;; Length[tot]]];
del2 = Last[del1] + (del2 - First[del2]) * (Last[del1] - Last[del2]) / (First[del2] - Last[del2]);
metemis = Join[del1, del2];


Gmetan = 0.34 * Table[Exp[- (i - j) / τmetan] * UnitStep[i - j], {i, 1, n}, {j, 1, n}];
(* The factor 0.34 tunes 2019 methane concentration to around 1880 ppb *)
metan = Map[Max[#, 0] &, 700 + Gmetan.metemis];

Δfmetan = 0.036 * (Sqrt[metan] - Sqrt[700]);
Δfco2 = 5.35 Log[1 + (meanco2 - 280) / 280]; (* CO2 til forcing*)
Δfaer= -0.02tot;
Δfaer1 = Δfaer[[1 ;; Length[EM]]] ;
Δfaer2 = Drop[Δfaer, Length[EM]] ;
Δfaer2 = Map[Min[-0.4, #] &, Δfaer2];
Δfaer = Join[Δfaer1, Δfaer2];
Δf = Δfco2 + Δfaer + Δfmetan;
Δfliste = Append[Δfliste, Δf];
Δfaeroliste = Append[Δfaeroliste, Δfaer];
Δfghgliste = Append[Δfghgliste, Δfco2 + Δfmetan];

Tliste = {}; Do[ T2 = Klimaliste[[p]].Δf;

(* Remove this part to run the linear SRM comparison*)

Do[
T2 = Klimaliste[[p]].(Δf + 0.2 T2);
, {10}];

(* End of part *)

noise = σ2liste[[p]] * (Klimaliste[[p]].RandomReal[NormalDistribution[0, 1], Length[Δf]]);
noise = Drop[noise, 268 - 20];
T2 = T2 * (Γliste[[p]] / Log[4.]) / 5.35; T2 = Drop[T2, 268]; T2=1.1+T2-T2[[1]];
noiseliste = Append[noiseliste, noise]; Tliste = Append[Tliste, T2];
, {p, 1, Length[models]}];

middel = Table[Mean[Transpose[Tliste][[i]]], {i, 1, Length[Transpose[Tliste]]}];
upper = Table[Mean[Transpose[Tliste][[i]]] + StandardDeviation[ Transpose[Tliste][[i]]], {i, 1, Length[Trans-
pose[Tliste]]}];
lower = Table[Mean[Transpose[Tliste][[i]]] - StandardDeviation[ Transpose[Tliste][[i]]], {i, 1, Length[Trans-
pose[Tliste]]}];

RCB = Plus @@ Drop[tot, 270];
RCBliste = Append[RCBliste, RCB];
totliste = Append[totliste, tot];
alltliste = Join[alltliste, Tliste];
templiste = Append[templiste, middel];
uptempliste = Append[uptempliste, upper];
lowtempliste = Append[lowtempliste, lower];
, {u, 1, Length[data2]}]
, u];

In[1]:= Length[noise]
Out[1]= 103
```

```
In[]:= Length[T2]
Out[]= 83

In[]:= window=10;
noiseliste2 = Table[MovingAverage[noiseliste[[i]], window][[1 ;; Length[T2]]], {i, 1, Length[noiseliste]}];
noiseliste2 = Transpose[Partition[noiseliste2, 14]];

In[]:= Length[noiseliste2]
Out[]= 14

In[]:= Dimensions[noiseliste2]
Out[]= {14, 127, 83}

In[]:= Length[noiseliste2[[1]]]
Out[]= 127

In[]:= ListPlot[noiseliste2[[3]],Joined→True]
In[]:= ListPlot[Extract[templiste,p1],Joined→True]
In[]:= ListPlot[Extract[temp1,p1],Joined→True,Axes→False,Frame→True, FrameStyle → Directive[Black, 14],
FrameLabel → {None, "GMST increase (°C)"}]

In[]:= OURMODEL=Extract[templiste,p1];
MAGICC = Extract[temp1, p1];

In[]:= Length[OURMODEL]
Out[]= 86
In[]:= Length[MAGICC]
Out[]= 86

In[]:= ListPlot[{OURMODEL[[1]],MAGICC[[1]]}]

In[]:= parliste={};

Do[
x = Drop[MAGICC[[i]], 1];
y = OURMODEL[[i]][[{3, 13, 23, 33, 43, 53, 63, 73, 83}]]; par = Transpose[{x, y}];
parliste = Append[parliste, par];
, {i, 1, Length[OURMODEL]}]

In[]:= y=OURMODEL[[1]][[{3,13,23,33,43,53,63,73,83}]]
Out[]= {1.16787, 1.54466, 1.64649, 1.64045, 1.60513, 1.56572, 1.53297, 1.50672, 1.48457}
PL1 = ListPlot[parliste, AspectRatio → 1, PlotRange → {{0.5, 4}, {0.5, 4}}]; PL2 = Plot[zz, {zz, 0.5, 4}, PlotStyle →
Black];
gg = Fit[Partition[Flatten[parliste], 2], {zz, 1}, zz];
PL3 = Plot[gg, {zz, 0.5, 4}, PlotStyle → {Black, Dashed}];
Show[{PL1, PL2, PL3}, FrameStyle → Directive[Black, 14], Axes → False, Frame → True, FrameLabel →
{"MAGICC GMST (°C)", "Response model GMST (°C)"}]
(* All 774 datapoints *)
In[]:= parliste2={};

Do[
x = Drop[MAGICC[[i]], 1];
y = OURMODEL[[i]][[{3, 13, 23, 33, 43, 53, 63, 73, 83}]]; par = {Max[x], Max[y]};
parliste2 = Append[parliste2, par];
, {i, 1, Length[OURMODEL]}];

PL1 = ListPlot[Map[{#} &, parliste2],
AspectRatio → 1, PlotRange → {{0.5, 4}, {0.5, 4}}];

PL2 = Plot[zz, {zz, 0.5, 4}, PlotStyle → Black];
gg = Fit[parliste2, {zz, 1}, zz];
PL3 = Plot[gg, {zz, 0.5, 4}, PlotStyle → {Black, Dashed}]; Show[{PL1, PL2, PL3}, FrameStyle → Directive[Black,
```

```
14], Axes → False, Frame → True, FrameLabel → {"MAGICC maximum GMST (°C)", "Response model maximum
GMST (°C)"}]
(* Max temperature comparison for 86 scenarios *)
```